SOFTWARE RELEASE NOTICE

1. SRN Number: MGFS-SRN-241	
2. Project Title: Analysis of the HI-STORM Cask S/ystem AHC 2-27-01	**Project No.** 20-01405-041
3. SRN Title: ANSYS / LS-DYNA, version 5.7	
4. Originator/Requestor: P. A. Cox	**Date: 02/26/01**

5. Summary of Actions

- ■ Release of new software

- ☐ Release of modified software:

    - ☐ Enhancements made

    - ☐ Corrections made

- ☐ Change of access software

- ☐ Software Retirement

6. Persons Authorized Access

Name	Read Only/Read-Write	Addition/Change/Delete
P. A. Cox	R-W	A
Asad Chowdhury	R-W	A
Janet Banda	R-W AHC 5-3-2001	A
		AHC 5-3-2001

7. Element Manager Approval: _(signature)_   **Date:** 2-27-2001   5-3-2001

8. Remarks:

SOFTWARE SUMMARY FORM

01. Summary Date: 02/26/01	02. Summary prepared by (Name and phone) P. A. Cox, 522-2315	03. Summary Action: NEW
04. Software Date: released 02/01	05. Short Title: ANSYS / LS-DYNA	

06. Software Title: ANSYS / LS-DYNA, version 5.7	07. Internal Software ID: N/A

08. Software Type: ☐ Automated Data System ■ Computer Program ☐ Subroutine/Module	09. Processing Mode: ☐ Interactive ☐ Batch ■ Combination	10. Application Area a. General: ■ Scientific/Engineering ☐ Auxiliary Analyses ☐ Total System PA ☐ Subsystem PA ☐ Other b. Specific: Structural Dynamics

11. Submitting Organization and Address: CNWRA/SwRI 6220 Culebra Road San Antonio, TX 78228	12. Technical Contact(s) and Phone: P. A. Cox, 210-522-2315 Asad Chowdhury, 210-522-5151

13. Software Application: Analysis of the HI-STORM cask System for Dynamic Loading

14. Computer Platform PC	15. Computer Operating System: Windows 2000	16. Programming Language(s): C++	17. Number of Source Program Statements: Many
18. Computer Memory Requirements: 512 Mb	19. Tape Drives: N/A	20. Disk Units: Removable, 45 Gb	21. Graphics: VGA

22. Other Operational Requirements   N/A

23. Software Availability: ■ Available ☐ Limited ☐ In-House ONLY	24. Documentation Availability: ■ Available ☐ Preliminary ☐ In-House ONLY

25. _(handwritten: 5 AHC 5-4-2001 4-3-2001)_

Software Developer: ANSYS, INC   Date: 02/26/01   _(Arrived at SwRI - BSu 5/3/2001)_

CNWRA Form TOP-4-1 (05/98)

TO: Bruce Mabrito

FROM: P. A. Cox

SUBJECT: Installation of ANSYS / LS-DYNA, version 5.7

DATE: February 26, 2001

The ANSYS / LS-DYNA program, version 5.7, is distributed as an executable. It is designed to run on many platforms. For this application it has been installed on a stand-alone PC, running WINDOWS 2000, that has been placed in a secure room (room 123, Bldg. 88). We purchased a 6-month license for the program.

On February 19, 2001, I installed and ran ANSYS / LS-DYNA successfully on the PC platform. To validate the installation, two supplied verification cases were executed on February 24, 2001, and results are attached. The verification cases are designed to replicate problems for which there are closed-form solutions. Results obtained with the program on the PC platform are in close agreement with test case values. One test case represents an impact event and the other a time dependent transient load. These two cases best represent the types of analyses we will be performing with the program.

The program also provides for stand-alone execution of LS-DYNA. This feature permits execution of input files that have not been created with the ANSYS pre-processor. It has been used successfully with LS-DYNA input files supplied by the NRC.

CENTER FOR NUCLEAR WASTE REGULATORY ANALYSES
DESIGN VERIFICATION REPORT FOR CNWRA SOFTWARE

ACQUIRED CODE - NOT TO BE MODIFIED[1]

Software Title/Name: *ANSYS/L.S. DYNA*

Version: *5.7*

Demonstration workstation: *PC*

Operating System: *Windows 2000*

Developer: *ANSYS, INC.*

---

1. Output: TOP-018, Section 5.5.4

Software designed so that individual runs are uniquely identified by Date, Time, Name of software and version?

Yes: ☐   No: ☐   N/A: ☑

Date and time of run: _____ *N/*

Name and version: _____ */A*

Notes: Acquired code that is not to be modified is accepted as is.

2. Medium and Header Documentation: TOP-018, Section 5.5.6

The physical labeling of software medium (tapes, disks, etc.) contain required information?

Yes: ☑   No: ☐   N/A: ☐

ANSYS/LS-DYNA

Program Name: *SwRI Project 20.01405.041/NRC Contract-02-97-009*

Module/Name/Title: *N/A   ANSYS/LS-DYNA Version 5.7*

Module Revision: *N/A*

File Type (ASCII, OBJ, EXE): *EXE*

Recording Date: *N/A   2/28/2001   QS   5/3/2001*

Operating System of Supporting Hardware: *Windows 2000*

Notes: Acquired code that is not to be modified may not have all above elements.

---

[1] See TOP-018. Table 1 for criteria.

3. User's Manual: TOP-018, Section 5.5.5

a) Is there a Users' Manual for the software?

Yes: ☑   No: ☐   N/A: ☐

User's Manual Version and Date: _**5.7**_

Notes: _Small Users manual with P.A. Cox, SwRI Div 18, Ext. 2315_

b) Are there basic instructions for the use of the software?

Yes: ☑   No: ☐   N/A: ☐

Location of Instruction: _Located on The CD_

Notes:

4. Acceptance Testing: TOP-018, Section 5.6

a) Has installation testing been conducted for each intended computer platform and operating system?

Yes: ☑   No: ☐   N/A: ☐

Platform(s): _PC - in Bldg 88, in Room 123._

Operating System(s): _Windows 2000_

Location of Test Results: _QA Records Room_

Notes:

5. Configuration Control: TOP-018, Section 5.7

a) Is the Software Summary Form completed and signed?

Yes: ☑   No: ☐   N/A: ☐

Software Summary Form Approval Date: _3 Apr 2001_

Notes:

b) Is a software technical description prepared, documenting the essential mathematical and numerical basis?

Yes: ☑   No: ☐   N/A: ☐

Location Technical Description: _Theoretical Information on The_
Notes: _CD describes essential mathematical basis._

c) Is the source code available (or, is the executable code available in the case of (acquired/commercial codes)?

Yes: ☑   No: ☐   N/A: ☐

Location of Source Code: _QA Records Room_

Notes:

6. Configuration Control, continued: TOP-018, Section 5.7

Have all the script/make files and executable files been submitted to the Software Custodian?

Yes: ☑   No: ☐   N/A: ☐

Location of Script/Make Files: _QA Records Room_

Notes:

7. Software Release: TOP-018, Section 5.9

Upon acceptance of the software as verified above, has a Software release Notice, Form TOP-6 been issued?

Yes: ☑   No: ☐   N/A: ☐

Version number on software (1.0 for 1st issue): _5.7_

Version number on SRN: _5.7_

Notes:

8. Software Validation: TOP-018, Section 5.10

a) Has a Software Validation Test Plan (SVTP) been prepared for the range of application of the software?

Yes: ☐   No: ☑   N/A: ☐

Version/Date of SVTP: ___

Date reviewed and approved via QAP-002: ___

Notes:

b) Has a Software Validation Test Report (SVTR) been prepared that documents the results of the validation cases, interpretation of the results, and determination if the software has been validated?

Yes: ☐   No: ☑   N/A: ☐

Version/Date of SVTR: ___

Date reviewed and approved via QAP-002: ___

Notes:

Additional Remarks:

5-3-2001   5-3-2001
AHC
5-5-2001   5/3/2001

_____   _____
CNWRA Software Developer/Date   CNWRA Software Custodian/Date

# VME2: Drop Analysis of a Block Onto a Spring Scale

Name

VME2 --

Overview

Reference:	Beer & Johnston, [Ref 8: Vector Mechanics for Engineers: Statics and Dynamics], pg. 635
Analysis Type(s):	Explicit Dynamics with ANSYS/LS-DYNA
Element Type(s):	Explicit 3-D Structural Solid (SOLID164) Explicit Spring-Damper (COMBI165)
Input Listing:	vme2.dat

Test Case

A 30 kg block is dropped from a height of 2 m onto a 10 kg pan of a spring scale. The maximum deflection of the pan will be determined for a spring with a stiffness of 20 kN/m.

Figure 1. Drop Analysis Of A Block Onto A Spring Scale Problem Sketch and Finite Element Model
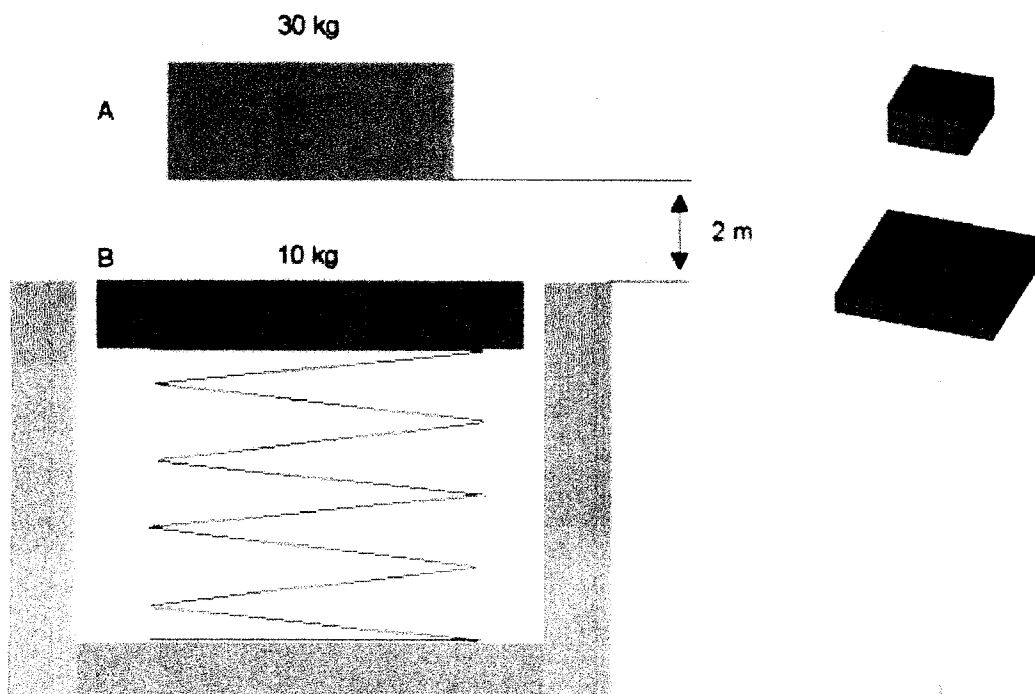
Problem Sketch   Representative Finite Element Model

Material Properties	Geometric Properties	Loading
Block	**Block**	The block is dropped from rest at a height of 2 m.
E = 207 GPa	base = 1 m	$g = 9.81$ m/sec^2
$\rho = 60$ kg/m^3	width = 1 m	
υ = .29	height = .5m	
Pan	**Pan**	
E = 207 GPa	base = 2 m	
$\rho = 10$ kg/m^3	width = 2 m	
υ = .29	height = .25 m	
Spring	**Spring**	
k = 20 kN/m	length = 6m	

Analysis Assumptions and Modeling Notes

The sizes of the block, pan, and spring have been arbitrarily selected. The densities of the block and pan, however, are based on the respective volumes of each component. A relatively course mesh was chosen for both the block and pan.

Results Comparison

	Target	ANSYS	Ratio
Maximum Uy of Pan	.230	.238	1.035

```
/COM,ANSYS MEDIA REL. 57 (11/17/00) REF. VERIF. MANUAL: REL. 57
/VERIFY,VME2
JPGPRF,500,100,1                    ! MACRO TO SET PREFS FOR JPEG PLOTS
/SHOW,JPEG

/title,VME2, Drop Analysis Of A Block Onto A Spring Scale
/stitle,1,Reason COMPARE differences are acceptable:
/stitle,2,  Leading zero before decimals, Accuracy
! Beer and Johnson, Vector Mechanics for Engineers, pg 635
/PREP7
ET,1,164
R,1
MP,EX,1,207E9
MP,NUXY,1,.29
MP,DENS,1,60
BLOCK,-.5,.5,8.25,8.75,-.5,.5,
VMESH,1
CM,BLOCK,NODE

ET,2,164
R,2
MP,EX,2,207E9
MP,NUXY,2,.29
MP,DENS,2,10
EDMP,RIGID,2,6,7
TYPE,2
REAL,2
MAT,2
BLOCK,-1,1,6,6.25,-1,1,
VMESH,2
ET,3,165
R,3
MP,EX,3,207E9
MP,NUXY,3,.29
MP,DENS,3,10
TB,DISC,3,,,0
TBDATA,1,20000

TYPE,3
REAL,3
MAT,3
N,1000
E,143,1000
NSEL,S,NODE,,1000
D,ALL,ALL
ALLS

NSEL,S,LOC,Y,6.25
CM,N1,NODE
NSEL,S,LOC,Y,8.25
CM,N2,NODE
EDCGEN,NTS,N2,N1
ALLS

*DIM,TIME,ARRAY,2
*DIM,ACCL,ARRAY,2
TIME(1)=0
TIME(2)=1.5
ACCL(1)=9.81
ACCL(2)=9.81
```
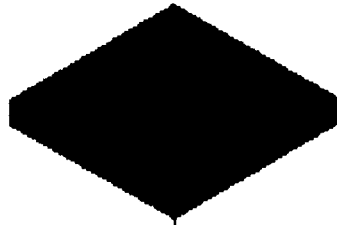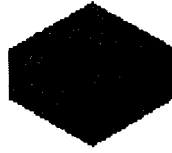
```
EDLOAD,ADD,ACLY,,BLOCK,TIME(1),ACCL(1)
/VIEW,1,1,1,1
/ANG,1
/AUTO,1
EPLOT
FINI

/SOLU
TIME,.75
EDRST,10
EDHT,50
NSEL,S,NODE,,143
CM,SCALE,NODE
EDHIST,SCALE
ALLS
SAVE
/COM    &COMPARE,NOCOMPARE
SOLVE
/COM    &COMPARE,NORMAL

/POST26
FILE,vme2,his
NSOL,2,143,U,Y,DISPY
PLVAR,2
PRVAR,2
*GET,RES1,VARI,2,EXTREM,VMIN, ,
*DIM,LABEL,CHAR,1
*DIM,RES,,1,3
LABEL(1) = 'MAX Uy'
*VFILL,RES(1,1),DATA,0.225
*VFILL,RES(1,2),DATA,ABS(RES1)
*VFILL,RES(1,3),DATA,ABS(RES(1,2)/RES(1,1))
/OUT,vme2,vrt
/COM,
/COM,------------------ VME2 DYNA RESULTS COMPARISION
--------------------
/COM,
/COM,         | TARGET | ANSYS | RATIO |
/COM,
*VWRITE,LABEL(1),RES(1,1),RES(1,2),RES(1,3)
(1X,A8,'    ',F5.3,'        ',F5.3,'      ',F5.3)
/COM,
/COM,-------------------------------------------------------------
----
/OUT
*LIST,vme2,vrt
*DELETE,vme2,db
FINISH
```
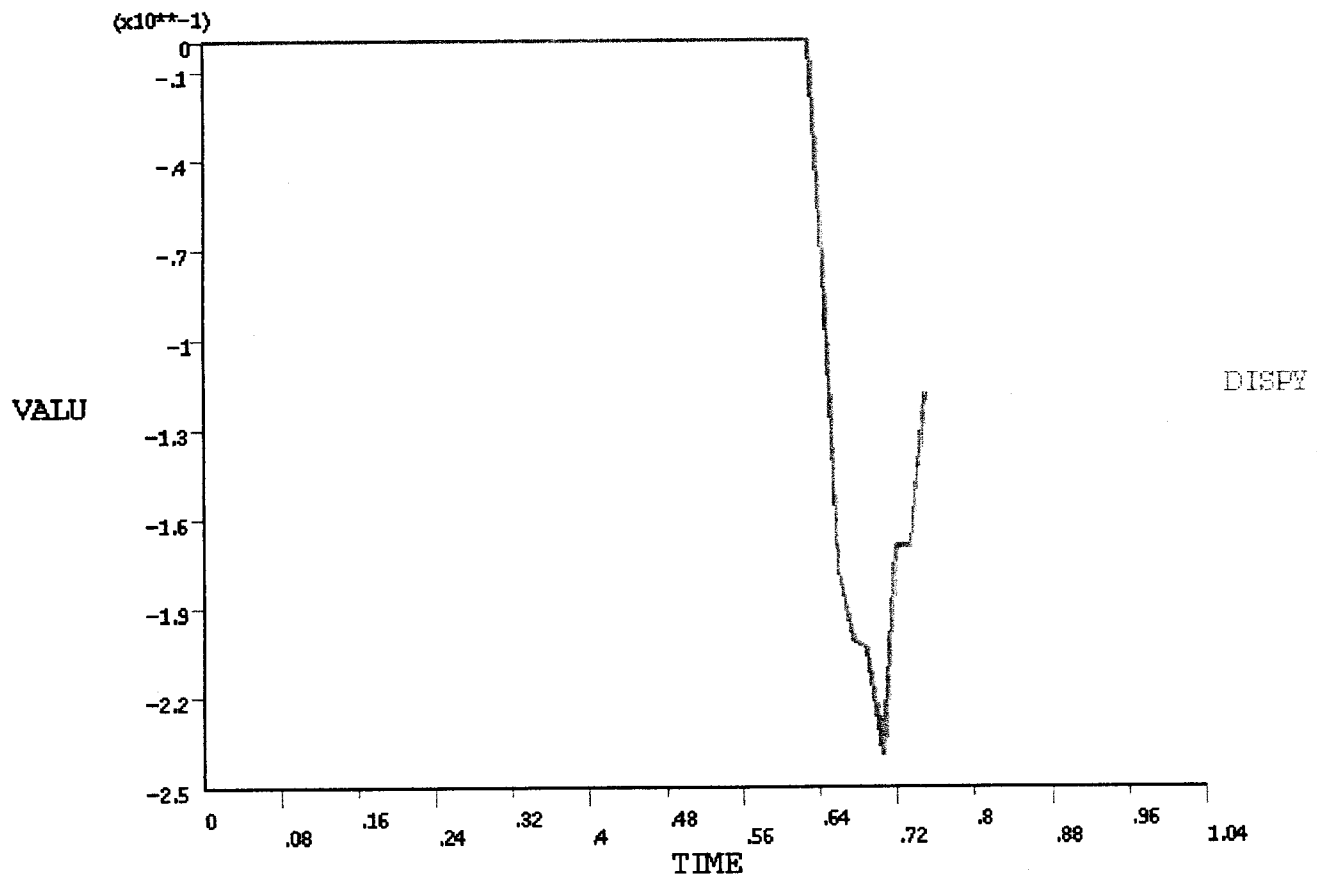
VME2, Drop Analysis Of A Block Onto A Spring Scale

(x10**-1)

VALU

DISPY

0
-.1
-.4
-.7
-1
-1.3
-1.6
-1.9
-2.2
-2.5

0   .08   .16   .24   .32   .4   .48   .56   .64   .72   .8   .88   .96   1.04

TIME

VME2, Drop Analysis Of A Block Onto A Spring Scale

```
-------------------- VME2 DYNA RESULTS COMPARISION --------------------

          |  TARGET  |  ANSYS  |  RATIO  |

MAX Uy       0.225      0.239     1.062

-----------------------------------------------------------------------
```

VME3: Response of Spring-Mass-Damper System

Name

VME3 --

Overview

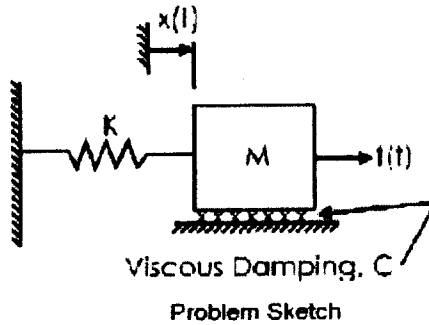| Reference:	Close & Frederick, [Ref 77: Modeling and Analysis of Dynamic Systems], pp. 314-315 Franklin, Powell & Emami-Naeini, [Ref 78: Feedback Control of Dynamic Systems], pp. 126-127
Analysis Type(s):	Explicit Dynamics with ANSYS/LS-DYNA
Element Type(s):	Explicit 3-D Structural Mass (MASS166) Explicit Spring-Damper (COMBI165)
Input Listing:	vme3.dat

Test Case

The one-DOF system consists of a spring, K, and mass, M, with viscous damping, C. There are two loading cases:

- Case 1: f(t) = A = constant (step input)

- Case 2: f(t) = At (ramp input)

For this underdamped system, the displacement of M for Case 1 overshoots the steady-state static displacement. The overshoot and the peak time, t_p are compared to theory outlined in [Ref 77: Modeling and Analysis of Dynamic Systems]. Based on the discussion in [Ref 78: Feedback Control of Dynamic Systems], the mass velocity in response to the ramp input, in theory, is equal to the mass displacement due to the step input.

Figure 1. Response of Spring-Mass-Damper System

Viscous Damping, C

Problem Sketch

Material Properties	Geometric Properties
Mass M = 1.0 kg **Spring** $K = 4\pi^2$ N/m **Damper** C = 0.21545376	**Spring** Length = 1 m

Loading
Case 1: A step force input, $f(t) = 4\pi^2$ on the mass M in the +x direction.   Case 2: A ramp force input, $f(t) = (4\pi^2)t$, on the mass M in the +x direction.

Analysis Assumptions and Modeling Notes

The magnitude of the step force input for Case 1 was chosen to equal the spring stiffness constant to produce a steady-state static deflection of unity. The ramp input for Case 2 was defined such that the input for Case 1 is the time derivative of the input for Case 2. The value of the stiffness constant was chosen so that the system undamped natural frequency equals 2 Hz. The damping constant was chosen to produce a damping ratio that results in a theoretical 50% overshoot of the steady-state deflection for the step input.

As outlined in [Ref 78: Feedback Control of Dynamic Systems], for a single DOF system subjected to a step input, the relationship between overshoot, M_p, and damping ratio, ζ, is given by:

$$M_p = \exp(-\pi\zeta/\sqrt{1-\zeta^2})$$

For the system in *Support Structure Problem Sketch*:

$$M_p = (x_{max} - x_{steady\text{-}state})/x_{steady\text{-}state}$$

The expression for peak time, t_p which is the time to reach x_{max} is given by:

$$t_p = \pi / (\omega_n \sqrt{1 - \zeta^2})$$

where ω_n is the system undamped natural frequency in units of radians per second.

Results Comparison

Table 1. Case 1: Step Input

	Target	ANSYS	Ratio
Maximum Ux of Mass	1.5000	1.5001	1.000
Peak Time for Mass Ux	0.2560	0.2559	1.000

Table 2. Case 2: Ramp Input

	Target	ANSYS	Ratio
Maximum Vx of Mass	1.5000	1.5001	1.000
Peak Time for Mass Vx	0.2560	0.2559	1.000

```
/COM,ANSYS MEDIA REL. 57 (11/17/00) REF. VERIF. MANUAL: REL. 57
/VERIFY,vme3
/CONFIG,NRES,3000
JPGPRF,500,100,1                 ! MACRO TO SET PREFS FOR JPEG PLOTS
/SHOW,JPEG

/TITLE,VME3,Response of Spring-Mass-Damper System
! Modeling And Analysis of Dynamic Systems,
! Close and Frederick, page 314
PI=3.1415927
ZETA=0.21545376             ! zeta=damping ratio.
M=1.0                       ! m=mass.
K=(4*PI)**2.0               ! k=spring stiffness.
WN=SQRT(K/M)                ! wn=system undamped natural frequency.
C=M*(2*ZETA*WN)             ! c=damping constant.
/PREP7                      ! Enter preprocessor.
N,1,0,0,0          ! Node 1 will be the fixed end.
N,2,1,0,0          ! The applied force will be at node 2.
ET,1,166           ! Define element type 1 as MASS166.
ET,2,165           ! Define element type 2 as COMBIN165.
R,1,M              ! Real constant for MASS166 is the value of the mass.
R,2
MP,EX,1,30E6             ! Define modulus of elasticity.
MP,DENS,1,.000733 ! Define density.
MP,NUXY,1,0.29          ! Define poisson's ratio.

MP,EX,2,30E6
MP,DENS,2,.000733
MP,NUXY,2,0.29
TB,discrete,2,,,0
tbdata,1,K
TYPE,1
REAL,1
E,2                ! Create the MASS166 element at node 2.

TYPE,2
REAL,2
MAT,2
E,1,2              ! Create the COMBIN165 element with end nodes 1 and 2.
NSEL,S,NODE,,2
CM,MASS,NODE             ! Create a nodal component at node 2 named
"mass"
ALLSEL
D,1,UX,0           ! Constrain all deflections at node 1.
D,1,UY,0
D,1,UZ,0
D,2,UY,0           ! Constrain uy and uz deflections at node 2.
D,2,UZ,0
EDDAMP,ALL,0,C/M   ! Define alpha damping.
FINI
/SOLU
EDRST,1000
EDHTIME,1000
EDHIST,MASS        ! Specify the mass component for time history output.
EDCTS,,0.001            ! Set a time step scaling factor to 0.001.
*DIM,T,ARRAY,2          ! Dimension array for time values.
*DIM,FSTEP,ARRAY,2      ! Dimension array for step force input.
*DIM,FRAMP,ARRAY,2      ! Dimension array for ramp force input.
T(1)=0,1
FSTEP(1)=K,K       ! The step input magnitude equals k so x=1 at steady-
```

```
state.
FRAMP(1)=0,K          ! The ramp input is the integral of the step input.
EDLOAD,ADD,FX,,MASS,T,FSTEP   !Specify the load for the step input
solution.
TIME,1                        !Specify the solution time.
/COM   &COMPARE,NOCOMPARE
SOLVE
/COM   &COMPARE,NORMAL
FINI
/POST26                       !Enter the time history post-processor.
NSOL,2,2,U,X,DISPLACE         !Define variable 2 - node 2 ux deflection
EXTREM,2                       !Print the max deflection and peak time
*GET,RES1,VARI,2,EXTREM,VMAX,,
*GET,TMAX1,VARI,2,EXTREM,TMAX,,
/solu                         !Return to the solution processor.
EDLOAD,ADD,FX,,MASS,T,FRAMP   !Redefine the load for a ramp input.
/COM   &COMPARE,NOCOMPARE
SOLVE
/COM   &COMPARE,NORMAL
FINI
/POST26
NSOL,2,2,V,X,VELOCITY         !Define variable 2 - node 2 velocity.
PLVAR,2
EXTREM,2                       !Print the max velocity and peak time
*GET,RES2,VARI,2,EXTREM,VMAX,,
*GET,TMAX2,VARI,2,EXTREM,TMAX,,
save
*DIM,LABEL,CHAR,4
*DIM,RES,,4,3
LABEL(1) = 'MAX Ux','PK TIME','MAX Vx','PK TIME'
*VFILL,RES(1,1),DATA,1.5,0.256,1.5,0.256
*VFILL,RES(1,2),DATA,RES1,TMAX1,RES2,TMAX2
*DO,I,1,4
   *VFILL,RES(I,3),DATA,(RES(I,2)/RES(I,1))
*ENDDO
/OUT,vme3,vrt
/COM,
/COM,-------------------- VME3 DYNA RESULTS COMPARISION
--------------------
/COM,
/COM,          | TARGET | ANSYS | RATIO |
/COM,
*VWRITE,LABEL(1),RES(1,1),RES(1,2),RES(1,3)
(1X,A8,'     ',F5.3,'        ',F5.3,'     ',F5.3)
/COM,
/COM,------------------------------------------------------------
----
/OUT
*LIST,vme3,vrt
/GOPR
FINISH
```

```
-------------------- VME3 DYNA RESULTS COMPARISION --------------------

          |  TARGET  |  ANSYS  |  RATIO  |

MAX Ux      1.500      1.499     0.999
PK TIME     0.256      0.256     1.000
MAX Vx      1.500      1.499     1.000
PK TIME     0.256      0.256     1.000


----------------------------------------------------------------------
```
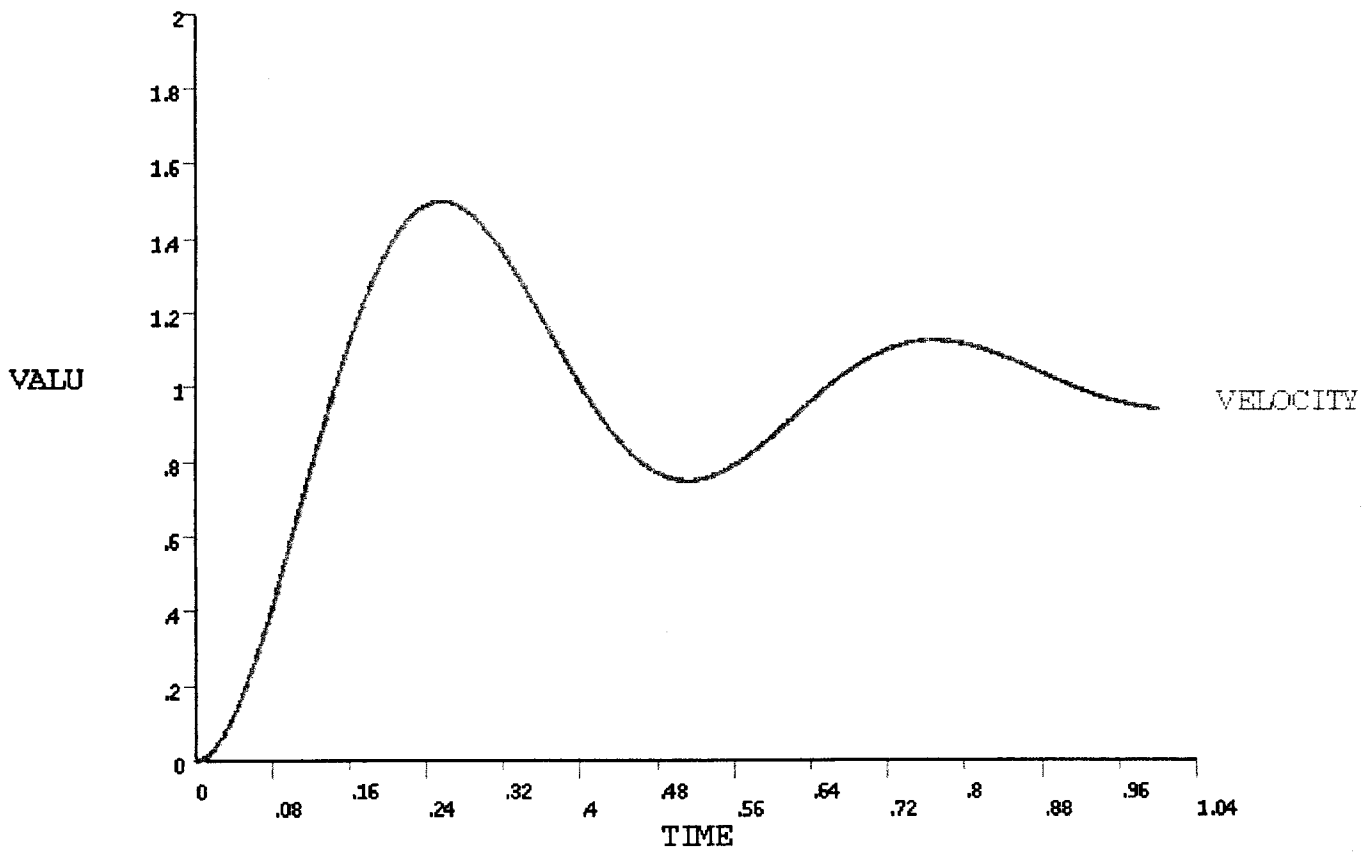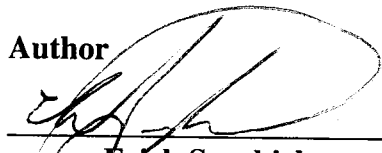
VME3,Response of Spring-Mass-Damper System

Software Validation Test Report

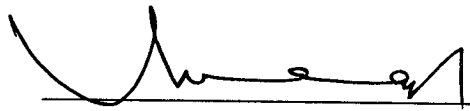# SOFTWARE VALIDATION TEST PLAN FOR ANSYS /LS-DYNA VERSION 5.7

January 18, 2002

Center for Nuclear Waste Regulatory Analyses
Southwest Research Institute
San Antonio, Texas

Author

Erick Sagebiel

1/18/02
Date

Element Manager

Asadul Chowdhury

1-18-02
Date

1

1.0 Scope of the Validation

Table 1 shows a list of features and options in the LS-Dyna code that the validation plan encompasses. The features and options listed in Table 1 were either used in previous CNWRA work or are likely to be used in future CNWRA projects.

Table 1. Feature and Options for Validation

Feature Number	Feature	Validation Case				
		1	2	3	4	5
1	Symmetric surface to surface contact		X			
2	Discrete nodes to surface contact	X	X	X	X	X
3	Spot welded nodes surface contact		X	X		
4	Nodes to surface contact constraint method		X			
5	Automatic nodes to surface contact			X		
6	Automatic surface to surface contact		X	X		
7	Rigid-wall surfaces	X	X	X	X	X
8	Solid elements				X	X
9	Beam elements			X		
10	Shell elements	X	X	X	X	
11	Piecewise linear plasticity material model (with and without rate effects; with and without finite failure strain)	X	X	X	X	X
12	Plastic-kinematic material model			X		
13	Pseudo-tensor material model				X	
14	EOS tabulated compaction material model				X	
15	Flexible to rigid conversion				X	
16	Rigid body motions				X	
17	Elastic deformations	X	X	X	X	X
18	Plastic deformations	X	X	X	X	
19	Large deformations	X	X	X	X	
20	Load curves	X	X	X	X	
21	Boundary node constraints	X				
22	Pressure loads	X	X	X	X	
23	Gravity loads	X	X	X	X	
24	Stiffness dampening					X
25	Mass dampening					X
26	Prescribed boundary motion					X

Validation for LS-DYNA will occur by comparing results from a series of test cases.

Therefore, five test cases will be run on both ABAQUS/ Explicit and LS-Dyna, both are explicit finite element analysis codes. Validation testing will be performed following procedures outlined in Section 5.10 of CNWRA Technical Operating Procedure TOP-018, Revision 8, change 01. If additional features are required in future projects, additional validation testing may be required.

2.0 References

ANSYS/LS-DYNA User's Guide, Version 5.6, November 1999
LS-DYNA Keyword User's Manual Volume 1&2, Version 960, March 2001
Center for Nuclear Waste Regulatory Analysis Technical Operating Procedure, TOP-018,
        Revision 8, October 2001
ANSYS/LS-DYNA Verification Manual , Version 5.7, December 2000
LS-DYNA Examples Manual, Version 960, June 2001

Other Documents as seen necessary

3.0 Environment

3.1 Software

pc environment:
ANSYS/LS-Dyna, version 5.7 (LS-Dyna Version 960) is the code being validated. The personal computer version runs under the Microsoft Windows Professional 2000 operating system. ANSYS/ LS-Dyna is acquired software being used to model large deformations and strain behavior under intense blast and earthquake loading. LS-Dyna is the solution package and ANSYS was the pre-processor. Lspost.exe (2.0 Beta, 2001) was used to process the results. McAfee VirusScan NT, current version

workstation environment:
ANSYS/LS-Dyna, version 5.7 is run under the Solaris 8 operating system. LS-Dyna is acquired software being used to model large deformations and strain behavior under intense blast and earthquake loading. LS-Dyna is the solution package and ANSYS was the pre-processor. Lspost.exe (2.0 Beta, 2001) was used to process the results.

Beowulf environment:
LS-Dyna version 960 is run under the Linux- Mandrake version 3.4.7 operating system. LS-Dyna is acquired software being used to model large deformations and strain behavior under intense blast and earthquake loading. LS-Dyna is the solution package and TrueGrid was the pre-processor. Lspost.exe (2.0 Beta, 2001) was used to process the results.

3.2 Hardware

ANSYS/LS-DYNA was used on two platforms:

1) Personal Computer equipped with:
   - Two (2) INTEL P3-1GbEBF Flip Chip CPU's
   - Four (4) PC-100 512 Mb SD-Ram
   - Mitsumi 1.44 Mb FLOPPY
   - Acer CD-RW 10x4x32 drive
   - KDS 21" color monitor
   - Vision Tek Geforce 2 GTS video card
   - IBM Deskstar 46.1 GB Removable Hard Drive
   - Logitch 3-Button PS/2 Mouse
   - Keytronix 104 PS/2 Keyboard
   - Seagate 20 GB Travan Tape Drive
   - HP Deskjet 720c color printer
   - Iomega 250 Zip drive

2) Workstation:
   - Sun 420R Server class machine w/ 4 processors
   - Solaris 8 operating system

3) Beowulf system:
   - 16 node cluster each with:
     - 900 MHz Athalon Thunderbird processor
     - 512 MB RAM
     - 20 GB Hard drive
   - 1 Master
     - 1 GHz Athalon Thunderbird processor
     - 1 GB RAM
     - 95 GB Hard drive cluster
   - Connection
     - 1 Gbit Ethernet connectors
     - 1 Gbit switch

4.0 Prerequisites

None

5.0 Assumptions and Constraints

None

6.0 Test Cases

There will be a series of five test cases run. These cases will include the features of the code

4

used in previous analyses. Each case will be modeled in both ANSYS/LS – Dyna and ABAQUS/ Explicit. The results will then be compared for verifications of each code. Comparisons will concentrate on plastic strain in highly loaded areas and maximum deformations. Case 3, 4, and 5 will be run on both the personal computer platform and workstation platform described above. These three cases are chosen because cases 1 and 2 are contained within them. For comparison, equivalent constitutive models and element formulations will be sought. If they do not exist, similar models will be sought and a sensitivity study may be required, to show the influence of different element formulations and constitutive models on results.

6.1.1 Test Case Number 1: Pressure Load on a Pipe

This case is a simple problem which makes sure ANSYS/LS – Dyna and ABAQUS/ Explicit are yielding similar results. The problem (shown in Figure 1) is a triangular pressure load on the top half of a thin walled pipe. The pipe geometry will utilize shell elements. Gravity loads will also be considered in this problem. The pipe along with all other structures in other cases will utilize discrete nodes to surface contact to interact with the rigid plane modeled as a Rigid-wall surface.

(1) Symmetric surface to surface contact –N/A
(2) Discrete nodes to surface contact – cylinder contacting rigid surface
(3) Spot welded nodes surface contact –N/A
(4) Nodes to surface contact constraint method–N/A
(5) Automatic nodes to surface contact–N/A
(6) Automatic surface to surface contact–N/A
(7) Rigid-wall surfaces – bottom surface to which cylinder is connected
(8) Solid elements–N/A
(9) Beam elements–N/A
(10) Shell elements – cylinder elements
(11) Piecewise linear plasticity material model (with and without rate effects; with and without finite failure strain)- shells
(12) Plastic-kinematic material model–N/A
(13) Pseudo-tensor material model–N/A
(14) EOS tabulated compaction material model–N/A
(15) Flexible to rigid conversion–N/A
(16) Rigid body motions–N/A
(17) Elastic deformations – certain cylinder deformations due to loading
(18) Plastic deformations – certain cylinder deformations due to loading
(19) Large deformations – certain cylinder deformations due to loading
(20) Load curves – the load applied is a function of time
(21) Boundary node constraints–the geometry may constrained on the centerline and cut in half
(22) Pressure loads – the load applied is distributed like a pressure load
(23) Gravity loads – the cylinder weight may be applied

(24) Stiffness dampening –N/A
(25) Mass dampening–N/A
(26) Prescribed boundary motion–N/A

Case 1
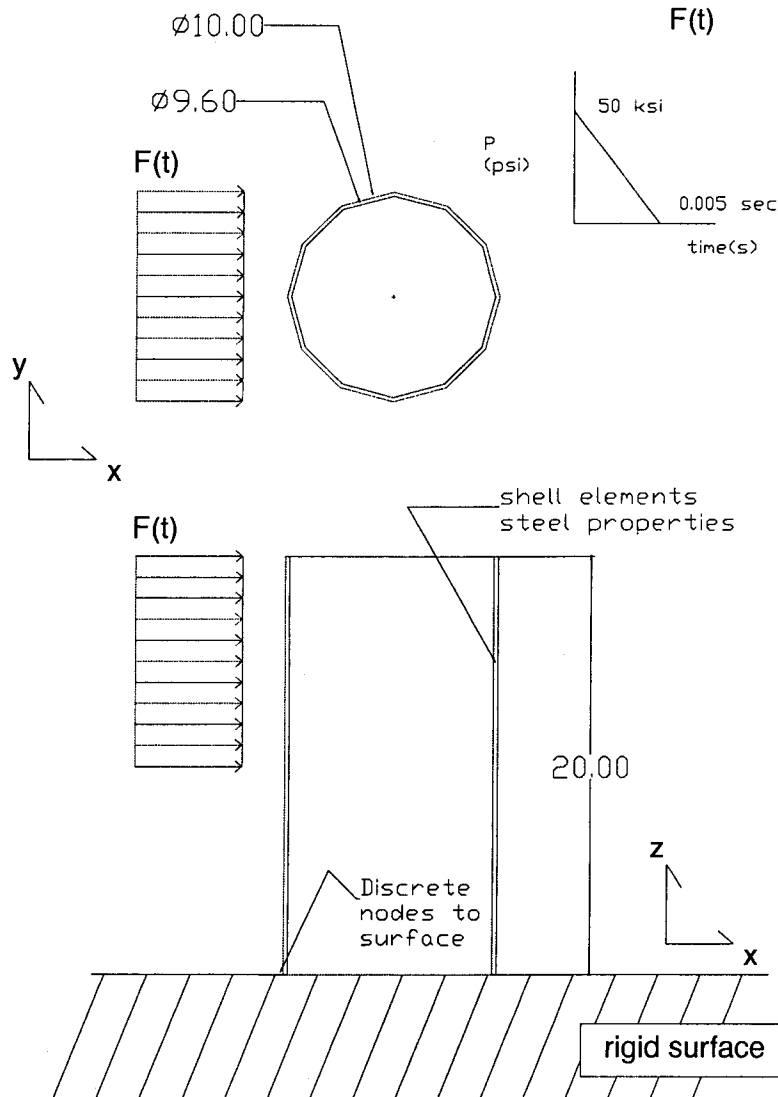
Figure 1. Case 1

6.1.2 Test Input

The model will be created with grid resolution similar to that used in the analyses. The

magnitude of the loading has been estimated. If it is seen that the damage to the model is to severe or too little deformation occurs, the magnitude of the load will be changed accordingly so elastic, plastic, and large deformations are observed.

6.1.3 Test Procedure

Case 1 will be modeled in both codes, and then results will be compared.

6.1.4 Test Results

The codes are not expected to give exactly the same results due to the complexity of the explicit codes. Therefore, requirements for code agreement will be determined on a case-by-case basis.
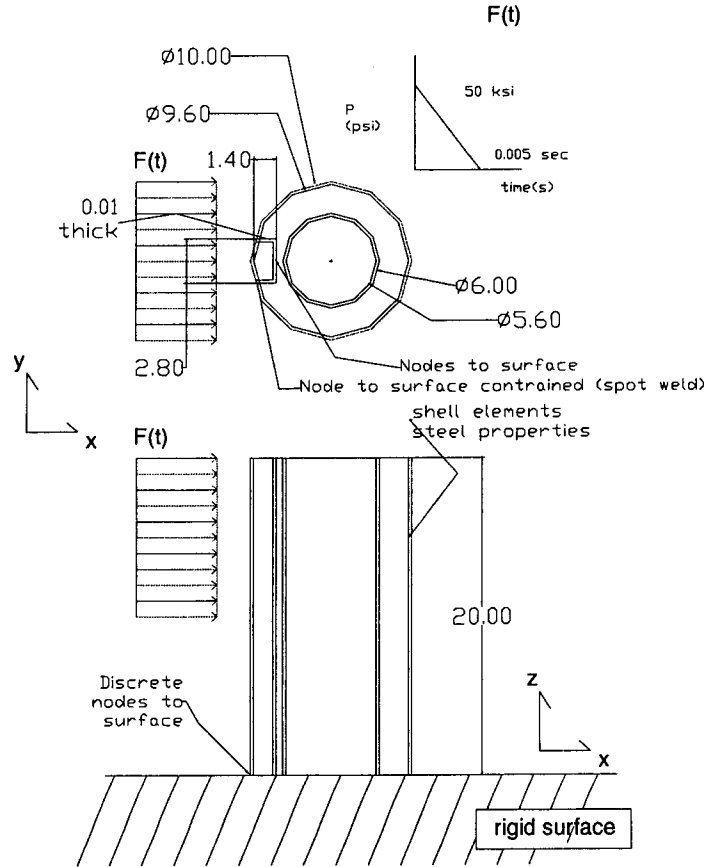
6.2.1 Test Case Number 2: Concentric Pipes with a Channel

Case 2 (shown in Figure 2) will build upon the Case 1 geometry. A concentric thin walled pipe will be placed inside of the previously modeled pipe. A channel shape will, also, be added to the model. The channel will be spot welded to the outer pipe and node to surface constraints will be added from the channel to the inner pipe. Symmetric surface to surface contact will be utilized between the two cylinders. This test will also test the same features as Case 1.

    (1) Symmetric surface to surface contact–occurs between the cylinders
    (2) Discrete nodes to surface contact – cylinder contacting rigid surface
    (3) Spot welded nodes surface contact – initial channel to outer cylinder contact
    (4) Nodes to surface contact constraint method–between channel and outer cylinder
    (5) Automatic nodes to surface contact–N/A
    (6) Automatic surface to surface contact – interaction between channel and inner
cylinder
    (7) Rigid-wall surfaces – bottom surface to which cylinder is connected
    (8) Solid elements–N/A
    (9) Beam elements–N/A
    (10) Shell elements – cylinder and channel elements
    (11) Piecewise linear plasticity material model (with and without rate effects; with and
          without finite failure strain) – shell elements
    (12) Plastic-kinematic material model–N/A
    (13) Pseudo-tensor material model–N/A
    (14) EOS tabulated compaction material model–N/A
    (15) Flexible to rigid conversion–N/A
    (16) Rigid body motions–N/A
    (17) Elastic deformations – certain cylinder deformations due to loading
    (18) Plastic deformations – certain cylinder deformations due to loading
    (19) Large deformations – certain cylinder deformations due to loading
    (20) Load curves – the load applied is a function of time
    (21) Boundary node constraints–N/A

(22) Pressure loads – the load applied is distributed like a pressure load

(23) Gravity loads – the cylinder weight may be applied

(24) Stiffness dampening –N/A

(25) Mass dampening–N/A

(26) Prescribed boundary motion–N/A

Case 2

Figure 2. Case 2

6.2.2 Test Input

Same procedure as Case 1.

6.2.3 Test Procedure

Same procedure as Case 1.

8

6.2.4 Test Results

Same procedure as Case 1.

6.3.1 Test Case Number 3: Beam Elements inside Concentric Pipes

Case 3 (shown in Figure 3) will build upon the Case 2 geometry. Two beams will be placed inside the inner pipe. These beams will utilize beam elements and will allow for beam-to- beam interactions using automatic single surface contact algorithms. This test will also test the same features as Case 2.

(1) Symmetric surface to surface contact–N/A
(2) Discrete nodes to surface contact – cylinder contacting rigid surface
(3) Spot welded nodes surface contact – initial channel to outer cylinder contact
(4) Nodes to surface contact constraint method–N/A
(5) Automatic nodes to surface contact– interaction between beams and inner cylinder
(6) Automatic surface to surface contact – interaction between channel and inner cylinder
(7) Rigid-wall surfaces – bottom surface to which cylinder is connected
(8) Solid elements–N/A
(9) Beam elements – beam element inside inner cylinder
(10) Shell elements – cylinder and channel elements
(11) Piecewise linear plasticity material model (with and without rate effects; with and without finite failure strain)- shell elements
(12) Plastic-kinematic material model – beam elements
(13) Pseudo-tensor material model –N/A
(14) EOS tabulated compaction material model–N/A
(15) Flexible to rigid conversion–N/A
(16) Rigid body motions–N/A
(17) Elastic deformations – certain cylinder deformations due to loading
(18) Plastic deformations – certain cylinder deformations due to loading
(19) Large deformations – certain cylinder deformations due to loading
(20) Load curves – the load applied is a function of time
(21) Boundary node constraints–N/A
(22) Pressure loads – the load applied is distributed like a pressure load
(23) Gravity loads – the cylinder weight may be applied
(24) Stiffness dampening –N/A
(25) Mass dampening–N/A
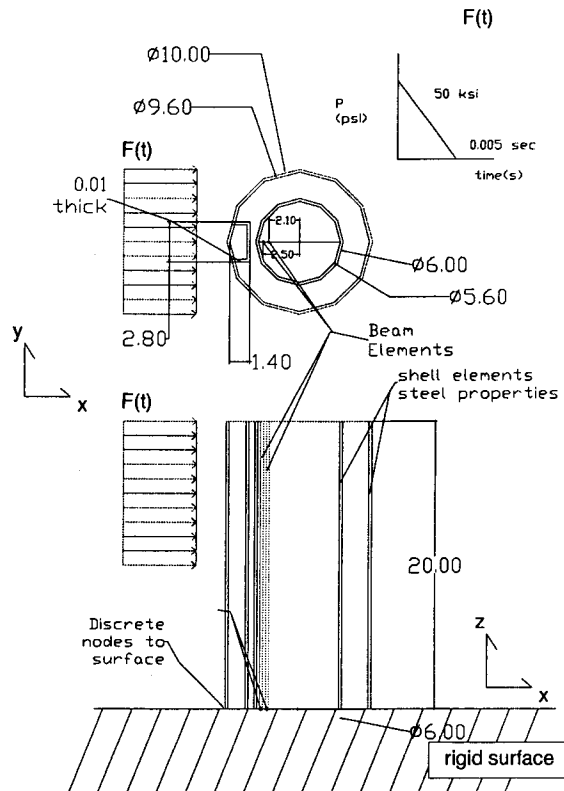(26) Prescribed boundary motion–N/A

Case 3

Figure 3. Case 3

6.3.2 Test Input

Same procedure as Case 1.

6.3.3 Test Procedure

Same procedure as Case 1.

6.3.4 Test Results

Same procedure as Case 1.

6.4.1 Test Case Number 4: Thin walled Pipe filled with Concrete

Case 4 (shown in Figure 4) will build upon the Case 1 geometry. The thin- walled pipe will be filled concrete. The concrete and pipe will not share common nodes: Interactions between the pipe and concrete will be controlled with contour surface. Before the pipe system

10

interacts with the soil wall the pipe system will be changed from flexible to rigid yielding rigid body motions. Both the concrete and the soil will utilize solid elements. The concrete will utilize the EOS tabulated compaction material model. This case will, also, test the same features as Case 1.

(1) Symmetric surface to surface contact–N/A
(2) Discrete nodes to surface contact – cylinder contacting rigid surface
(3) Spot welded nodes surface contact –N/A
(4) Nodes to surface contact constraint method–N/A
(5) Automatic nodes to surface contact–N/A
(6) Automatic surface to surface contact –N/A
(7) Rigid-wall surfaces – bottom surface to which cylinder is connected
(8) Solid elements – soil and concrete in model
(9) Beam elements –N/A
(10) Shell elements – cylinder elements
(11) Piecewise linear plasticity material model (with and without rate effects; with and without finite failure strain) – shell elements
(12) Plastic-kinematic material model–N/A
(13) Pseudo-tensor material model- concrete solid elements
(14) EOS tabulated compaction material model – concrete inside cylinder
(15) Flexible to rigid conversion - cylinder will be switched to rigid body before impact
(16) Rigid body motions – cylinder will be switched to rigid body before impact
(17) Elastic deformations – certain cylinder deformations due to loading
(18) Plastic deformations – certain cylinder deformations due to loading
(19) Large deformations – certain cylinder deformations due to loading
(20) Load curves – the load applied is a function of time
(21) Boundary node constraints–N/A
(22) Pressure loads – the load applied is distributed like a pressure load
(23) Gravity loads – the cylinder weight may be applied
(24) Stiffness dampening –N/A
(25) Mass dampening –N/A
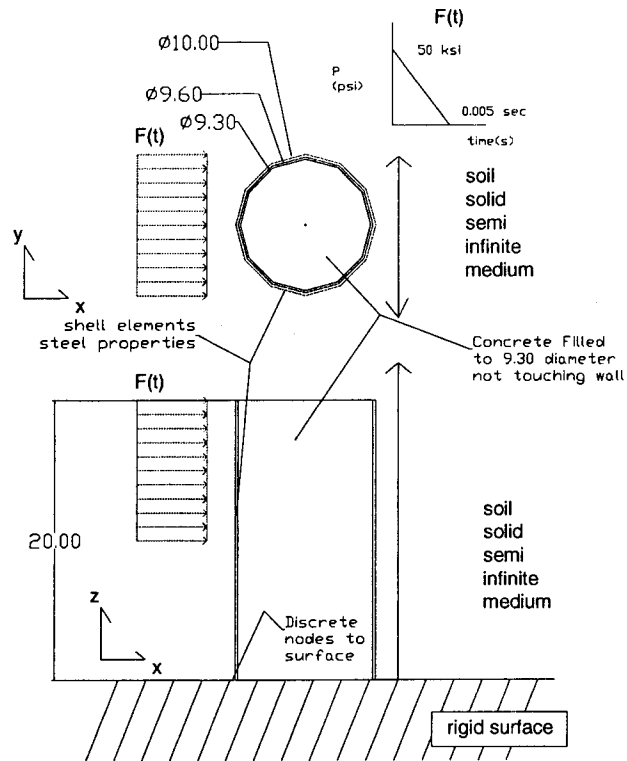(26) Prescribed boundary motion–N/A

Case 4

Figure 4. Case 4

6.4.2 Test Input

Same procedure as Case 1.

6.4.3 Test Procedure

Same procedure as Case 1.

6.4.4 Test Results

Same procedure as Case 1.

6.4.1 Test Case Number 5: Mass Vibrating on Cylinder with Dampening

Case 5 (shown in Figure 5) is a simple case to verify both mass and stiffness dampening are correctly working. The problem consists of a rigid cube mounted on top of a cylinder constructed out of solid elements containing the two dampening properties. The rigid cube is loaded by a large impulse.

(1) Symmetric surface to surface contact–N/A
(2) Discrete nodes to surface contact – cylinder contacting rigid surface
(3) Spot welded nodes surface contact –N/A
(3) Automatic nodes to surface contact–N/A
(4) Nodes to surface contact constraint method–N/A
(5) Automatic surface to surface contact –N/A
(7) Rigid-wall surfaces – bottom surface to which cylinder is connected
(8) Solid elements – block and cylinder
(9) Beam elements –N/A
(10) Shell elements –N/A
(11) Piecewise linear plasticity material model (with and without rate effects; with and without finite failure strain) - cylinder
(12) Plastic-kinematic material model–N/A
(13) Pseudo-tensor material model–N/A
(14) EOS tabulated compaction material model –N/A
(15) Flexible to rigid conversion –N/A
(16) Rigid body motions –N/A
(17) Elastic deformations – certain cylinder deformations due to loading
(18) Plastic deformations –N/A
(19) Large deformations –N/A
(20) Load curves – N/A
(21) Boundary node constraints–N/A
(22) Pressure loads –N/A
(23) Gravity loads –N/A
(24) Stiffness dampening – used in cylinder motions
(25) Mass dampening – used in cylinder motions
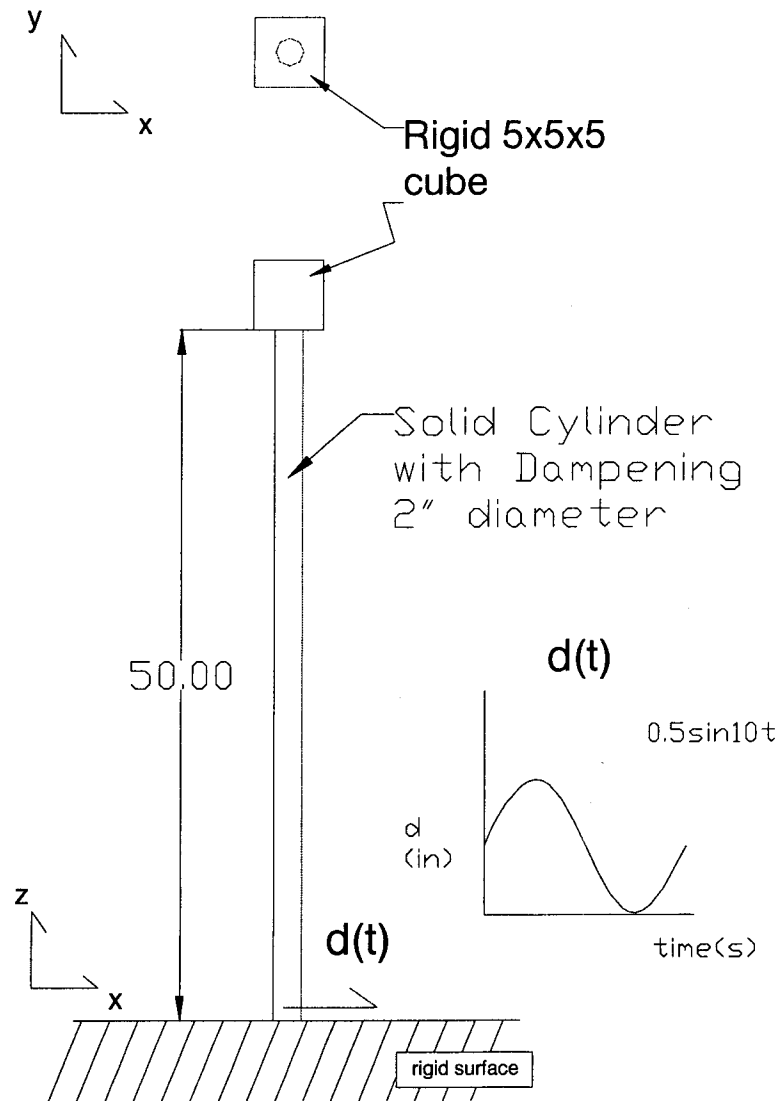(26) Prescribed boundary motion–at the base of the cylinder

Case 5

Figure 5. Case 5

6.4.2 Test Input

Same procedure as Case 1.

6.4.3 Test Procedure

14

Same procedure as Case 1.

6.4.4 Test Results

Same procedure as Case 1.

SOFTWARE VALIDATION FOR
LS-DYNA 960

Prepared for

Prepared by

E.J. Sagebiel
C.J. Waldhart
P.A. Cox

Center for Nuclear Waste Regulatory Analyses
San Antonio, Texas

1 Introduction

A series of numerical simulations have been performed for the Center for Nuclear Waste Regulatory Analyses (CNWRA) using LS-DYNA, a commercial finite element analysis software package. Following CNWRA operating procedures (CNWRA TOP 018), validation of the LS-DYNA computer program for modeling various physical systems is required. To this end, a validation plan was developed entitled "Software validation test plan for ANSYS/LS-DYNA Version 5.7" dated January 18, 2002[1]. This document presents the results of the validation effort.

In the validation plan, five test cases were described that address a wide range of analysis options employed in previous numerical simulations using LS-DYNA at the CNWRA. The features associated with each test case and the report section describing them are presented in Table 1-1. Table 1-2 cross-references the case numbers and title with the report section numbers. Two commercially available finite element codes were utilized for each analysis in the validation process:

> 1.) LS-DYNA[2] version 960 and
>
> 2.) ABAQUS/Explicit[3] (ABAQUS) version 6.2-1.

LS-DYNA 960 is the version of LS-DYNA most commonly used in conjunction with ANSYS/LS-DYNA 5.7 for previous CNWRA analysis. The resulting validation is based on agreement between the solutions provided by the two codes.

During the execution of the validation plan, it was determined that it was not possible to adequately assess the agreement of the solutions using just the five test cases defined in the plan. Additional sub-cases were created to investigate subsets of each test case. For example, one unit case may examine just the input material model for a single element while another may investigate the behavior of spot weld failures in the two codes. Upon completion of the five test cases, several analysis options in the validation plan remained unaccounted for and were addressed separately. These analysis options included:

- Strain-rate dependent plasticity,
- Strain failure of elements, and
- Deformable to rigid body conversion.

The first two options were examined in both ABAQUS and LS-DYNA. The last option was performed only in LS-DYNA because ABAQUS does not support an equivalent option. As such, the validation of the LS-DYNA deformable to rigid conversion option was accomplished independently from ABAQUS by utilizing previously validated analysis options associated with deformable bodies.

---

[1] E.Sagebiel, "Software validation test plan for ANSYS/LS-DYNA Version 5.7", January 18, 2002

[2] Livermore Software Technology Corporation, Livermore, CA, United States of America

[3] ABAQUS, Inc. (formerly Hibbitt, Karlson, and Sorensen, Inc.), Pawtucket, RI, United States of America

Several options outlined in the validation plan were not addressed in either LS-DYNA or ABAQUS:

- Equation of state (EOS) tabulated compaction material model,
- Stiffness damping, and
- Beam-to-beam contact.

The EOS material model present in ABAQUS does not employ comparable inputs to that in LS-DYNA. Without a comparable material model, it is not possible to make a fair comparison between the analysis codes. Stiffness damping in both codes was examined briefly; however, it was determined for the cases being considered that stiffness damping did not introduce significant variations in the model response in either finite element code. Lastly, beam-to-beam contact options were not addressed because the version of ABAQUS used to conduct the validation does not support this type of contact.

When taken together, the five initial test cases, the sub-cases, and the additional analyses provide a basis for validating portions of the LS-Dyna code against the ABAQUS code, which has been previously validated by the CNWRA. Before performing more analyses with LS-Dyna, users should consult the validation plan and results to verify that their intended use will be covered by the validation.

Table 1-1. Validation Analysis Features Outline

Feature	Case	1	2	3	4	5	6	7	8	9	10	11
	Section	2	3	4	5	6	5	2	3	7	7	8
Shell elements		X	X	X	X			X	X	X	X	
Elastic, perfectly plastic material		X	X	X	X		X	X				X
Elastic deformations		X	X	X	X	X	X		X			
Plastic deformations		X	X	X	X		X	X		X	X	
Large deformations		X	X	X	X	X		X		X	X	
Load curves		X	X	X	X	X	X	X	X			
Boundary node constraints		X	X	X	X		X	X	X	X	X	
Pressure loads		X	X	X	X							
Spot welds				X					X			
Surface to surface contact				X	X							X
Surface to node contact					X							
Beam elements					X							
Solid elements					X	X	X					
Prescribed boundary motion					X		X	X		X	X	
Rigid elements					X							
Mass damping							X					
Multi-linear, isotropic hardening material model										X		
Strain-rate dependent material										X		
Strain failure criterion											X	
Rigid body motion												X
Deformable to rigid conversion												X
Gravity					X							

Table 1-2. Section/ Case Cross Reference

Description	Case Number	Section Number
Cylinder Under Transient Pressure Loads	1	2
Concentric Cylinders with Spotweld Channel Sections	2	3
Cylinder Beam Interactions	3	4
Partially Filled Cylinder Impacting Wall	4	5
Pendulum/ Dampening Problem	5	6
Single Solid Element	6	5
Single Shell Element	7	2
Spotweld Problem	8	3
Shell with Strain Rate Dependant Material Model	9	7
Shell with Strain Failure Material Model	10	7
Deformable to Rigid Problem	11	8

2 Cylindrical Shell Under Applied Lateral Pressure (Case 1)

Case 1 examined the effect of a large lateral pressure applied to a thin walled, cylindrical shell. The applied loading induced significant yielding of the structure and resulted in large deformations.

2.1 Geometry

This simulation consisted of a cylinder 20 inches tall, 4.9 inch radius, and a thickness of 0.2 inches. The bottom nodes of the cylinder are fixed in space from all translations and rotations while an inward facing pressure is applied at the top of the cylinder.

2.2 Material Definition

An elastic, perfectly plastic material defined in Cauchy stress-logarithmic strain space was used in both codes:

- Elastic modulus of 30×10^6 psi,
- 0.333 Poisson's ratio,
- Density of 7.40×10^{-4} lb sec^2 in^{-4}, and
- Yield stress of 45,000 psi.

2.3 Element Selection

The elements selected for this portion of the validation effort were chosen with the following characteristics in mind:

- Capable of addressing moderately thick shells,
- Handling large deformations, and
- Developing finite strains.

The description of single element loading comparisons between the ABAQUS S4R and LS-DYNA Belytschko-Tsay shell elements used for Case 1 are presented in Section 2.3.1.

2.3.1 Single Shell Element Unit Problem (Case 7)

The first step in verifying the Case 1 analyses was to perform single element studies in both ABAQUS and LS-DYNA. This isolated several key features needed in the Case 1 model: the elastic, perfectly plastic material definition defined in Section 2.2 and the ability of the shell formulation to handle both axial and bending loading conditions.

2.3.1.1 Geometry

The single shell element geometry was defined to be:

- 1.0-inch by 1.0-inch square and
- Uniform thicknesses of 0.05, 0.10, or 0.20 inches were evaluated.

2.3.1.2 ABAQUS S4R Shell Element

The S4R shell was used in the ABAQUS single shell analyses. This is a four-noded, reduced integration shell element capable of addressing thick or thin shells and it is suitable for large-strain analyses as it can account for finite membrane strains and large rotations. The use of the *SHELL SECTION option calculated cross-sectional behavior for each element based on numerical integration thereby permitting the requisite nonlinear material model behavior to occur.

2.3.1.3 LS-DYNA Belytschko-Tsay Element

The default shell element is the Belytscko-Tsay shell element that is based on a combined co-rotational and velocity-strain formulation. Lobatto integration was used so stresses and strains could be easily extracted from the outer surfaces of the shell.

LS-DYNA offers several different shell formulations including the following (numbering is not sequential but rather refers to the input card in LS-DYNA):

1)   Hughes-Liu,

2)   Belytschko-Tsay,

6)   S/R Hughes-Liu,

7)   S/R co-rotational Hughes-Liu,

8)   Belytschko-Leviathan shell,

10)   Belytschko-Wong-Chiang,

11)   Fast (co-rotational) Hughes-Liu, and

16)   Fully integrated shell element.

The Belytschko-Tsay, type 2 element was selected for this single element model. This element is a reduced integration element based on a combined co-rotational and velocity-strain formulation. While only the Belytscko-Tsay, type 2 element was used in this single element model, Case 1 utilized all of the element types listed above in this validation study to examine the effects of element formulation on the solution and subsequently on the agreement between ABAQUS and LS-DYNA.

2.3.1.4 Loading Conditions

Two different cyclic loading conditions were examined:

1) Axial extension-compression and

2) Out-of-plane bending.

2.3.1.5 Axial Extension-Compression On Single Shell Element

2.3.1.5.1 Applied Loading and Boundary Conditions

The boundary conditions for the axial extension-compression shell model are shown in Figure 2-1.

$u_y = 0.15 \sin(500t)$

No out of plane displacement

All nodal rotations = 0 radians

Y

X
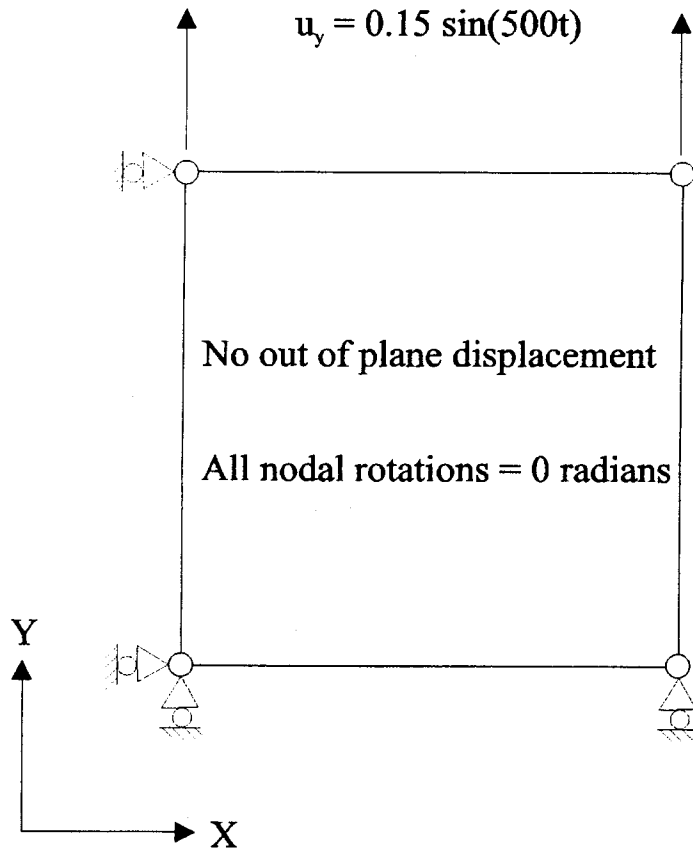
Figure 2-1. Model boundary conditions for single shell element uniaxial extension-compression.

The boundary conditions applied are as follows:

Node at (0.0, 0.0, 0.0): $u_x = u_y = u_z = 0.0$ inches

$\theta_x = \theta_y = \theta_z = 0.0$ radians

Node at (1.0, 0.0, 0.0): $u_y = u_z = 0.0$ inches

$\theta_x = \theta_y = \theta_z = 0.0$ radians

Node at (0.0, 1.0, 0.0): $u_x = u_z = 0.0$ inches

$u_y = 0.15 \sin(500t)$ inches

$\theta_x = \theta_y = \theta_z = 0.0$ radians

Node at (1.0, 1.0, 0.0): $u_z = 0.0$ inches

$u_y = 0.15 \sin(500t)$ inches

$\theta_x = \theta_y = \theta_z = 0.0$ radians

For the nodes with a non-zero u_y, the sine function is defined using a tabular sequence of 31 pairs of equally spaced values out to 0.21 seconds. The displacement was then varied linearly between each increment during the analyses resulting in a multi-linear approximation to the desired sine wave.

7

2.3.1.5.2 Axial Extension-Compression Results

A 0.10-inch thick shell subjected to the loadings in Section 2.3.1.5.1 was analyzed using ABAQUS and LS-DYNA. Two results components will be examined:

- Mid-plane strain in the y direction and

- Mid-plane stress in the y direction.

Because the model is free to expand or contract in the x or z directions, no normal stresses will be developed in these directions. Likewise, the x and z strains caused by Poisson's contraction and expansion can be inferred by examining the agreement in the normal stress oriented in the y direction because it is affected by all strain components.

The mid-plane strains in the y direction for the single shell element under the applied cyclic displacement as calculated by ABAQUS and LS-DYNA are shown in Figure 2-2.
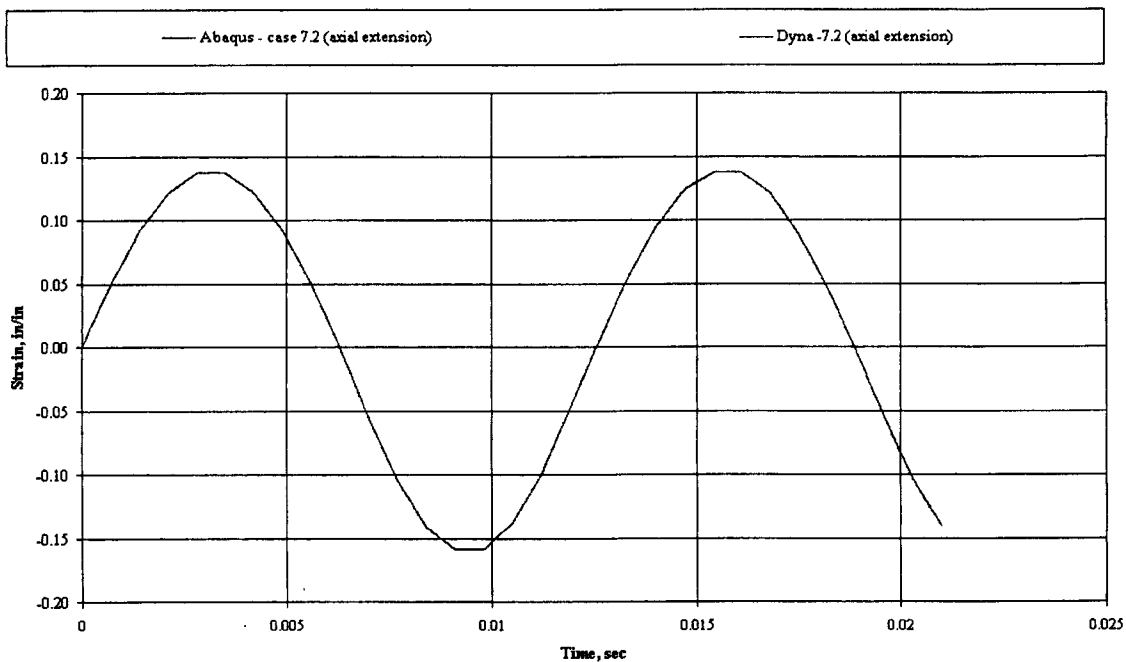
Figure 2-2. Mid-plane strain in y direction versus time for cyclic extension-compression of single shell element.

The reason that the maximum strains observed in Figure 2-2 are not equivalent to the maximum applied nominal strain of 0.15 in/in is that both ABAQUS and LS-DYNA report logarithmic strains:

$$\varepsilon_{\ln} = \ln(1 + \varepsilon_{nom}).$$
Eqn 3-1

This results in the logarithmic strains being slightly smaller in magnitude than the nominal strain for tension and slightly larger in compression. Excellent agreement is observed between the ABAQUS and LS-DYNA solutions throughout the entire load history examined.

Mid-plane y stress is plotted against time in Figure 2-3.

8
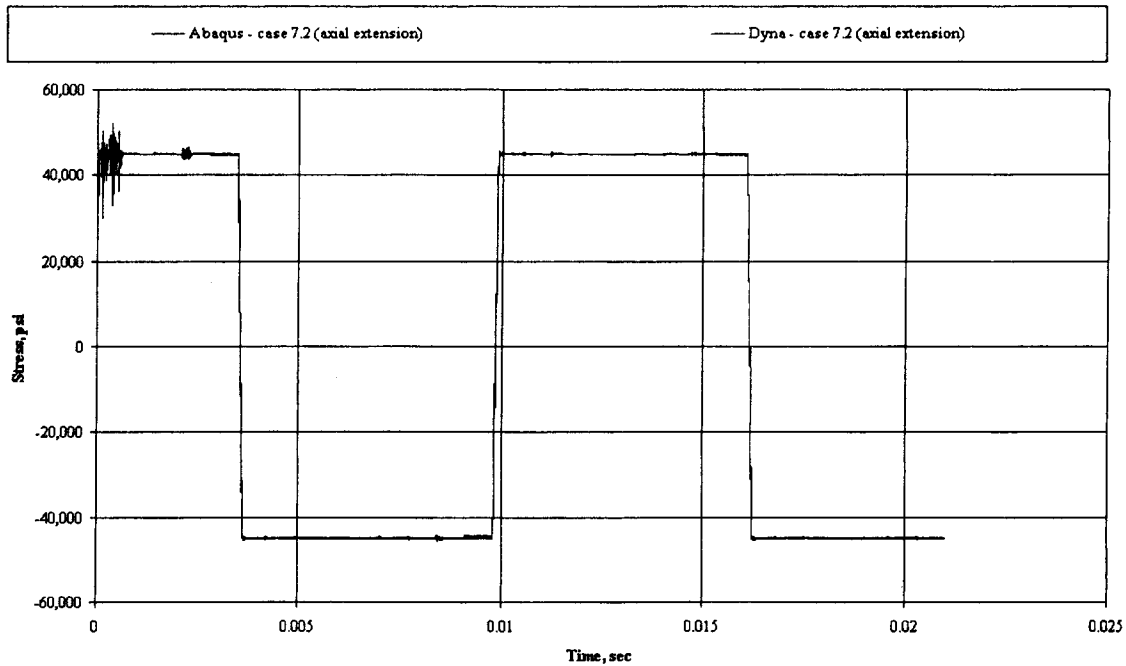
Figure 2-3. Mid-plane stress in y direction versus time for cyclic extension-compression of single shell element.

As expected from the excellent agreement observed with the y direction strains, the stresses are also similar. In each case the shell element rapidly reaches its elastic limit (45,000 psi), at which no further stresses can be accommodated. The primary difference between the two codes exists at the initial loss of stiffness associated with the onset of perfectly plasticity. In this case, the ABAQUS solution shows oscillations in the stress value both above and below the anticipated stress levels.

An investigation into the source of the variations between the two codes focusing on the analysis time steps for each code was performed. The results presented in Figure 2-3 utilized a 4.0×10^{-6} second time step in ABAQUS and a smaller increment of 2.3×10^{-6} seconds in LS-DYNA. Since the LS-DYNA solution did not encounter as large an oscillation as ABAQUS, a smaller time increment was used in ABAQUS through the following command:

*DYNAMIC,EXPLICIT, Fixed Time Incrementation, Scale Factor=0.2

The presence of the smaller time step in ABAQUS virtually eliminated the stress oscillations. An inverse tact was taken in LS-DYNA where the time step was increased to approximately 4.0×10^{-6} seconds, inline with the baseline time step in ABAQUS. Despite increasing the time step by almost a factor of two, no noticeable variation in stress was observed in the stress calculated by LS-DYNA.

Overall, excellent agreement was obtained between the ABAQUS and LS-DYNA single shell element models subjected to cyclic axial loading. There was some unanticipated oscillations in the calculated stress in the ABAQUS solution however they were not deemed to be a critical issue at this point.

9

2.3.1.6 Out-Of-Plane Bending On Single Shell Element

2.3.1.6.1 Out-Of-Plane Bending Applied Loading

Using the same element presented in Figure 2-1, the applied boundary conditions are as follows:

Node at (0.0, 0.0, 0.0):	$u_x = u_y = u_z = 0.0$ inches
	$\theta_x = \theta_y = \theta_z = 0.0$ radians
Node at (1.0, 0.0, 0.0):	$u_y = u_z = 0.0$ inches
	$\theta_x = \theta_y = \theta_z = 0.0$ radians
Node at (0.0, 1.0, 0.0):	$u_x = 0.0$ inches
	$\theta_y = \theta_z = 0.0$ radians
	$\theta_x = 0.15 \sin(500t)$ radians
Node at (1.0, 1.0, 0.0):	$\theta_y = \theta_z = 0.0$ radians
	$\theta_x = 0.15 \sin(500t)$ radians

Defining the shell rotations in this manner allows the plate to develop curvature about only the x axis. As with the axial extension-compression case, the sine function was approximated with 31 pairs of equally spaced time-rotation pairs out to 0.21 seconds. The applied rotations in the analyses were then linearly interpolated between the input pairs.

2.3.1.6.2 Out-Of-Plane Bending Results

Unlike the axial extension-compression loading case, three different thickness were examined under the in-plane bending loading condition: 0.05, 0.10, and 0.20 inches to determine the presence of any thickness dependencies. The shell thicknesses used for the different analyses are summarized in Table 2-1.
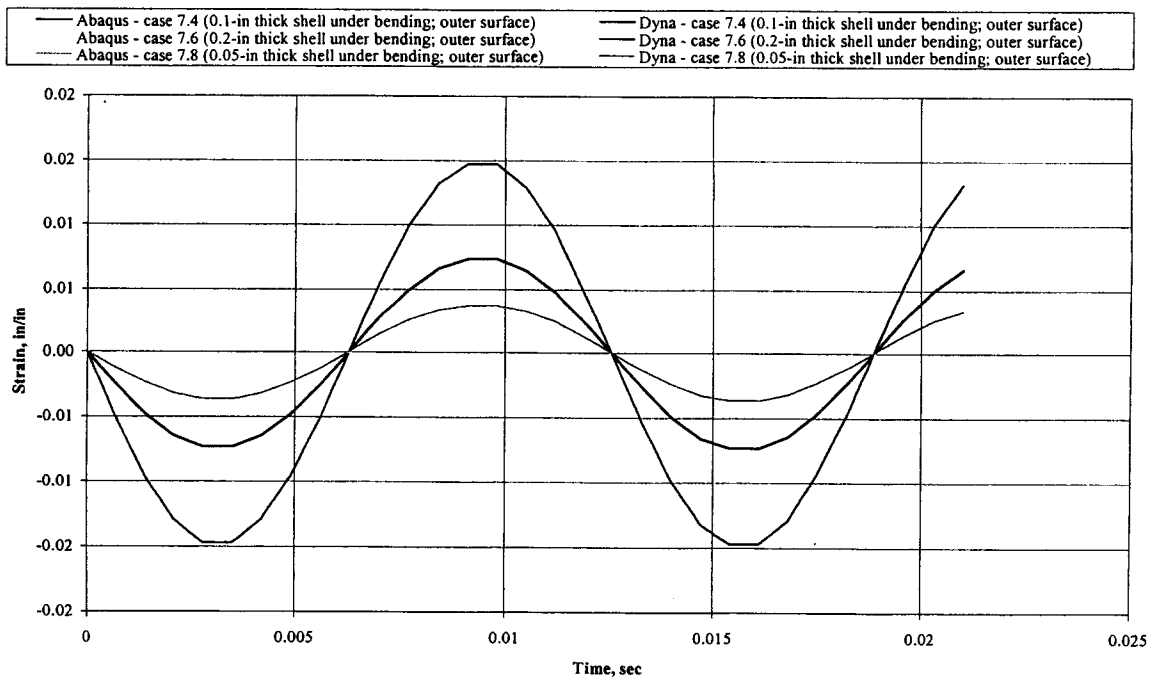
Table 2-1. Wall Thickness for Cyclic Bending Analyses

Case	Shell Thickness (in)
7.4	0.10
7.6	0.20
7.8	0.05

The axial stress and strain versus time are plotted for the three cases identified in Table 2-1 in Figure 2-4 and Figure 2-5, respectively.
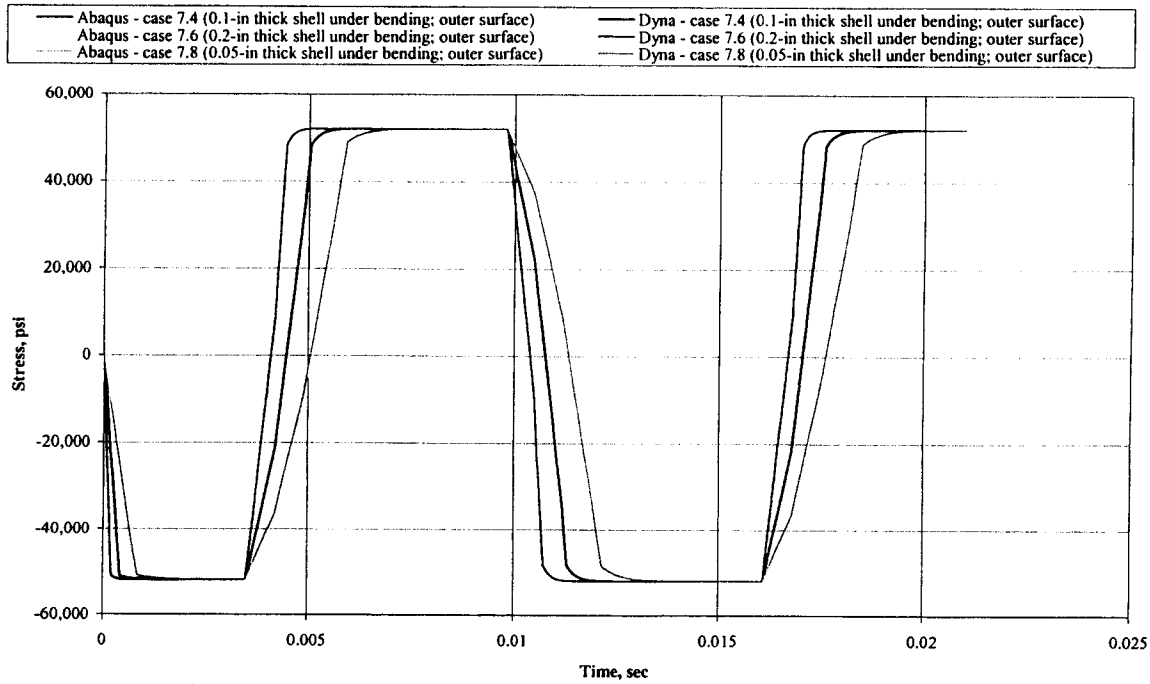
Figure 2-4. Positive surface stress in y direction versus time for cyclic bending of single shell element.

Figure 2-5. Positive surface strain in y direction versus time for cyclic bending of single shell element.

11

In Figure 2-4, all the surface stresses for a given element thickness are virtually identical for the two codes. Another important point is that the ABAQUS stress results for the bending load case do not experience the oscillations at the onset of perfect plasticity observed in the axial extension-compression case. This is a result of the cross section gradually losing stiffness with increasing load as opposed to the instantaneous yielding of the entire cross section under axial loading. As expected from the stress results, Figure 2-5 shows excellent agreement in the strains as well between the two codes.

2.3.1.7 Single Element Conclusion

Based on the single element cases examined, both LS-DYNA and ABAQUS appear to offer excellent agreement for the applied loading conditions and material properties. As such, the S4R and Belytscko-Tsay elements were utilized in ABAQUS and LS-DYNA, respectively, for Case 1 simulations.

2.4 Case 1 Loading Conditions

The displacement boundary conditions applied to the cylindrical model described in Section 2.1 fixed the base of the cylinder from displacing in all degrees of freedom (translation and rotation).

A pressure load was applied to the cylinder from h=10 to 20 inches around a 60 degree arc of the cylinder as shown in Figure 2-6. The pressure magnitude and corresponding time interval are described in Table 2-2.
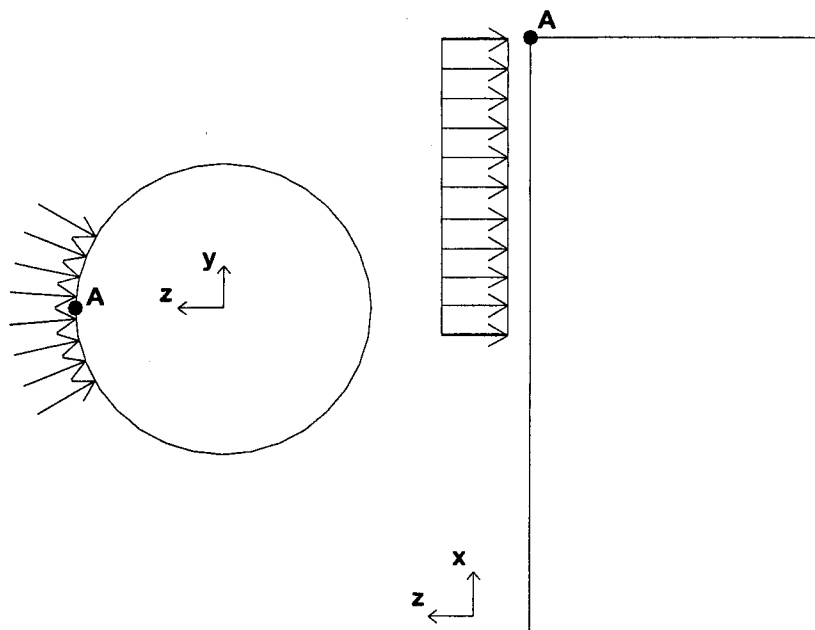
Figure 2-6. Pressure loading applied to Case 1 cylinder (note that the cylinder is clamped at x = 0.0).

Table 2-2 Case 1 Lateral Pressure Loading

| Time (s)	Pressure (psi)
0	0
2.5×10^{-5}	40
5.0×10^{-5}	100
2.5×10^{-4}	200
5.0×10^{-4}	400
5.0×10^{-3}	400
1.0	400

2.5 Case 1 Mesh Density Convergence Study

Prior to presenting the results, a brief study was performed to assess the effect of mesh densities on the calculated results. This study would indicate if a comparable mesh density in ABAQUS and LS-DYNA offers the same degree of convergence for a solution. Table 2-3 indicates the four different mesh densities that were examined in LS-DYNA.

Table 2-3 LS-DYNA Mesh Densities Used for Case 1

Model Designation (Order of Increasing Refinement)	Mesh Density (elements in axial by circumferential))
1.22	20 x 24
1.21	40 x 48
1.20	80 x 96
1.23	160 x 192

In each model, the number of elements is doubled in both the axial and circumferential directions.

The convergence criteria for each code being examined will be the lateral deflection of the top node centered about the pressure loading (largest deformation in the model), i.e. point A in Figure 2-6. The resulting displacement versus time plots obtained from the four cases are shown in Figure 2-7 for both ABAQUS and LS-DYNA.

13
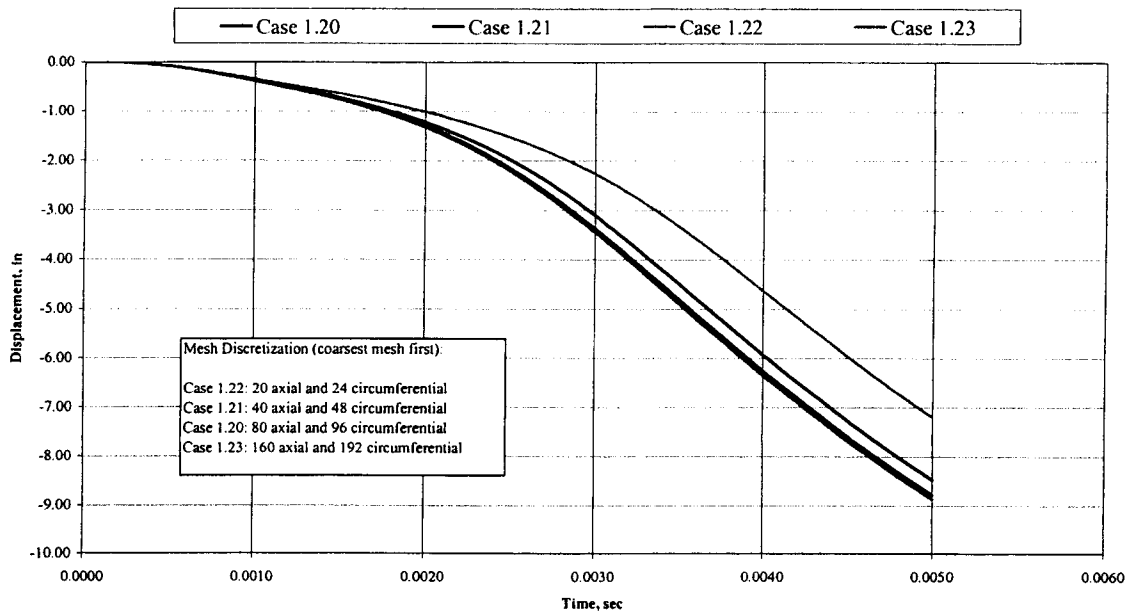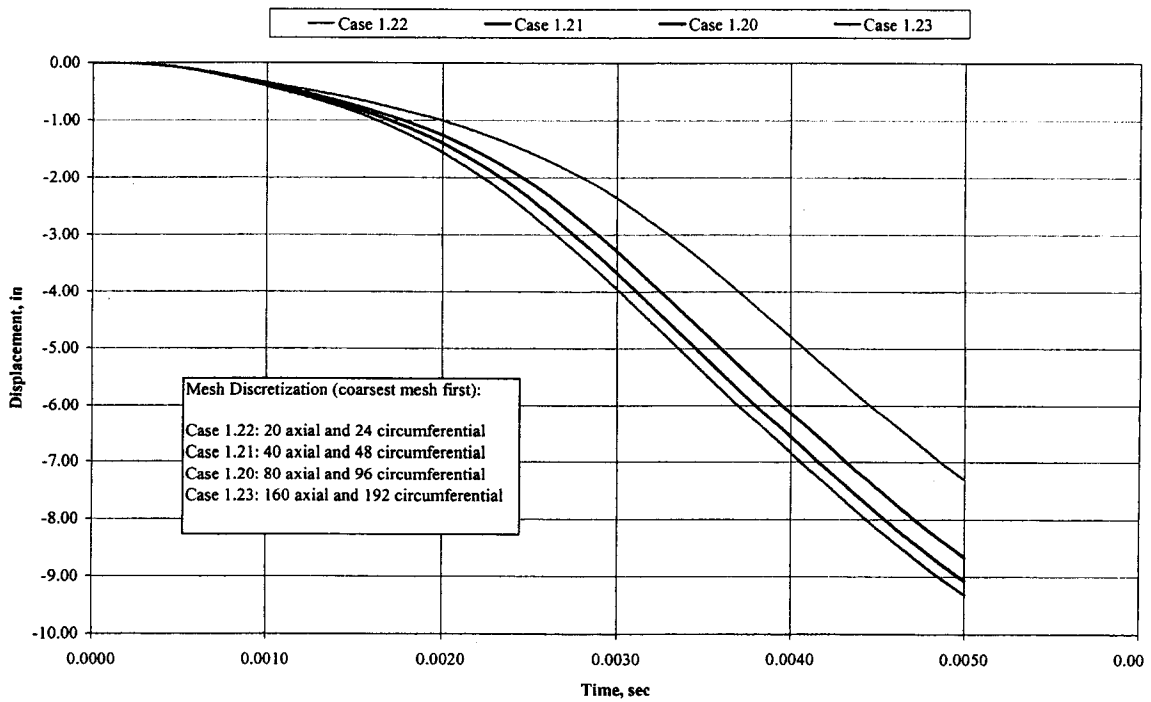
(a) ABAQUS

(b) LS-DYNA

Figure 2-7. Convergence of lateral deflection at point A versus time for Case 1 solution in ABAQUS and LS-DYNA.

14

Similar trends are observed in the lateral deflection of point A for the mesh refinements in both ABAQUS and LS-DYNA:

- Variation between subsequent mesh refinements in a given code decrease with increasing mesh density

- Mesh refinement creates a more flexible system

Table 2-4 summarizes the lateral deflection of point A at 0.005 seconds (maximum deflection reached during analyses).

Table 2-4 Case 1 Point A Lateral Deflection at 0.005 Seconds

Model	ABAQUS		LS-DYNA	
	Deflection	Δ%	Deflection	Δ%
1.22	-7.2025	-15.0	-7.3185	-15.5
1.21	-8.4785	-3.50	-8.6659	-4.48
1.20	-8.7857	-0.98	-9.0719	-2.60
1.23	-8.8727	N/A	-9.3145	N/A

$$\Delta\% = \frac{\delta_{coarse} - \delta_{refined}}{\delta_{refined}} \times 100.$$

The rate of convergence for the lateral deflection is comparable in ABAQUS and LS-DYNA. Based on small relative change, less than 3.0 percent, in the lateral deflection of point A for both codes, it was decided that the 80 axial element and 96 hoop element mesh present in model 1.20 could be considered to be converged. A comparison of the lateral deflection of point A for the converged solution (model 1.20) is presented in Figure 2-8.
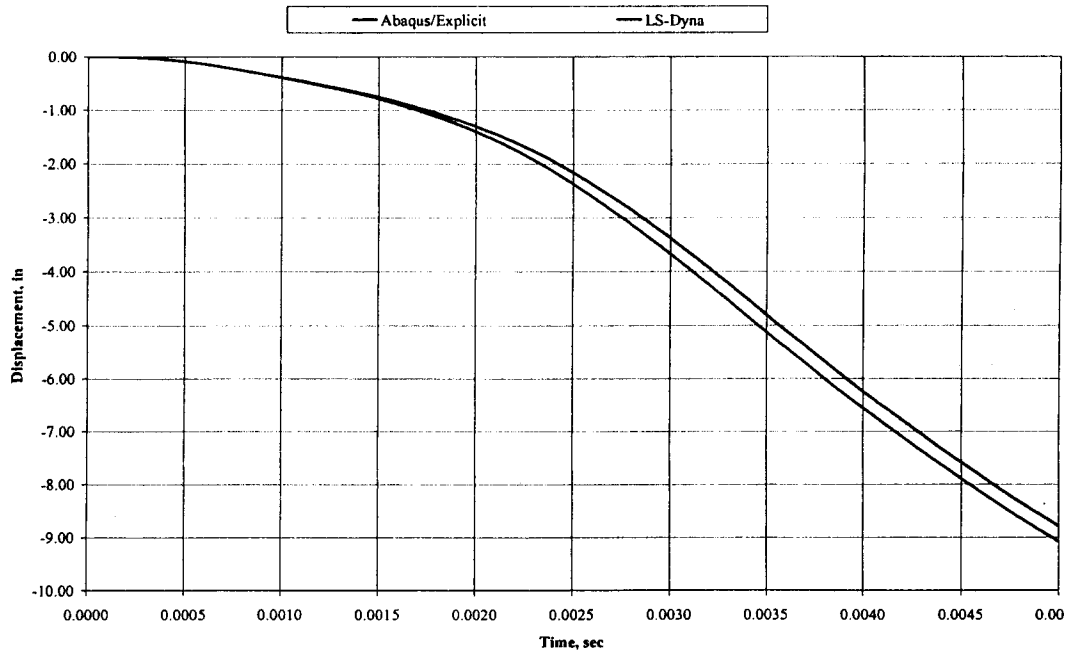
Figure 2-8. Point A lateral deflection versus time for Case 1 converged solutions.

After 0.0025 seconds and approximately 2.25 inch deflection, the curves are almost parallel, i.e. the offset introduced remains essentially constant.
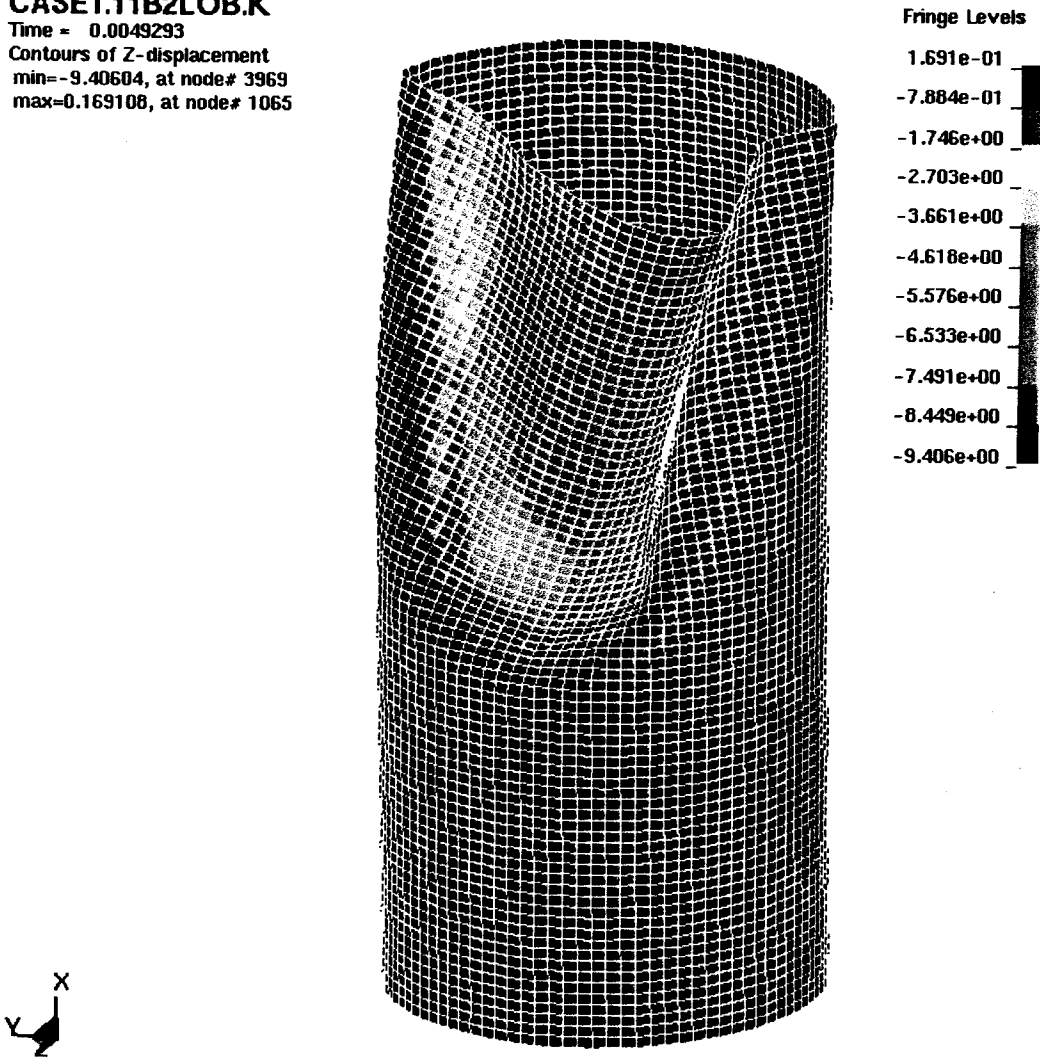
2.6   Case 1 Results Comparison

Two results will be compared for the analyses at the cylinder top at the center of pressure loading (Point A in Figure 2-6):

- Lateral deflection and
- Hoop strain.

Together, these results give an overall indication of the correlation between responses of the two analysis codes.

The resulting deformation, shown in Figure 2-9, indicated that a large dent was developed at the top of the cylinder due to the lateral pressure.

CASE1.11B2LOB.K
Time = 0.0049293
Contours of Z-displacement
min=-9.40604, at node# 3969
max=0.169108, at node# 1065

Fringe Levels

1.691e-01

-7.884e-01

-1.746e+00

-2.703e+00

-3.661e+00

-4.618e+00

-5.576e+00

-6.533e+00

-7.491e+00

-8.449e+00

-9.406e+00

X
Y

**Figure 2-9. Case 1 deformed shape (fringe values of z displacement in inches).**

The lateral deflection versus time plot for the Case 1 solutions of ABAQUS and LS-DYNA (case designations provided in Table 2-5) are indicated in Figure 2-10 with the hoop strain versus time provided in Figure 2-11.

17

Table 2-5 Case 1 Model Designations for LS-DYNA

Label	Shell Type
dyna1.11b_1	Hughes-Liu
dyna1.11b_2	Belytschko-Tsay
dyna1.11b_6	S/R Hughes-Liu
dyna1.11b_7	S/R co-rotational Hughes-Liu
dyna1.11b_8	Belytschko-Leviathan shell
dyna1.11b_10	Belytschko-Wong-Chiang
dyna1.11b_11	Fast (co-rotational) Hughes-Liu
dyna1.11b_16	Fully integrated shell element
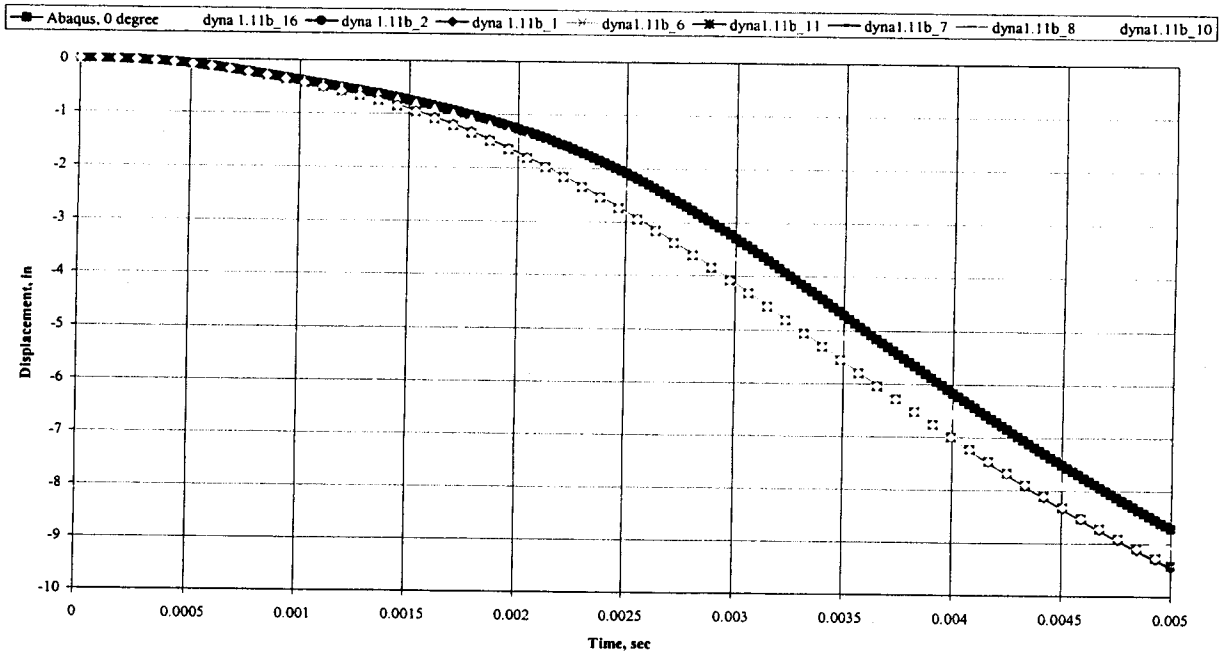
Figure 2-10. Lateral deflection versus time for Case 1 at cylinder top at center of applied pressure.
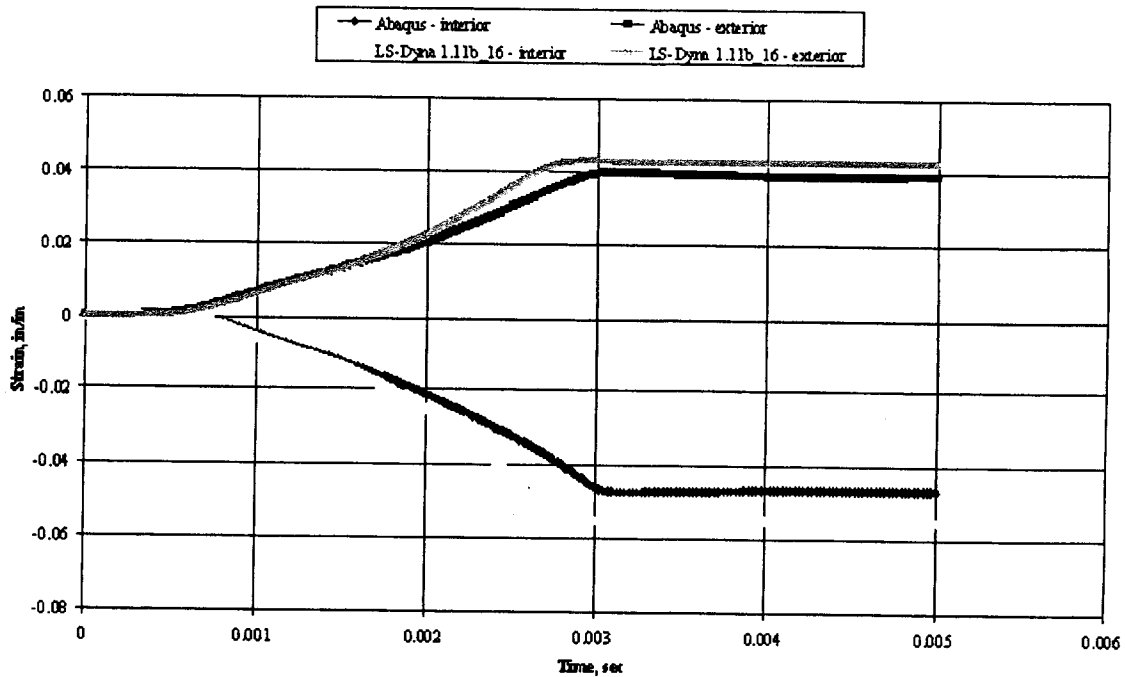
Figure 2-11. Hoop strain versus time for Case 1 at cylinder top at center of applied pressure.

After the pressure load reached its maximum value of 400 psi at 0.0005 seconds, the cylinder continued to buckle despite no additional load being applied. Figure 2-10 shows the different shell element types tried and the resulting deformation. The designations in Figure 2-10 are

19

according to shell type as listed for LS-DYNA on page 5. Even though many different shell elements were evaluated in this case, the fully integrated shell element (#16) gave the best correlation with ABAQUS results, which is in agreement with the single element studies described in Section 2.3. All other LS-DYNA shell elements are in good agreement with each other and are seen to be more flexible than the fully integrated shell (#16) and the ABAQUS SR4 shell elements; however, all of the other shell elements are much less expensive in terms of solution time than the fully integrated shell.

An interesting feature in Figure 2-11 is that both the ABAQUS and LS-DYNA hoop strains essentially become constant after approximately 0.003 seconds. This result is consistent with the deformed shape that tends to indicate a minimal change in the local curvature after that time. Without changes in curvature or membrane straining action, there is not a mechanism for altering the hoop strain.

In both figures, ABAQUS has smaller lateral deflection and smaller hoop strains. When taken together, these results indicate that the ABAQUS analysis represents a slightly stiffer system. Due to the complexity of the system, it is not possible to discern whether the result is caused by factors such as the plasticity progression through the cross section, solution quality (despite using comparable time steps and mesh densities), or another similar factor. Despite these variations, the magnitude and shape of the displacement and strain curves are similar to each other.
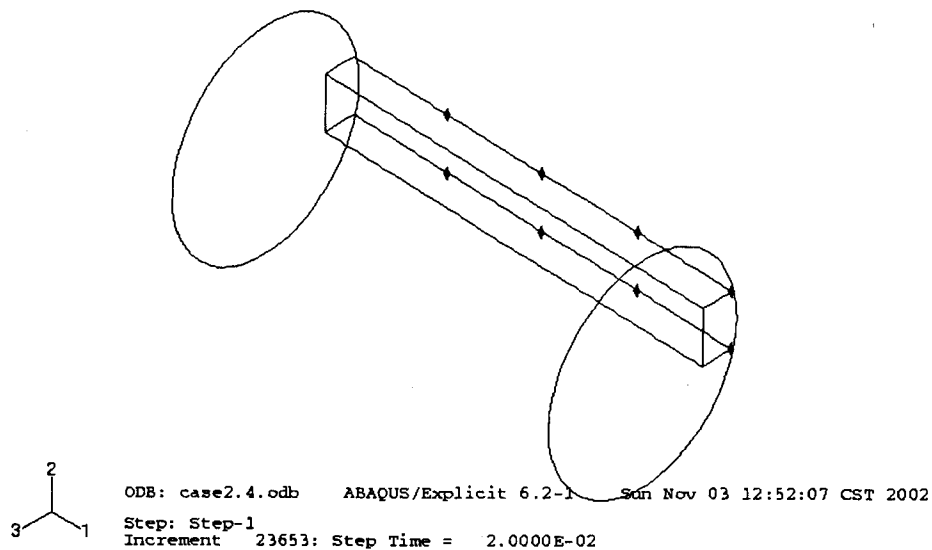
2.7 Case 1 Conclusions

The Case 1 model consisting of a cylindrical shell model subjected to lateral pressure was created in both ABAQUS and LS-DYNA. Based on the anticipated requirements for large deformations resulting from the applied load, a series of single element models were used to assess the performance of the pertinent ABAQUS and LS-DYNA shell elements. Following the excellent agreement between these single element models, the Case 1 model was run. The general trends were present in both analysis codes with the LS-DYNA model offering consistently more flexible responses.

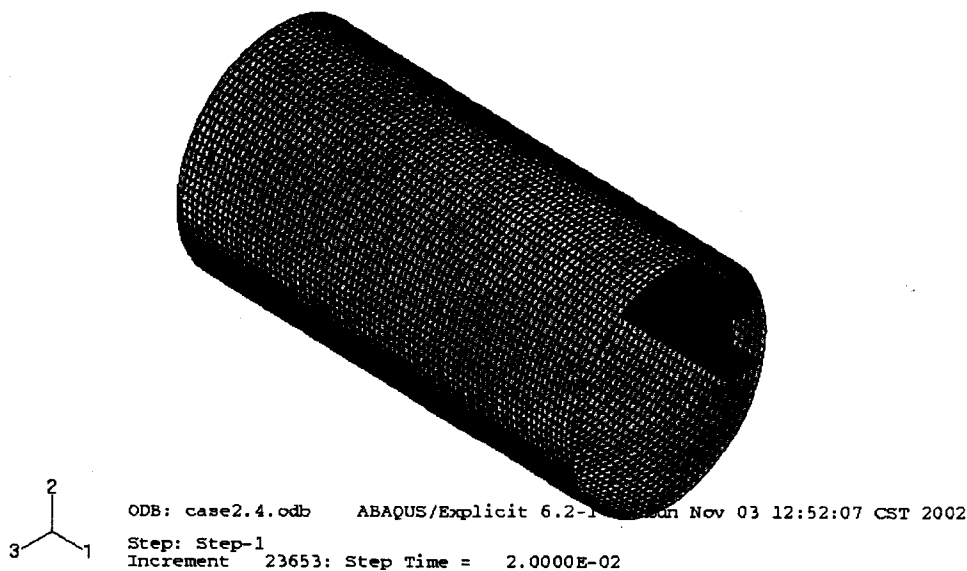# 3 Concentric Cylinders with Spot Welded Channel Section (Case 2)

The Case 2 model consisted of two concentric, thin-walled steel cylinders with a channel section spot welded to the outer cylinder placed between them. The primary features being addressed in Case 2 are the surface contact algorithms and spot weld capabilities.

3.1 Geometry

The outer cylinder in Case 2 had a 4.90-inch mean radius, 0.20-inch thickness, and a height of 20 inches. A channel section with a 2.5 inch web and 1.5 inch flanges was spot welded to the outer cylinder at 8 locations (4 on each side) at 5.00-inch increments along the outer cylinder's length. A geometry schematic with corresponding finite element mesh is shown in Figure 3-1.

ODB: case2.4.odb   ABAQUS/Explicit 6.2-1   Sun Nov 03 12:52:07 CST 2002
Step: Step-1
Increment   23653: Step Time =   2.0000E-02

(a) Case 2 schematic showing external cylinder, internal channel, and spot welds (diamond markers)

ODB: case2.4.odb   ABAQUS/Explicit 6.2-1   Sun Nov 03 12:52:07 CST 2002
Step: Step-1
Increment   23653: Step Time =   2.0000E-02

(b) Case 2 mesh

Figure 3-1. Case 2 geometry schematic and finite element mesh.

3.2   Material Definition

An elastic, perfectly plastic material was used in both codes:

- Elastic modulus of 30×10^6 psi,
- 0.333 Poisson's ratio,
- Density of 7.40×10^{-4} lb sec^2 in^{-4}, and
- Yield stress of 45,000 psi.

21

3.3 Element Formulation

The elements selected for this portion of the study were chosen with the following characteristics in mind:

- Capable of addressing moderately thick shells,
- Handling large deformations,
- Developing finite strains,
- Accommodate spot welds, and
- Accommodate contact surfaces.

The S4R element in ABAQUS and the fully integrated shell element (#16) in LS-DYNA utilized in Case 1 (see Section 2.3) met all of these requirements.

3.4 Spot Weld Interaction

One of the key features present in Case 2 is the use of spot welds to join the outer cylinder to the channel. The key spot weld issues examined were the initial load input into the welds and the failure behavior after exceeding certain thresholds. As such, a series of unit problems were created consisting of two shell element groups joined by spot welds at their corners subjected to normal, shear, and multi-axial loading.

The discussion that follows will summarize how the spot welds are formulated in each analysis code, the spot weld models, and, finally, a series of unit problems examining the effect of different loading and spot weld strength scenarios.

3.4.1 Spot Weld Formulation

A brief summary of the spot weld formulations in ABAQUS and LS-DYNA will be presented next. There are subtle differences between the two codes, primarily in the spot weld failure definition.

3.4.1.1 Spot Weld Formulation in ABAQUS

Spot welds in ABAQUS are considered a type of mechanical interaction that couples translational degrees of freedom at various locations between two different surfaces. The welds themselves are assumed to be sufficiently small so that no torque or moment can be transmitted and, hence, no rotational stiffness is present at the weld.

Simple failure mechanisms can be included in the spot weld definitions based on the load carried in the joint:

$$\left(\frac{\max(F^n, 0)}{F_f^n}\right)^2 + \left(\frac{F^s}{F_f^s}\right)^2 \leq 1.0$$

where: F^n = normal force,

F^s = shear force,

F_f^n = normal failure force, and

F_f^s = shear failure force.

Eqn 3-1

During some spot weld analyses, significant noise may be observed in the normal and shear forces calculated for the weld. The analyses in these cases may indicate failure of the spot weld whereas a filtered solution might indicate that the strength capacity of the weld has not been reached. Rather than implementing a filter on the solution, ABAQUS provides various post-failure options to address how the spot weld behaves after exceeding its maximum load carrying capacity. However, these features were not addressed in this effort.

3.4.1.2 LS-DYNA

The spot weld used for the LS-DYNA simulations was the *CONSTRAINED_GENERALIZED_WELD_SPOT formulation. In this option the spot weld acts like a massless rigid beam that can connect two non-contiguous nodal pairs. Therefore, nodal rotations and displacements are coupled until the weld breaks. Simple failure mechanisms can be included in the spot weld definitions based on the load carried in the joint:

$$\left(\frac{|f_n|}{S_n}\right)^N + \left(\frac{|f_s|}{S_s}\right)^M \leq 1.0$$

where: f_n = normal force,

f_s = shear force,

S_n = normal failure force

S_s = shear failure force

N = exponent on normal force ratio

M = exponent on shear force ratio.

Eqn 3-2

For the analysis N and M were set equal to 2 to allow for a direct comparison between LS-DYNA and ABAQUS. LS-DYNA also allows solution filtering and plastic strain limits before the weld fails to stabilize the solution. These later options were not used in the final comparison.

3.4.2 Spot Weld Unit Problem (Case 8)

In order to assess the agreement between the two finite element codes handling of spot weld interaction, a unit problem was created that minimized the complexity inherent in spot weld analyses and permitted the isolation of normal and shear failure modes as well as progressive failure of a series of spot welds.

3.4.2.1 Spot Weld Unit Problem Geometry

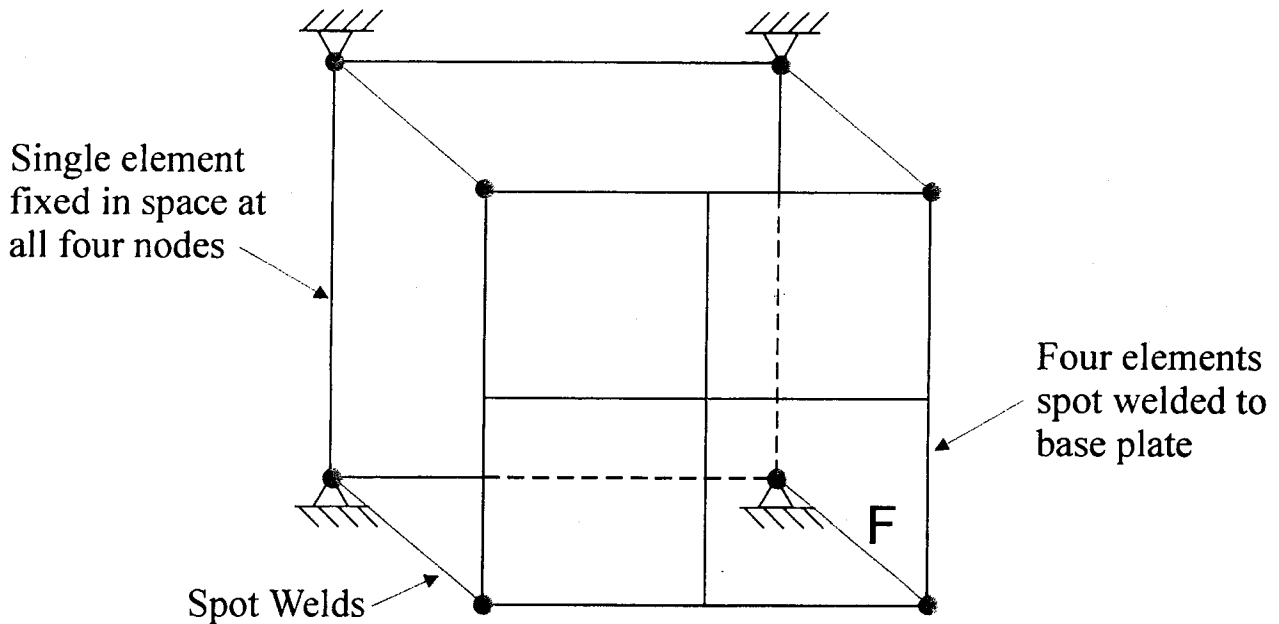The base configuration is shown in Figure 3-2.

Figure 3-2. Case 8 spot weld unit problem schematic.

The base configuration consisted of a single 2.00-inch square shell element fixed in space at all four corner nodes so that no translations or rotations were permitted. A second group of four coplanar shells was placed in front of the fixed shell as shown in Figure 3-2. Unless noted, the shell thickness was 0.5 inches. Spot welds of varying strength were placed between the 8 corresponding nodes of the front and back shells. The loading was applied at the center of the four coplanar elements. In the case of Figure 3-2, a normal load is applied.

3.4.2.2 Spot Weld Unit Problem Material Definition

For all the unit spot weld problems examined, an elastic material was used in both codes:

- Elastic modulus of 30×10^6 psi,
- 0.333 Poisson's ratio, and
- Density of 7.40×10^{-4} lb sec^2 in^{-4}.

3.4.2.3 Loading Conditions and Spot Weld Strengths

Various combinations of normal and shear loads were applied to the base model described in Figure 3-2. Different spot weld strengths were utilized with the different loading conditions in an effort to better characterize the spot weld failure mechanism. Table 3-1 summarizes the applied loading and spot weld strength for the cases examined.

Table 3-1 Case 8 Spot Weld Unit Problem Loading and Spot Weld Strength Summary

Case	Applied Force		Spot Weld Strength Description	
	Normal	Shear	Normal	Shear
8.0	Yes	No	Finite	Infinite
8.1	No	Yes	Infinite	Finite
8.2	Yes	Yes	Finite	Finite
8.49	Yes	No	Finite	Finite

With the exception of Case 8.49, all models had constant spot weld strength. For Case 8.49, a combination of normal loading and variable strength spot welds was used to observe a progressive failure mode. The use of infinite strength spot welds was done to facilitate the load to failure estimates and minimize the possible interaction between the normal and shear failure modes. The exact values of the loading and spot weld strengths will be discussed in more detail in Section 3.4.2.4, where the individual cases and their results are discussed in detail.

3.4.2.4 Spot Weld Unit Problem Results

3.4.2.4.1 Case 8.0 – Spot Weld with Normal Loading

Case 8.0 examined two spot welded 0.5-inch thick plates subjected to an applied normal load. The applied normal force was linearly increased from 0.0 lbs at the start of the analysis to 4.1 lbs at 1.0 seconds, after which it was held constant at 4.1 lbs. No shear force was applied.

The spot welds utilized in this model were intended to focus on the normal strength failure mode. Because a 4.1 lb load was applied, the normal failure strength for each spot weld was set to 1.0 lb. In order to isolate the normal failure mode, the shear failure strength, F_f^s (see Eqn 3-1), was set at 1.0×10^7 lb. As a result, any shear force present in the spot welds would have a minimal influence on the overall failure of the spot weld.

A plot of the normal deflection of the top plate versus time is presented in Figure 3-3.
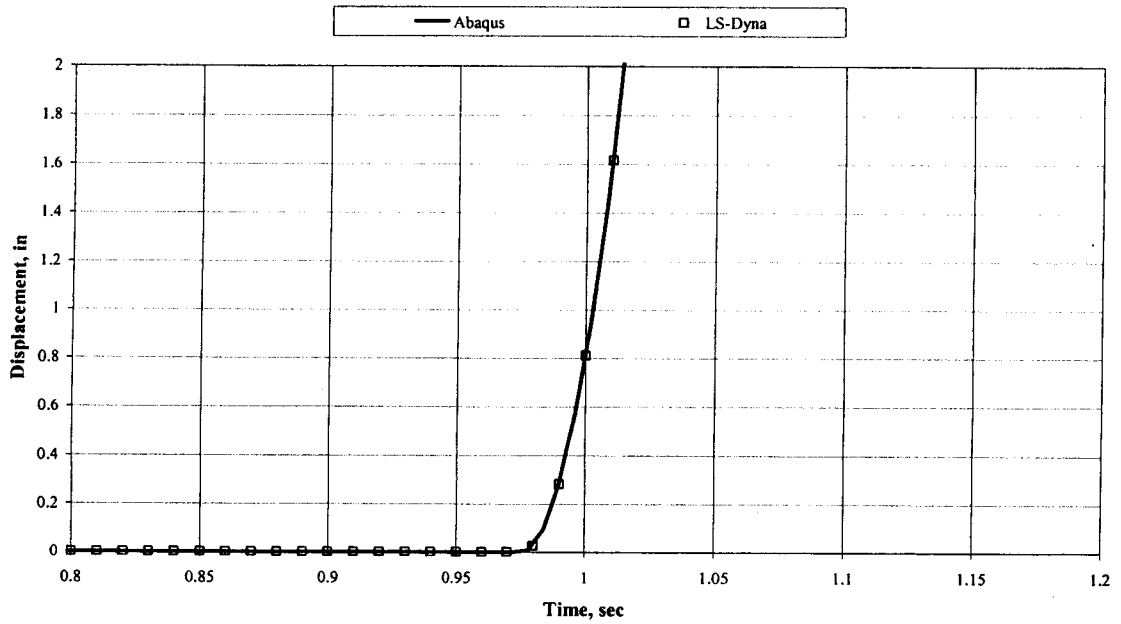
Figure 3-3. Normal deflection versus time for Case 8.0 (normal loading of spot weld unit problem).

This figure shows that the top plate separates from the bottom one at approximately 0.976 seconds in both the ABAQUS and LS-DYNA analyses. The agreement of the displacement of the top plate center node indicates that the spot welds failed at comparable times.

3.4.2.4.2 Case 8.1 – Spot Weld with Shear Loading

Case 8.1 examined the case where only a shear load was applied to the center of the top plate as shown in Figure 3-4.

26
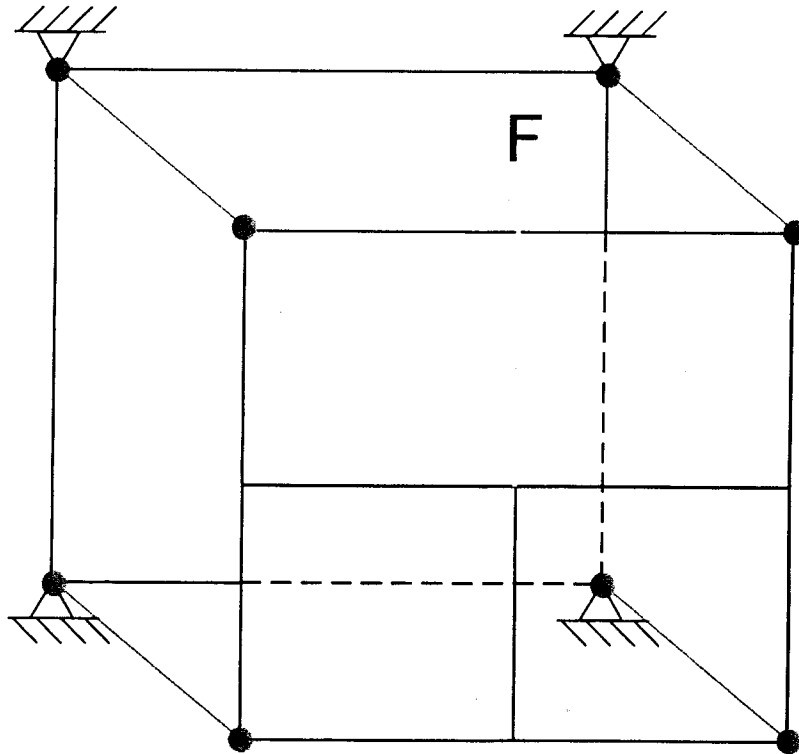
Figure 3-4. Case 8.1 spot weld shear loading unit problem schematic.

The applied shear loading was linearly increased from 0.0 lbs at the start of the analysis to 4.10 lbs 1.0 second later. The applied force was then held constant at 4.10 lbs. No normal force was applied to the plate.

The spot welds utilized in this model were intended to focus on the shear strength failure mode. Because a 4.1 lb load was applied, the shear failure strength for each spot weld was set to 1.0 lb. In order to isolate the shear failure mode, the normal failure strength, F_f^n (Eqn 3-1), was set at 1.0×10^7 lb. As a result, any normal force present in the spot welds would have a minimal influence on the overall failure of the spot weld.

A plot of the normal deflection of the top plate versus time is presented in Figure 3-5.
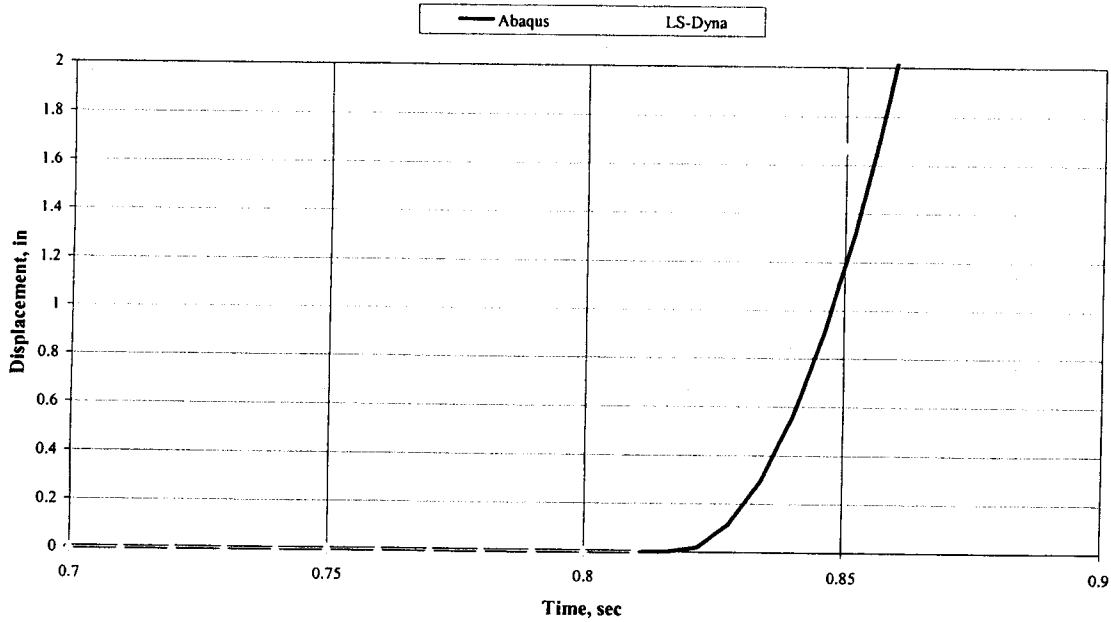
Figure 3-5. Normal deflection versus time for Case 8.1 (shear loading of spot weld unit problem).

Unlike the normal loading applied in Case 8.0, the shear loading in Case 8.1 illustrates a variation in the results calculated by the two codes. The spot weld failures in LS-DYNA occurred earlier in time (i.e., at lower loads), than in ABAQUS. However the failure time in LS-DYNA was only 0.7 percent earlier than that in ABAQUS. This earlier failure time in LS-DYNA corresponds to a 0.7 percent lower failure load due to the linearly increasing the applied load with respect to time in both models. After the welds fail, the body motions of the upper plates were consistent for the two analyses.

3.4.2.4.3 Case 8.2 – Spot Weld with Normal and Shear Loading

Case 8.2 considered spot weld behavior under both normal and shear loading (i.e., normal and shear load were applied to the center of the top plate). The two loads were linearly ramped from 0.0 lb at the start of the test to 2.828 lb after 1.0 second and then maintained at 2.828 lb for the remainder of the analysis.

Unlike the spot weld behavior in Cases 8.0 and 8.1, the spot weld failure condition addressed finite weld strength in both the normal and shear directions. The normal and shear weld strengths were specified to be 1.0 lb at each joined node (i.e., spot weld).

28
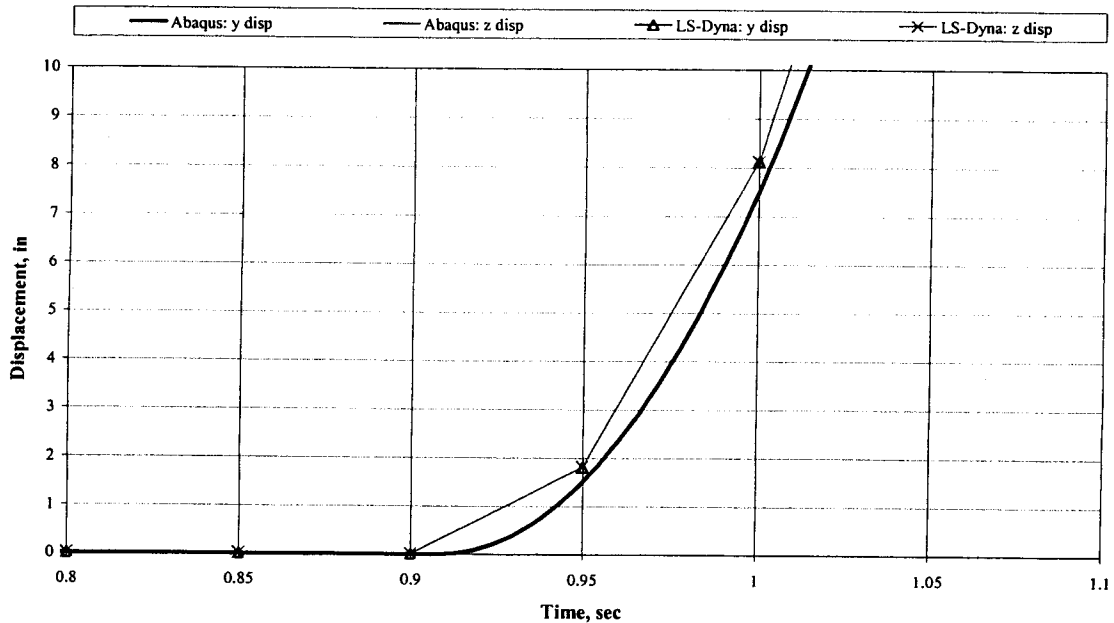
Figure 3-6. Displacement versus time for Case 8.2 (normal and shear loading of spot weld unit problem).

Because the structure is symmetrical with respect to the applied loading condition and the normal and shear loads are equal in magnitude, the resulting y and z displacements were identical for a each analysis code. However, there is a slight difference in when the spot welds fail and the plates begin to completely separate in ABAQUS and LS-DYNA. ABAQUS indicates that the top plate begins to separate from the bottom one after approximately 0.91 seconds while the LS-DYNA solution indicated a slightly earlier separation (i.e., 0.90 seconds). This is not unexpected given the results of the shear loading analysis, where the LS-DYNA solution predicted an earlier weld failure under the shear loading. In this case the percent difference in both time and load to failure is approximately 1%.

3.4.2.4.4 Case 8.4 – Spot Weld with Normal Loading and Variable Spot Weld Strength

Case 8.4 was designed to examine a progressive failure of the spot welds. To achieve this objective, four different spot weld strengths were assigned in the model as indicated in Table 3-2.

Table 3-2 Normal Spot Weld Failure Strength for Case 8.4

Corner Spot Weld Node Numbers		Normal Spot Weld Failure Force (pounds)
Fixed Shell	Coplanar Shell	
1	5	4.0
2	7	2.0
3	11	0.75
4	13	0.25

While the normal strengths varied at each spot weld, the shear spot weld strength was defined to be 1.0×10^7 lb for each weld. The shell thickness was reduced to 0.1 inches for both the top and bottom plates to make the model more flexible.

A normal force was applied to the center of the top plate utilizing a linear ramp over the first 1.0 seconds of the analysis. Upon reaching the maximum normal load of 8.0 lb at 1.0 seconds, the load was maintained at 8.0 lb for the remainder of the analysis. In order to simplify the variables being included in the analysis, no shear loading was applied to the center of the top plate.

The goal of Case 8.4 is to assess the progression of the spot weld failures in the models. As such, the results will focus on the normalized spot weld loads being carried by each weld. The normalized load is defined using Equation 3-1 such that

$$\overline{F} = \left(\frac{\max\left(F^n, 0\right)}{F_f^n} \right)^2 + \left(\frac{F^s}{F_f^s} \right)^2$$

where: $\overline{F}$ = normalized spot weld force,

F^n = normal force,   Eqn 3-3

F^s = shear force,

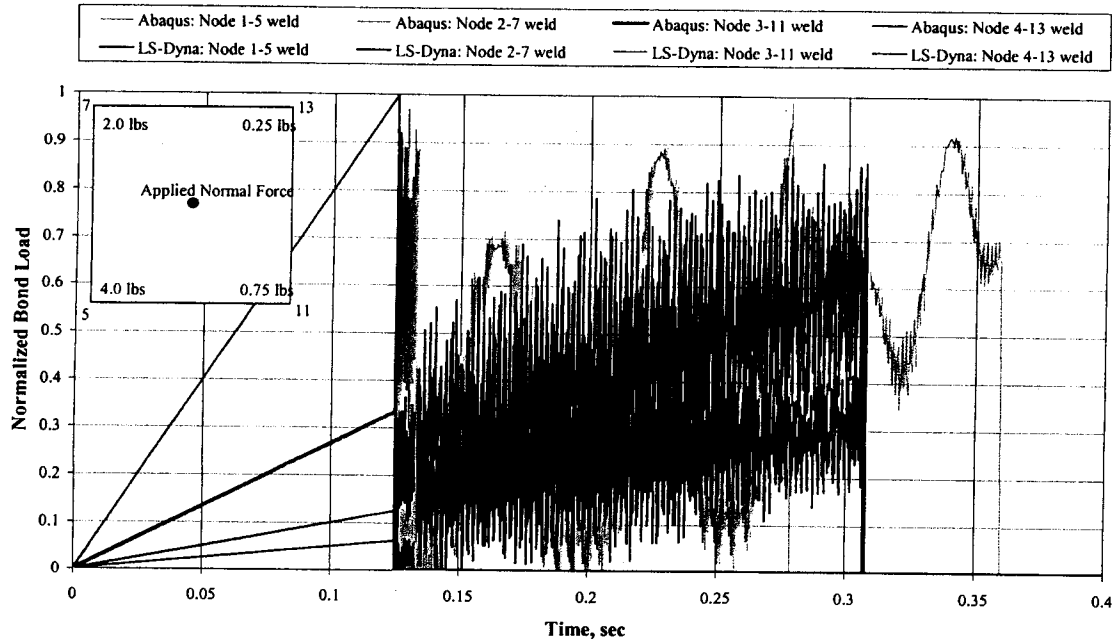F_f^n = normal failure force, and

F_f^s = shear failure force.

Using this definition means that when the normalized force in a spot weld reaches 1.0, failure of the spot weld occurs.
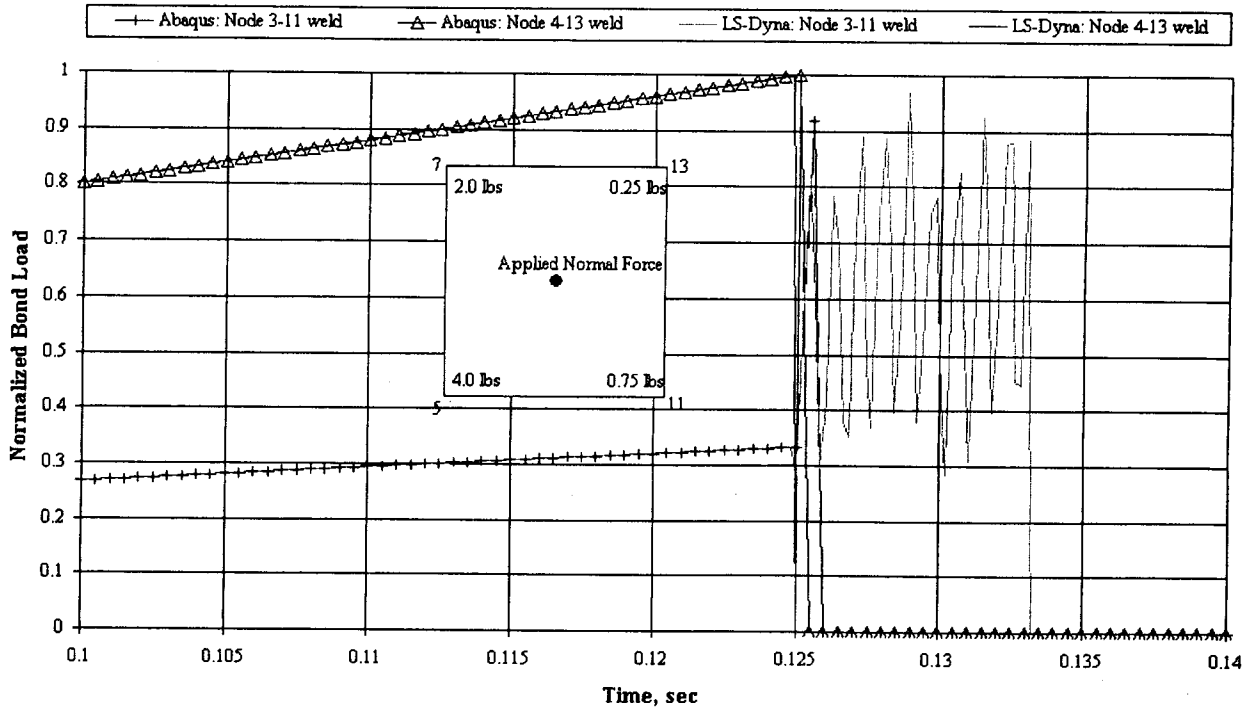
The normalized spot weld load versus time for Case 8.4 is presented in Figure 3-7.

Figure 3-7. Normalized spot weld load versus time for Case 8.4 (normal loading applied and variable strength spot welds present).

Note that the corner nodes of the top plate and the corresponding weld strengths are indicated in the inset image. Figure 3-7 indicates that there is a gradual and consistent progression of failure across the spot welds predicted by ABAQUS and LS-DYNA. However, the calculated failure times are different for the two codes.

In order to simplify the presentation of the spot weld failures, Figure 3-8 shows only the two lowest strength spot welds.

Figure 3-8. Normalized spot weld load versus time for two weakest spot welds in Case 8.4 (normal loading applied and variable strength spot welds present).

The failure time and load for the weakest spot weld are virtually identical between LS-DYNA and ABAQUS. After the first spot weld fails, the plate begins to vibrate thereby introducing high frequency oscillations in the remaining spot weld loads. The boundary conditions present for the plates at this point are different due to the assumed spot weld constraints in the two codes. ABAQUS only constrains displacement degrees of freedom while the LS-DYNA constraint creates a stiffer system by coupling displacement and rotation degrees of freedom. For the case under consideration, the resulting oscillations are such that the first peak following the initial spot weld failure causes the 0.75-lbs spot weld to fail in ABAQUS. LS-DYNA, however has a slightly different plate response that allows the spot weld to maintain its integrity through several oscillations. The 0.75-lb spot weld in LS-DYNA maintains its integrity to a higher total applied load, 1.06 lb versus approximately 1.01 lbs for ABAQUS. While these loads are not significantly different, they do indicate a difference in how the two codes handle spot weld modeling.

An examination into possible additional sources for the variations in spot weld failure loads was performed addressing weld load filtering and contact options were examined in LS-DYNA. Coupling the weld failure methodology with weld load filtering allows the user to specify how the weld fails. For instance, the user can specify that the weld fails on the first occurrence in excess of the weld strength limit or make the failure occur when a filtered value exceeds that limit. The filtering option is not present in ABAQUS and was not addressed. Neither the weld load filtering consistent with the handling of spot weld failure in ABAQUS (no filtering) nor the contact options examined, significantly improved the agreement between the solutions for the Case 8.4 unit problem.

3.4.2.5 Case 8 Spot Weld Unit Problems Conclusions

The spot weld definitions in ABAQUS and LS-DYNA are different in the degree of constraint they offer and spot weld failure definition. ABAQUS considers the spot welds to transmit only translational constraint whereas LS-DYNA applies both translational and rotational constraints. While the weld failure definitions are different in the two codes, it is possible to develop spot weld failure formulations consistent with ABAQUS by selecting the appropriate failure exponent. The failure descriptions for the constant spot weld strength models (Case 8.0, 8.1, and 8.2) indicated reasonably close failure loads and subsequent deformation. Variable spot weld strengths were examined in Case 8.49 resulted in progressive spot weld failures that induced high frequency vibrations. These vibrations coupled with the differing restraint offered by the spot welds in the two codes result in slight variations between time to failure for the structure being considered. Overall, the spot weld behavior is sufficiently close enough from an engineering stand point to be utilized in Case 2.

3.5 Case 2 Loading Conditions

A pressure load is applied to the cylinder from h=10 to 20 inches and over 60 degrees (± 30 degrees from the xz axis) of the cylinder as indicated in Figure 3-9 with the corresponding pressure magnitude indicated in Table 3-3.
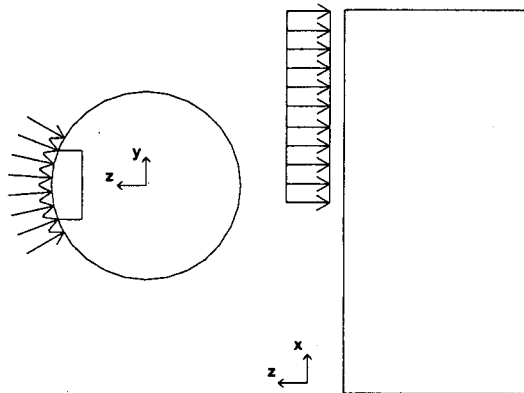

Figure 3-9. Case 2 loading conditions.

Table 3-3 Lateral Pressure versus Time For Case 2

Time (s)	Pressure (psi)
0	800
2.5×10^{-3}	400
5.0×10^{-3}	0.0
30.0	0.0

33

3.6 Case 2 Results

The Case 2 results will focus on two particular features of the analyses:

- The lateral deflection of the cylinder and
- The spot weld behavior.

These two results will provide insight into how LS-DYNA differs from ABAQUS in its treatment of spot weld models and the resulting impact on the structural stiffness.

The spot weld behavior in LS-DYNA and ABAQUS for the Case 2 model will be presented first as this has a direct impact on the resulting deflection of the structure. The primary measure of spot weld performance will be a normalized load carried by the spot welds. The spot weld load normalization is defined by Equation 3-2 in Section 3.4.1.2. The result of Equation 3-2 is that failure of the spot weld will occur when the normalized spot weld load, $\overline{F}$, reaches 1.00. At that point, the spot weld failure behavior of the two codes will be used to dictate the post-failure behavior.

A plot of the normalized spot weld load versus time for the Case 2 model being considered is presented in Figure 3-10.
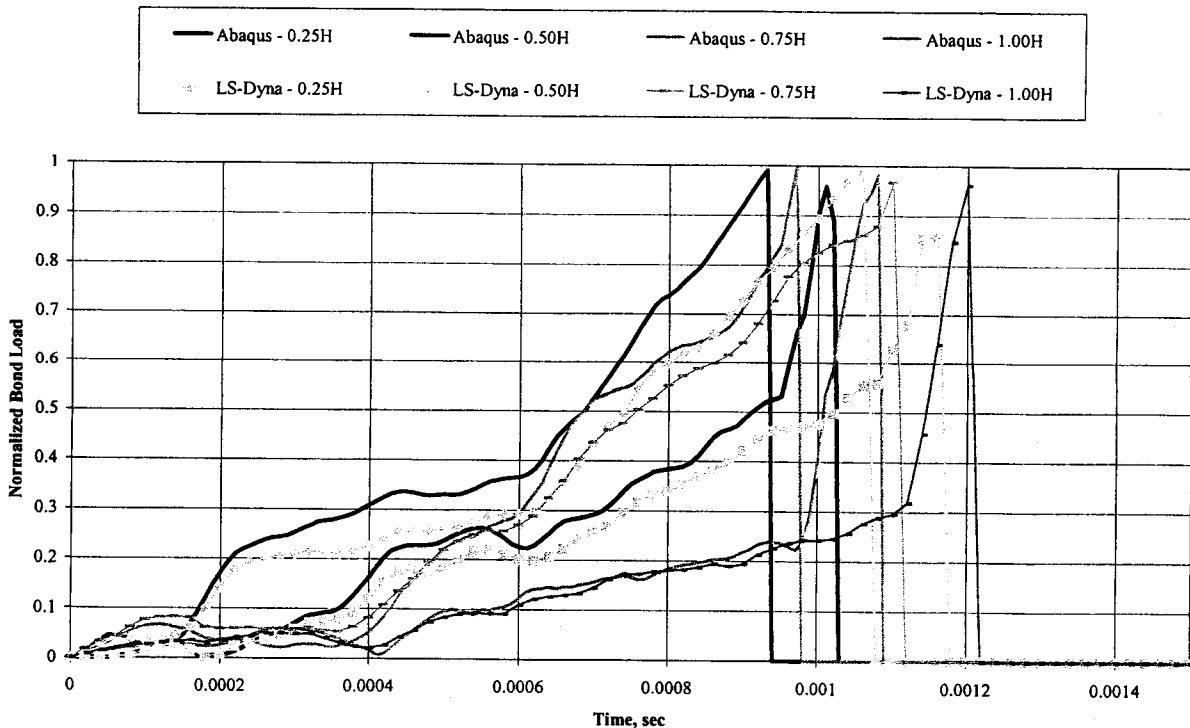

Figure 3-10. Case 2 normalized spot weld load versus time.

This figure shows four of the eight spot welds used in the model ranging from 0.25 to 1.00 times the cylinder height. Only four are required to fully understand the load carrying behavior of the spot welds because symmetry in the model geometry and loading.

34

The first point of interest is the progression of the spot weld failures. Table 3-4 summarizes the failure progression of the spot welds.

Table 3-4 Case 2 Spot Weld Failure Summary

Weld Location	Failure Time (sec)		Total Applied Load at Failure (lbs)		Percent Difference in Failure Time and Load
	ABAQUS	LS-DYNA	ABAQUS	LS-DYNA	
1.00H	1.09×10^{-3}	1.22×10^{-3}	174.4	195.2	11.9
0.75H	9.80×10^{-4}	1.12×10^{-3}	156.8	179.2	14.3
0.50H	9.41×10^{-4}	1.08×10^{-3}	150.6	172.8	14.8
0.25H	1.03×10^{-3}	1.18×10^{-3}	164.8	188.8	14.6

Both analysis codes demonstrated the same progression of the spot weld failures. In the order of occurrence, the spot welds failed at the following locations: 0.50, 0.75, 0.25, and 1.00 times the cylinder height. In each model, the progression from initial to final failure lasts approximately 1.5×10^{-4} seconds. While the failure interval was consistent, the ABAQUS spot welds typically failed approximately 1.20×10^{-4} seconds earlier than the corresponding ones in LS-DYNA.

Other quantities of interest are the lateral deflections for the cylinder at each spot weld height as presented in Figure 3-11.
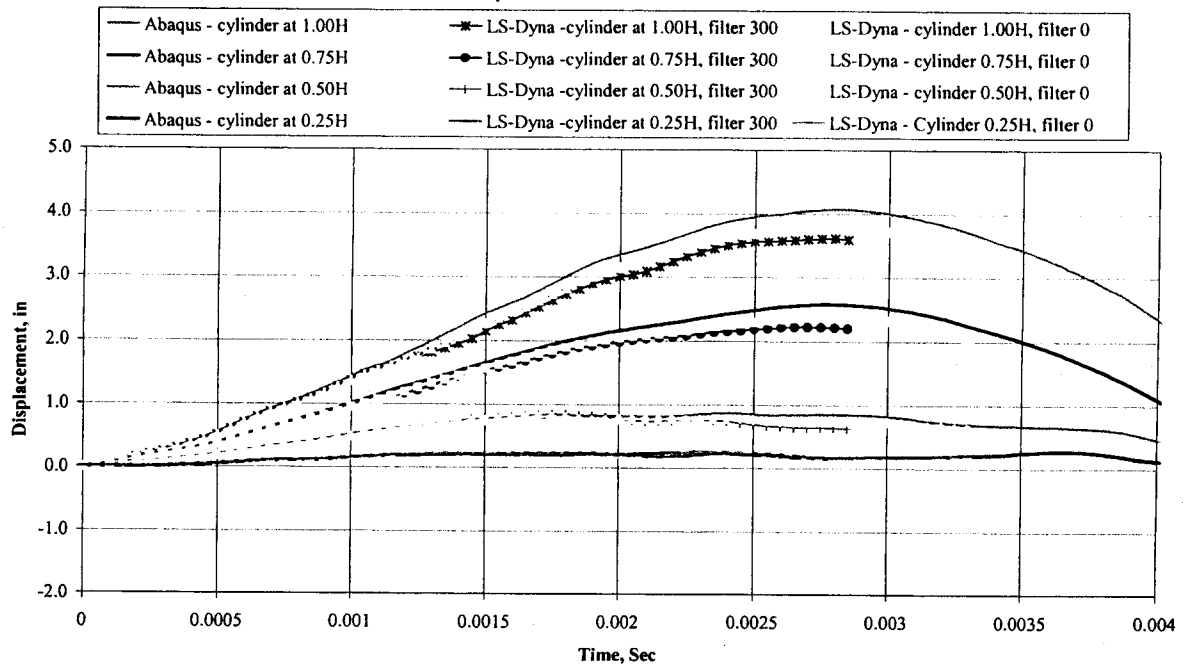
Figure 3-11. Case 2 lateral deflections versus time.

There is good correlation in the shape of the deflection of the structure through 0.330 seconds (termination of LS-DYNA run). For the top of the cylinder, ABAQUS predicts a maximum lateral deflection of approximately 4.07 inches, which is 7.7 percent higher than the 3.78-inch deflection in LS-DYNA (245_0). This behavior is consistent with the loss of stiffness in the ABAQUS models that accompanies the spot weld failures at an earlier time than in LS-DYNA.

3.7   Case 2 Conclusions

The primary feature examined in Case 2 was the presence of spot welds. Through the use of the four unit problems presented in Case 8 (Section 3.4.2), it was shown that for the simplest cases (pure normal or shear loadings and corresponding spot weld strengths) that the two codes agree very well with one another. Once progressive failure is introduced as in Case 8.49, the implementation of the spot weld failures begin to diverge. This divergence appeared to increase in severity once significant oscillations were encountered. It was shown in Case 2, however, that the behavior of the ABAQUS and LS-DYNA models were well correlated. The largest variations occurred in the failure time and it appears that this is a result of the stiffness variation associated with the differences in spot weld failures.

36

4 Cylinder-Beam Interactions (Case 3)

Case 3 was designed to address the contact interaction between a cylinder and a three-dimensional beam. The layout of Case 3 was modified from the initial statement of work in order to better isolate the interaction between shell and beam elements.

Initially, two concentric cylinders were to be present with two beams located inside the inner cylinder. However, the version of ABAQUS used to validate the LS-DYNA contact algorithm does not support beam to beam contact. Therefore, it was decided to remove one of the beams from consideration. The inner cylinder was also removed from the analysis in an effort to simplify the analysis. The resulting model is comprised of a single cylinder with a single beam located on the interior of the cylinder (see Figure 4-1).
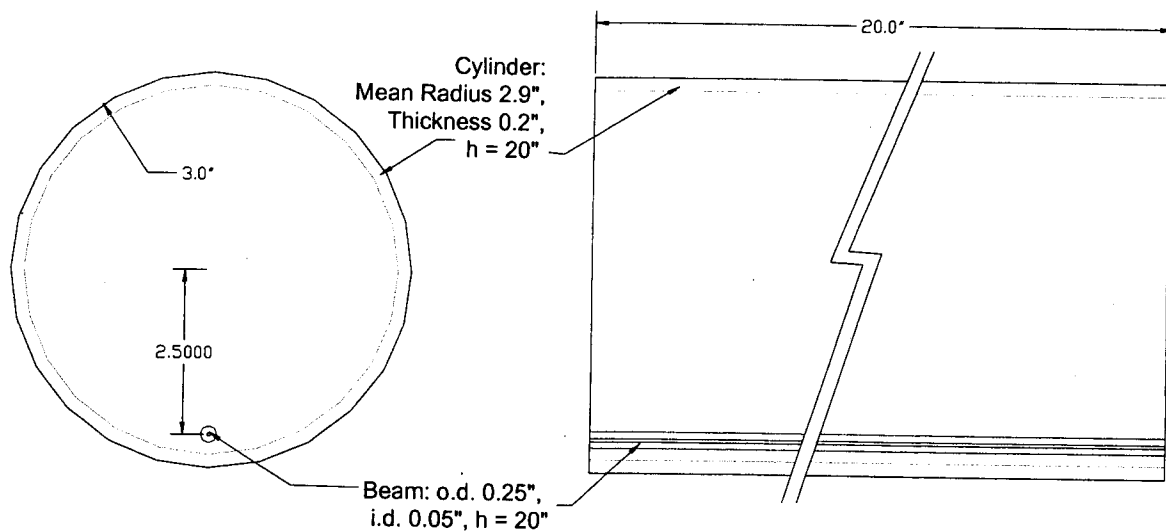

Figure 4-1. Cylinder-beam interaction (Case 3) geometry schematic.

4.1 Geometry

As shown in Figure 4-1, the 20-inch tall cylinder has a mean radius of 2.9 inches and a 0.2 inch wall thickness. A 20-inch tall beam was placed on the interior of the cylinder so that its base is 2.5 inches from the center of the cylinder. The beam has a hollow, circular cross section with a 0.25-inch outer diameter and a 0.05-inch inner diameter.

4.2 Material Definition

An elastic, perfectly plastic material was used in both structural members in each analysis code:

- Elastic modulus of 30×10^6 psi,
- 0.333 Poisson's ratio,
- Density of 7.40×10^{-4} lb sec^2 in^{-4}, and
- Yield stress of 45,000 psi.

4.3 Element Formulation

Case 3 utilized two different types of structural members:

- Shell elements for the cylinder and
- Beam elements for the internal beam.

The shell elements used in this case were identical to those used in Case 1 (Section 2.3) and Case 2 (Section 3.3).

The inner column is relatively tall and slender, and is approximated using beam elements. Beam elements reduce a three-dimensional solution to one-dimension, where the only variation is along the axis of the beam. This approximation is reasonable provided limitations such as the following are met:

- The distance between supports is large as compared to the dimension of the beam cross section and
- The beam cross-section remains planar during deformation.

In the Case 3 configuration, the beam approximation is reasonable because the 20-inch column height and the 0.25-inch outer diameter provide a sufficiently large slenderness ratio. The assumption that the beam cross-section remains planar prohibits an assessment of the beam failing by buckling in the analyses. A brief description of the beam element selection follows for each analysis code.

4.3.1 Beam Element Unit Problem (Case 3.2)

Prior to solving the cylinder-beam interaction problem, a unit problem was devised to assess the behavior of the beam elements in each analysis code. This model (Case 3.2) considered the tubular column 20 inches tall with a 0.40-inch outer diameter and a 0.20-inch inner diameter that is clamped at its base. The base is then translated and the structure is allowed to vibrate freely. The material model used is the same as in Case 3, which was summarized in Section 4.2.

4.3.1.1 Beam Element Unit Problem Loading Conditions

A translation in the z direction was applied to the base of the beam. The displacement was linearly ramped from its initial position to 0.3 inches at a time of 0.005 seconds. After 0.005 seconds, the base position was maintained at the 0.3-inch deflection. During this base motion all other degrees of freedom at the base were maintained at 0.0 inches.

4.3.1.2 ABAQUS B31 Beam Element

The B31 element was selected for modeling the beam in the ABAQUS Case 3 model. This element is a linear Timoshenko (shear flexible) beam with six degrees of freedom (three

displacement and three rotation) at each node. These elements can handle the large axial strains anticipated to occur when subjected to the applied load.

4.3.1.3 LS-DYNA Beam Element

Three different LS-DYNA beam elements were utilized in the beam unit problem:

- Belytschko-Schwer tubular beam with cross–section integration (Element Type 5),

- Hughes-Liu with cross-section integration (Element Type 1), and

- Belytschko-Schwer full cross-section integration (Element Type 4).

4.3.1.4 Beam Element Unit Problem Results

A total of four analyses were performed on the unit problem as presented in Table 4-1.

Table 4-1. Beam Element Unit Problem Analysis Element Type

Analysis Code	Analysis Designation	Beam Element Type
ABAQUS	3.2a	B31
LS-DYNA	3.2a	Type 5
	3.2b	Type 1
	3.2c	Type 4

The primary mechanism for comparison in Case 3.2 is the displacement at the top of the beam as shown in Figure 4-2.
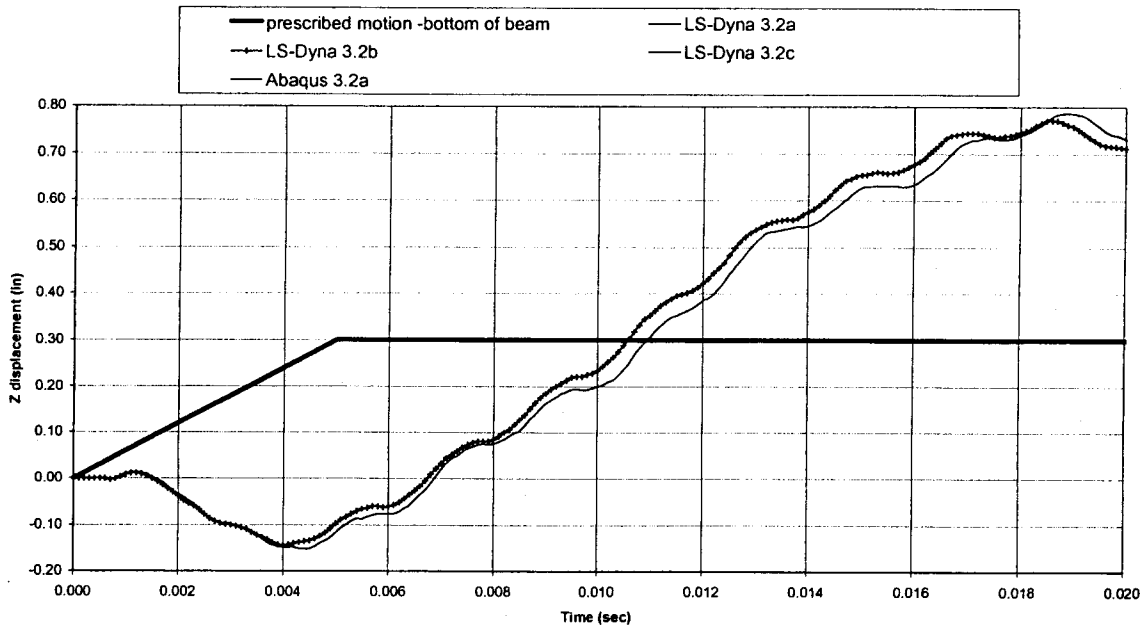
Figure 4-2. Displacement at top of beam versus time for Case 3.2 (beam element unit problem).

Figure 4-2 shows that the displacements in the three LS-DYNA analyses agree well with each other for this loading condition. They also agree well with the ABAQUS results through approximately 0.004 seconds. After this time, variations between the two codes become more significant. There appears to be a slight delay in the ABAQUS response compared to LS-DYNA. Also, the ABAQUS solution is slightly more flexible as indicated by an increase in the peak deflection to approximately 0.786 inches compared to 0.771 inches in LS-DYNA.

An additional study examining the effect of time step on the ABAQUS and LS-DYNA solutions was performed in an effort to determine if that could have contributed to the time delay between the two codes. The study did not reveal any significant variations on the solutions for either code with the reduction in time step.

4.3.1.5 Conclusions

While the applied displacement at the base of the model in Case 3.2 was not sufficient to induce plastic deformation, the two codes did provide reasonable correlation in both the magnitude of tip deflection and the time history of the vibration. Based on the similarity between the three LS-DYNA beam elements, it was decided to go with element type 5.

4.4 Case 3 Loading Conditions

A pressure load is applied to the cylinder from h=10 to 20 inches and across a 30 degree arc along the outer surface of the cylinder as shown in Figure 4-3.
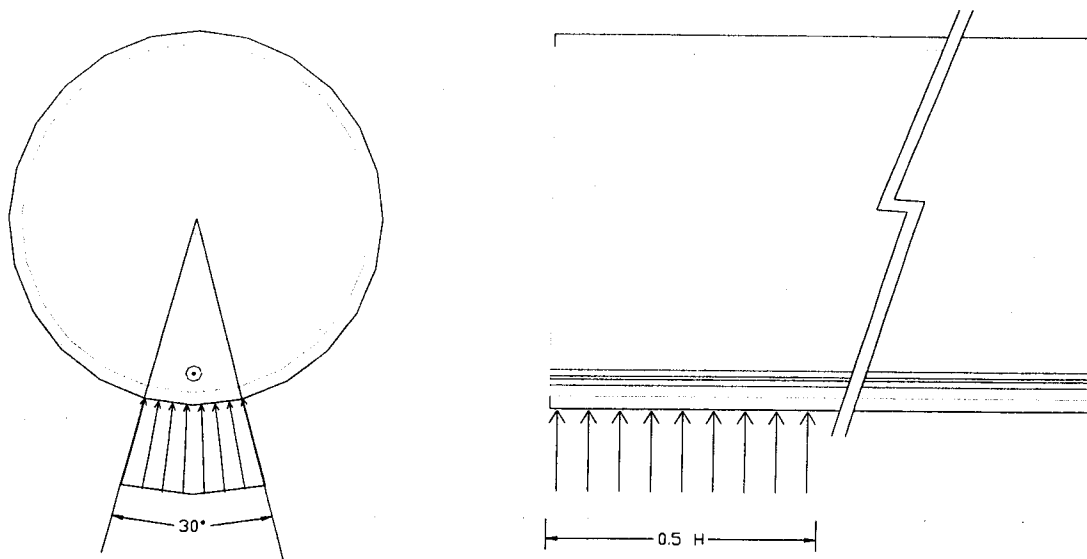
Figure 4-3. Applied loading for Case 3.

The pressure load was such that it was a maximum at the initiation of the analysis, 600 psi, and reduced linearly with time until it reached 0 psi at 0.010 seconds where it was held constant for the remainder of the analysis.

4.5   Shell-Beam Contact Formulation

The focus in the Case 3 analysis is the behavior of the contact algorithms when assessing shell-beam interactions. The primary difference between the two codes handling of this contact event is a direct result of what contact members are considered.

4.5.1   ABAQUS Shell-Beam Contact Formulation

The contact formulation in ABAQUS requires that a node-based surface be defined on beam elements. These nodal surfaces do not contain sufficient geometry definition so they must be maintained on the slave surface and employed in a pure master-slave configuration. In Case 3, this pure master-slave arrangement considers the shell elements as the master surface and beam nodes as the slave surface. The result of this is that contact will be initiated when the beam nodes intersect the corresponding master surface that, in this case, is defined to be the interior of the cylinder. Therefore, the initial contact gap is defined to be the distance from the inner surface of the shell to the center of the beam.

4.5.2   LS-DYNA Shell-Beam Contact Formulation

Options for performing contact interaction analyses between shell and beam elements in LS-DYNA include:

- Automatic, single surface,
- Nodes to surface, and
- Automatic nodes to surface.

The primary difference between these formulations is how the algorithms treat the thickness of the components. This determines when the components begin to interact with each other.

4.6 Case 3 Results

The primary concern in the Case 3 analyses is the beam to cylinder interaction. This interaction is most readily observed by examining the displacement histories of the top, center of the cylinder and the free beam tip. As the top of the cylinder is collapsed, the lateral deflections of the cylinder increase. Once the lateral deflection equals the appropriate clearance between the cylinder and the beam, the beam also will begin to deflect laterally. This clearance will depend upon the analysis code and the options utilized in it. A summary of the corresponding deflections and contact clearances are presented in Table 4-2.

Table 4-2. Case 3.0 Contact Clearance Summary

Analysis Code	Case Identifier	Contact Option	Clearance Description	Idealized Clearance (in)
ABAQUS	Case 3.0c	Default, pure master (cylinder)-slave (beam)	Beam center to inner shell surface	0.300
LS-DYNA	Case 3.0c	Automatic_single_surface		0.240
	Case 3.0d	Nodes_to_surface	Center of beam to center of shell	0.400
	Case 3.0f	Automatic_nodes_to_surface	Outside of beam to outside of shell	0.175

From the cases examined in Table 4-2, there is not a contact option in LS-DYNA that will reproduce the same idealized clearance as in ABAQUS. Therefore, all three cases will be examined in LS-DYNA to see how its three contact options affect the structural response relative to that in ABAQUS.

A plot of lateral deflection histories for the top of the cylinder and top of the beam through the first 0.002 seconds of the analysis is provided in Figure 4-4.

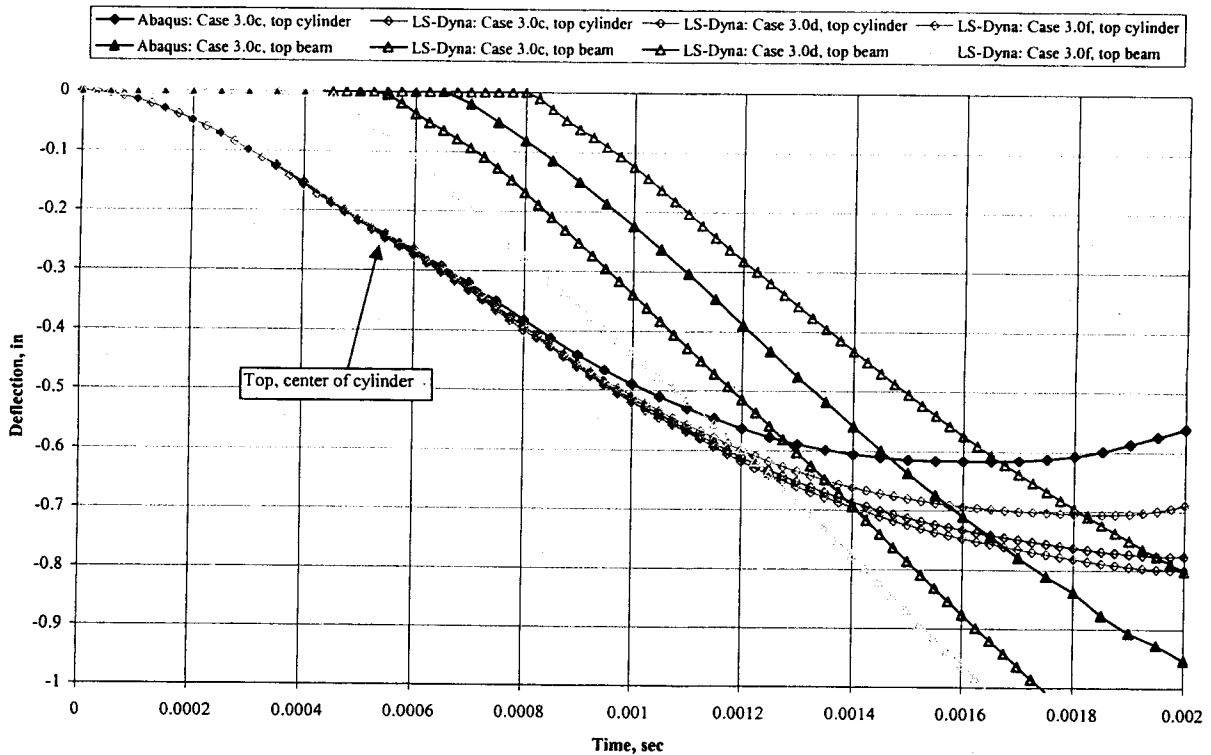Z Displacement ofNode at Top of Cylinder and Beam in Case3.0b Analyses

Figure 4-4. Lateral deflection of the top, center of the cylinder and the interior beam tip versus time for Case 3.0.

In each case, the initiation of the beam tip displacement presented in Figure 4-4 corresponds directly to the idealized clearance in Table 4-2.

While there is a significant variation in the idealized clearances, the variation in the cylinder deflection is essentially unchanged between all the analyses through the initial 0.001 seconds. Beyond that point, the LS-DYNA begins to significantly deviate from the ABAQUS Case 3.0c solutions indicating a softer solution. Of the LS-DYNA solutions, Case 3.0f appears to offer the stiffest solution as indicated by the smallest lateral deflection at the cylinder top.

Based on the studies performed throughout the course of this program it is unclear why the two codes experience response variations. It is believed that the mesh density (see Case 1 mesh convergence study in Section 2.4) and time step (see Section 4.3.1.4 for a brief discussion of the time step study on the unit beam problem) do not play a significant role in the observed variations. Remaining issues that may affect the structural stiffness include aspects such as the default damping present in both ABAQUS and LS-DYNA and the element formulations themselves.

4.7 Shell-Beam Interaction (Case 3) Conclusions

The Case 3 analyses addressed the contact interaction of shell and beam elements. First, a favorable comparison between the beam element solutions in ABAQUS and LS-DYNA was obtained. Next, the Case 3 model was analyzed where a pressure was applied to collapse a thin-

walled cylinder and the deformation introduced contact with an internal beam element. Several key variations were observed in the solutions of the two codes:
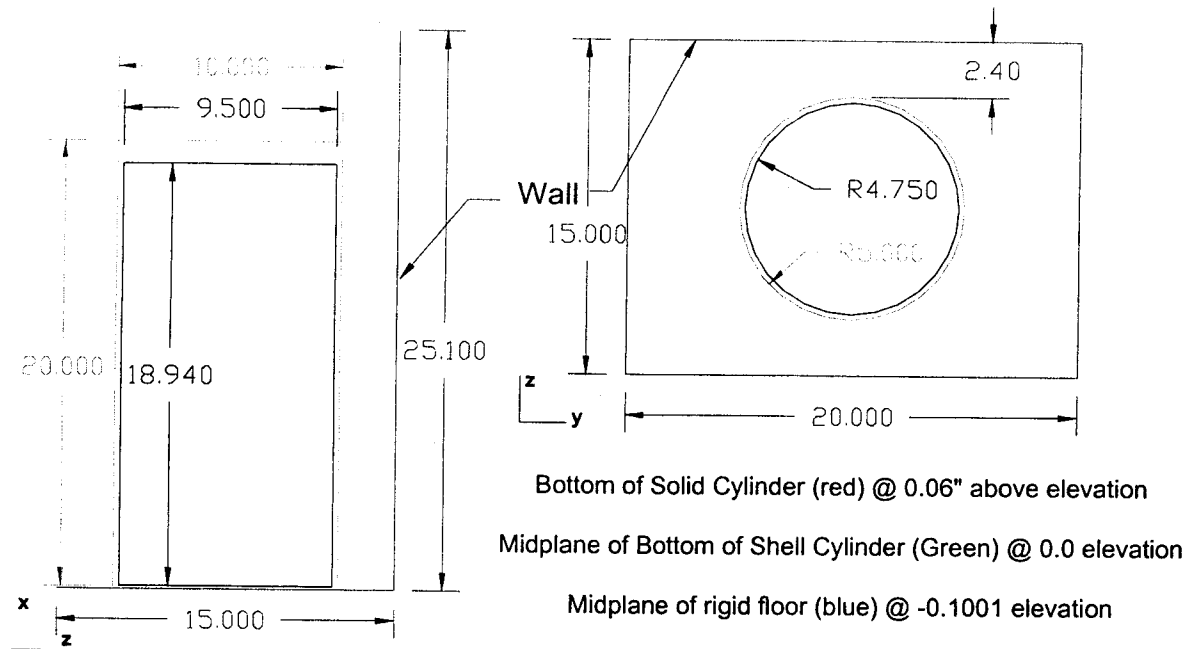
- The version of ABAQUS used for the validation exercise does not permit contact between two sets of beam elements,

- Options exist to adjust the clearance between contact bodies to account for issues such as shell thickness (ABAQUS and LS-DYNA) and beam geometry (LS-DYNA only), and

- As observed in Case 1 (Section 2.6), the cylindrical shell portion of the ABAQUS model is stiffer than that used in LS-DYNA; however the differences were small for the ABAQUS SR4 and the LS-DYNA fully integrated shell elements. Differences in this case appear greater and are influenced by the contact algorithm.

5 Partially Filled Drum Impacting a Wall (Case 4)

Case 4 investigates the behavior of a thin-walled drum filled with concrete as it impacts against a rigid wall. The model will address various contact algorithm issues (solid to shell and shell to rigid contact) as well as the inclusion of gravity as a loading variable.

5.1 Geometry

A schematic of the Case 4 geometry is provided in Figure 5-1.

Bottom of Solid Cylinder (red) @ 0.06" above elevation

Midplane of Bottom of Shell Cylinder (Green) @ 0.0 elevation

Midplane of rigid floor (blue) @ -0.1001 elevation

Figure 5-1. Case 4 configuration schematic.

Three distinct components are indicated in the figure:

1. 0.1-inch thick steel drum shown in green,
2. Concrete cylinder inside of steel drum shown in red, and
3. Rigid wall boundary shown in blue.

The concrete volume does not completely fill the steel drum. Rather there is a 0.20-inch radial clearance and a 1.01-inch vertical clearance from the concrete to the top of the drum.

5.2 Material Definition

Two different materials will be defined for Case 4: steel for the drum and concrete for the drum contents.

5.2.1 Steel Drum Material Model

An elastic, perfectly plastic material was used for the steel drum in each analysis code:

- Elastic modulus of 30×10^6 psi,
- 0.3333 Poisson's ratio,
- Density of 7.40×10^{-4} lb sec^2 in^{-4}, and
- Yield stress of 45,000 psi.

5.2.2 Drum/ Cylinder

The concrete cylinder contained in the steel drum was modeled as an elastic material:

- Tangent Elastic modulus of 3.6×10^6 psi,
- 0.3 Poisson's ratio, and
- Density of 2.20×10^{-4} lb sec^2 in^{-4}.

5.3 Element Formulation

Three different element types were utilized in Case 4:

1. Shell elements for the steel drum,
2. Solid elements for the concrete cylinder,
3. Rigid elements for the rigid walls (in ABAQUS).

The LS-DYNA model utilized the *RIGIDWALL_PLANAR command for the rigid wall. This command creates a rigid surface in space that is utilized by the contact algorithm. The shell elements used are identical to those used in Case 1, 2, and 3 (Sections 2.3, 3.3, and 4.3) and their description will not be repeated here. The following sections will provide information on the solid and rigid elements used.

5.3.1 Single Solid Element Unit Problem (Case 6)

The solid element behavior was examined through a single element test. While the solid element was used to model the elastic concrete cylinder in Case 4, it was decided to model the elastic, perfectly plastic steel material model provided in Section 5.2.1 in this unit problem. The rationale was that this would provide a more complicated system to validate as it includes not only the initial elastic behavior but also the plastic deformations.

5.3.1.1 Single Solid Element Unit Problem Element Selection

##### 5.3.1.1.1 ABAQUS C3D8R Solid Element

The C3D8R element is an 8-noded hexahedral, reduced integration element that can be used in nonlinear analyses involving effects such as contact, plasticity, and large deformations. There are three displacement degrees of freedom at each node.

5.3.1.1.2 LS-DYNA Type 3 Element

This is a fully integrated quadratic 8 node element with nodal rotations.

5.3.1.2 Single Solid Element Unit Problem Geometry

A single solid element 1.00 inch on each side was modeled as shown in Figure 5-2.
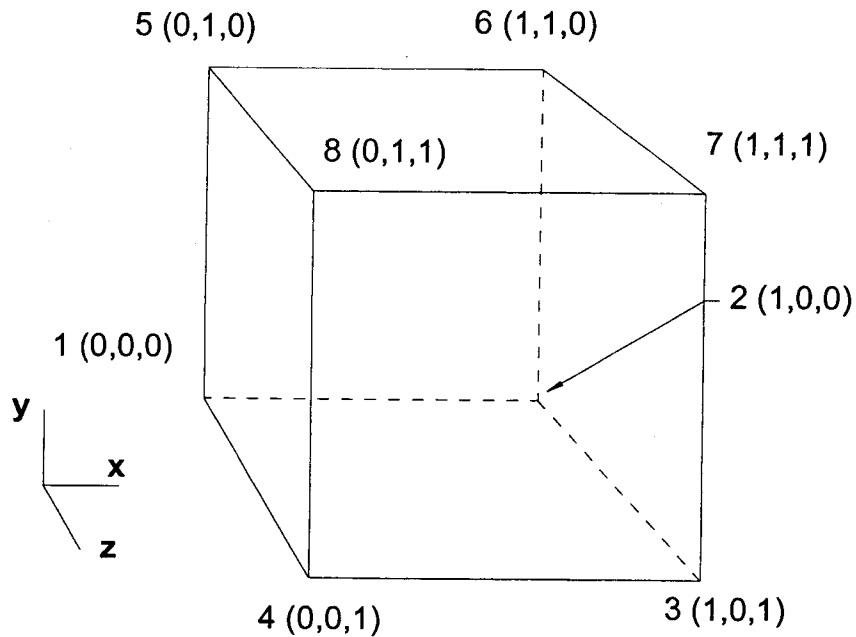
Figure 5-2. Single solid element model schematic.

Symmetry boundary conditions corresponding to the x=0, y=0, and z=0 planes were applied to the model. This required that no nodal displacement be permitted normal to the plane. The LS-DYNA model included additional restrictions that all nodal rotations be identically zero as well.

All four nodes on the y=1.00 plane had a non-zero displacement applied to them in the y direction by a sine function [y=0.15 sin(500t) inches] defined using a tabular sequence of 31 pairs of equally spaced values out to 0.021 seconds. The displacement was then varied linearly between each increment resulting in a multi-linear approximation to the desired sine wave.

5.3.1.3 Single Solid Element Unit Problem Results

An axial stress versus time plot for the single solid element unit problem is provided in Figure 5-3.
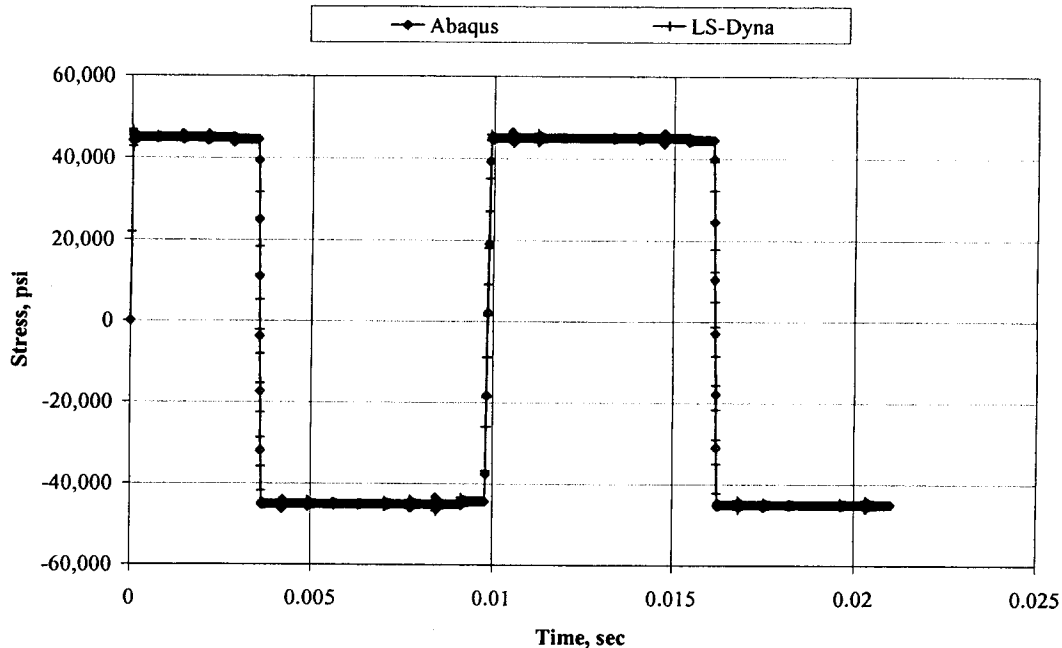
Figure 5-3. Axial stress versus time for the single solid element

The two codes exhibit excellent agreement for the applied loading condition throughout the entire analysis.

5.3.1.4 Conclusions

Based on the excellent agreement between the LS-DYNA and ABAQUS for the single solid element unit problem using an elastic, perfectly plastic material model, it was determined that the solid element selected should be applicable for an elastic material model.

5.3.2 Rigid Element Selection

The remaining element type utilized in Case 4 is the rigid elements used in ABAQUS to provide the floor and wall that the steel drum impacts.

5.3.2.1 ABAQUS R3D4 Rigid Element

R3D4 is a four noded quadrilateral element that has three degrees of freedom at each node. The nodal displacements are governed by the master node for the rigid element's corresponding rigid body. Similar to the S4R shell element, a thickness is defined for the rigid body in order to account for material in the case of contact. Boundary conditions can only be applied to the master node associated with the rigid body. The motion of this master node will dictate the motion of the remainder of the rigid body.

An alternative formulation in ABAQUS for the rigid surfaces was to use a rigid analytical surface instead of the rigid elements. However, the rigid analytical surface was not considered in this study.

48

5.3.2.2 LS-DYNA *RIGIDWALL_PLANAR Command

The *RIGIDWALL_PLANAR command was used to define the rigid wall surface instead of shell elements. Initial attempts using shell elements and defining them as a rigid material for the rigid wall surface provided erroneous results because nodes were being trapped behind the rigid wall elements.

5.4 Case 4 Loading Conditions

Gravity was applied gradually in the negative x direction. The ramping function was used to apply the acceleration and is given by Equation 5-1.

$$A = A_1 \left(\frac{t}{t_1}\right)^3 \left(10 - 15\left(\frac{t}{t_1}\right) + 6\left(\frac{t}{t_1}\right)^2\right) \qquad \text{Eqn 5-1}$$

"A" is the amplitude of the gravity at time (t), A_1 is the magnitude of the gravity, and t_1 is the time over which the gradual increase occurs. In this case, A_1 equaled 386.4 in/s^2 and t_1 equaled 4 ms.

A pressure load also was applied to a portion or the shell cylinder as shown in Figure 5-4.
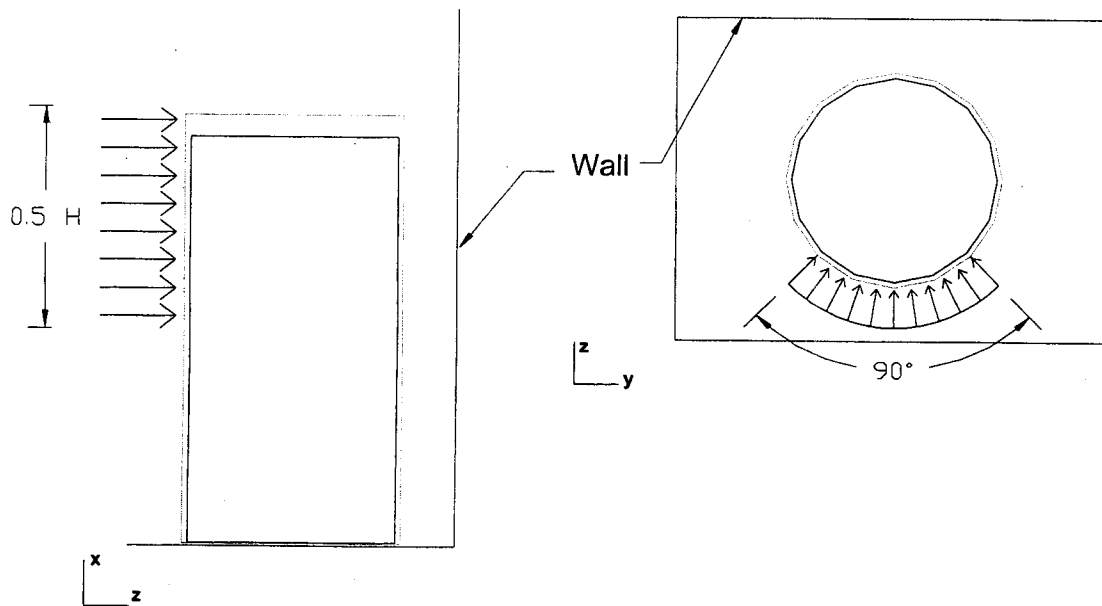
Figure 5-4. Case 4 applied loading.

The pressure acted on the top half of the cylinder from h= 10 to 20 inches. It was applied over a 90° segment on the –z surface of the shell. The pressure load curve provided in Table 5-1.

Table 5-1. Case 4 Pressure Load History

Time (s)	Pressure (psi)
0.0	0.0
3.99×10^{-3}	0.0
4.0×10^{-3}	1000.0
9.0×10^{-3}	0.0
30.0	0.0

In this case, the maximum pressure is applied at the same time that the gravity load has reached its maximum amplitude.

5.5 Results

The primary quantities examined in the Case 4 analyses are the displacement of the top and bottom corners of the steel drum that are closest to the wall. The points are designated "A" (top corner of drum) and "C" (bottom corner of drum) in Figure 5-5 and 5-6. As the lateral load is applied to the body, the drum will begin to tip over and slide. It will contact the inner drum and, eventually, this over-turning motion will result in the drum impacting the rigid wall.

The transverse and vertical deflection of points A and C versus time are provided in Figure 5-5 and Figure 5-6, respectively.
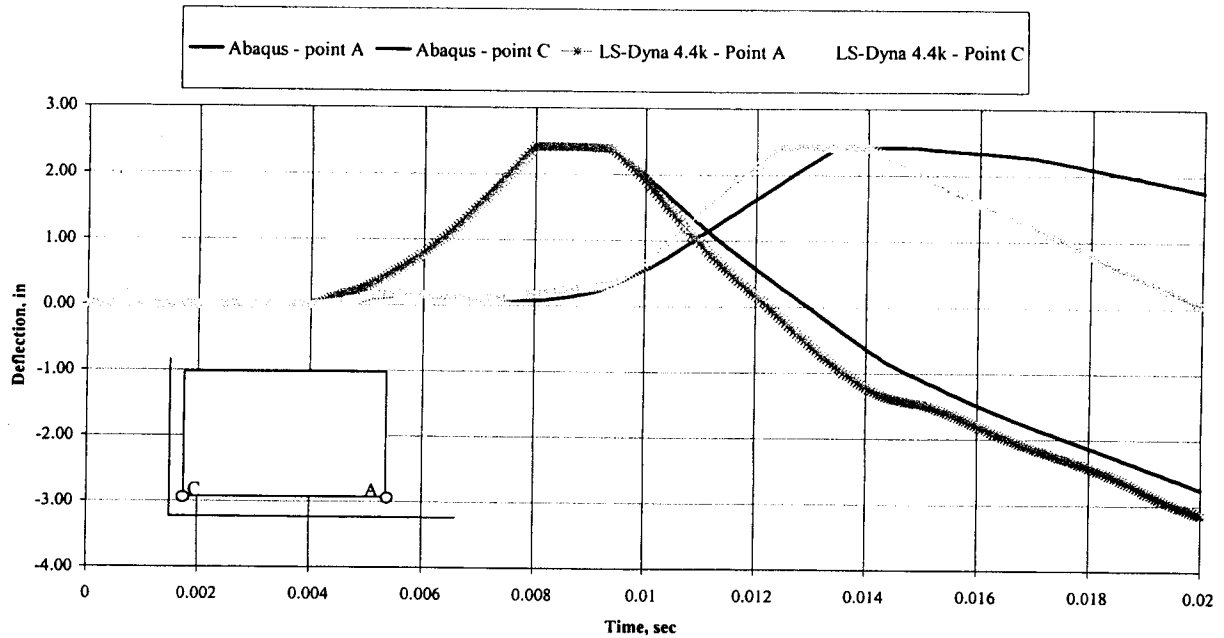
Figure 5-5. Lateral deflection (positive is towards rigid wall) versus time for points A and C on the steel drum in Case 4.
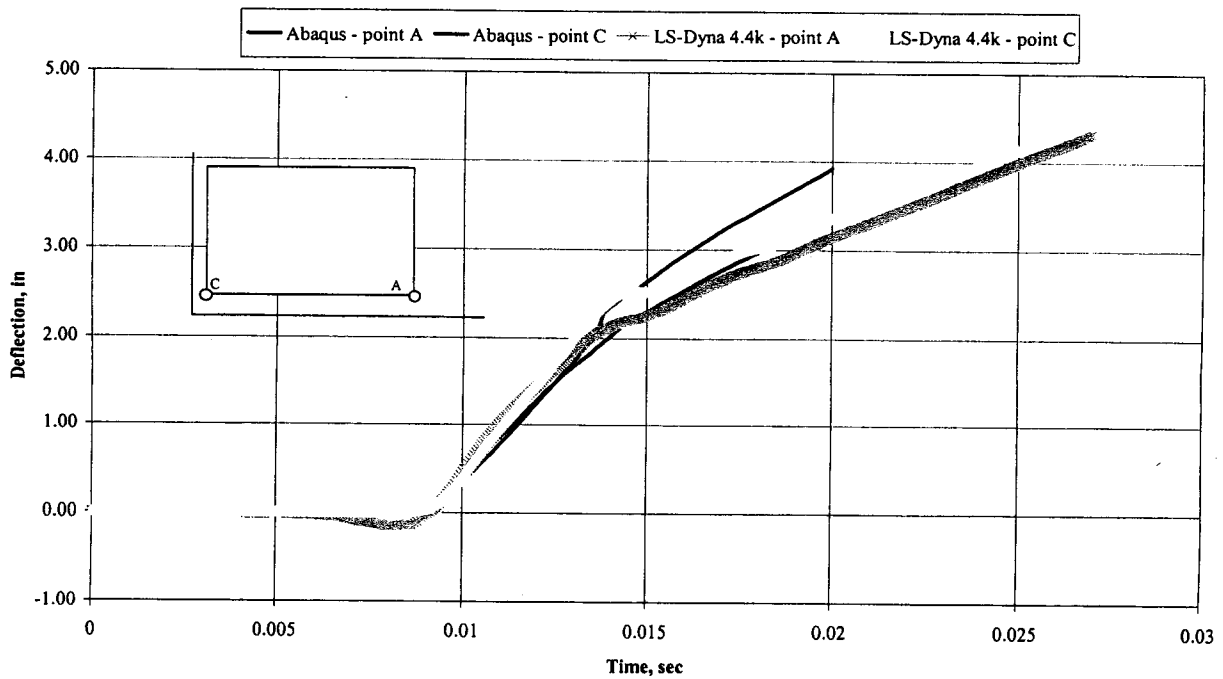

Figure 5-6. Vertical deflection (positive is upwards) versus time for points A and C on the steel drum in Case 4.

51

Overall, these two figures are in good agreement with one another in both general behavior and magnitude. Figure 5-5 shows excellent agreement between the two codes through the first 0.010 seconds. During this time, the drum is tipped towards the rigid wall by the lateral pressure. The Point A is the first point on the drum to impact the vertical rigid wall initially 2.4 inches away. After impacting the rigid wall, the drum remains in contact with the wall for approximately the next 0.001 seconds of the analysis. This is a result of the drum undergoing a significant plastic deformation on the corner. Eventually, the drum begins to rebound from the rigid wall. As this rebounding begins to occur, slight differences are observed in the two solutions. LS-DYNA indicates that Point C at the bottom of the drum will impact the wall slightly ahead of the ABAQUS solution. Despite this variation, the resulting durations of Point C remaining in contact with the rigid wall are comparable for the two codes. After 0.015 seconds, both analysis codes indicate that the drum has separated from the rigid wall with better agreement observed for Point A than Point C.

Figure 5-6 shows good agreement in the vertical displacement at Points A and C for the two codes through 0.015 seconds (separation from rigid wall). After 0.015 seconds, there is a slight difference in the resulting slope of the deflection-time curves indicating that the ABAQUS solution has a slightly higher post-impact velocity than that in LS-DYNA.

## 5.6 Partially Filled Drum Impacting a Wall (Case 4) Conclusions

An analysis of a steel drum partially filled with a concrete cylinder impacting a rigid wall was performed. After successfully verifying the material modeling for the concrete portion of the model with three-dimensional, solid elements the complete model was analyzed. The use of contact algorithms in ABAQUS and LS-DYNA with deformable to rigid bodies was successfully employed in Case 4. The primary difference in the algorithms used was that the LS-DYNA solution considered a rigid plane as opposed to the rigid elements in ABAQUS. This was required to prevent nodes from passing through the rigid elements in LS-DYNA. Results of these analyses indicate that the global behavior of the two models are similar. There were slight differences in the solutions following the initial impact of the drum with the wall but, overall, good agreement was observed.

6 Damping of an Inverted Pendulum (Case 5)

Case 5 investigated the effect of mass proportional damping on a simplistic structure representative of an inverted pendulum.

6.1 Inverted Pendulum Geometry

The inverted pendulum finite element geometry is provided in Figure 6-1.
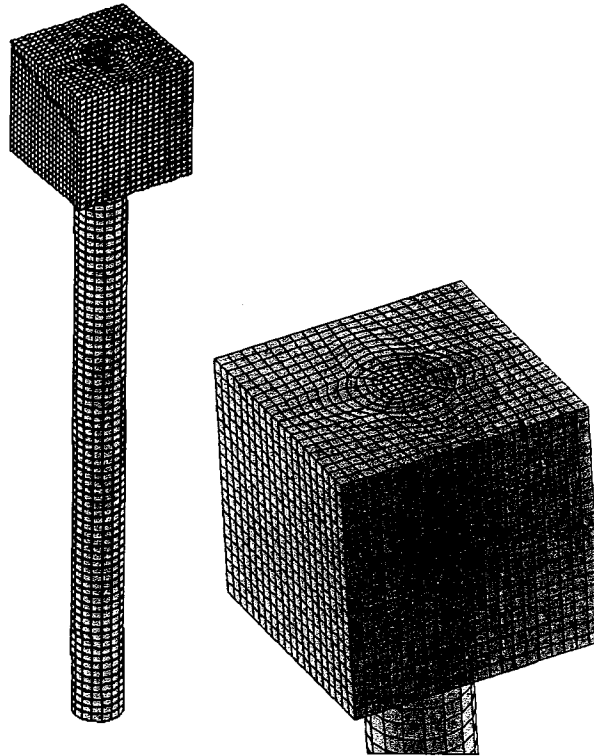
Figure 6-1. Inverted pendulum finite element geometry.

The geometry consists of a solid cylinder of height 25.0 inches and radius 1.0 inch. A solid cube with side lengths of 5.0 inches is centered on the top of the cylinder bringing the total height of the structure to 30.0 inches. The resulting structure is considered to be a single unit.

6.2 Material Definition

An elastic material was used in both codes:

- Elastic modulus of 30×10^6 psi,

- 0.333 Poisson's ratio, and

- Density of 7.40×10^{-4} lb sec^2 in^{-4}.

In addition to the elastic material properties, damping was also defined for the structure. Rayleigh damping present in both ABAQUS and LS-DYNA are comprised of two distinct modes:

1. Mass proportional damping and

2. Stiffness proportional damping.

This analysis focused on the effects of mass proportional damping on the structure.

Mass proportional damping is related to the period of the system being considered. In this case, it is possible to adjust the mass proportional damping to obtain a critically damped structure using solely the period of the undamped structure, T, as shown in Equation 6-1.

$$\alpha = \frac{4\pi}{T}$$

Eqn 6-1

6.3 Element Selection

The C3D8R and type 3 solid elements were used in the ABAQUS and LS-DYNA analyses, respectively. The elements are described in Section 5.3.1.1.

6.4 Inverted Pendulum (Case 5) Loading Conditions

A prescribed motion was applied to the nodes at the bottom of the cylinder. The motion is in the x direction, perpendicular to the cylinder axis, and is defined in Table 6-1.

Table 6-1. Prescribed Base Motion of Inverted Pendulum (Case 5)

Time (s)	Prescribed Motion (inches)
0.00	0.000
7.00×10^{-4}	0.160
1.40×10^{-3}	0.320
2.00	0.320

The remaining degrees of freedom at the cylinder base in the y and z directions are set to 0.0 so that there is only translation in the x direction.

6.5 Inverted Pendulum (Case 5) Results

Two series of analyses were performed:

1. Undamped system and

2. Mass proportionally damped system.

6.5.1 Undamped Inverted Pendulum Results

The first analysis performed did not apply any damping to the model so the natural period of the structure could be obtained. Figure 6-2 shows the lateral deflection at the top, center of the inverted pendulum versus time.
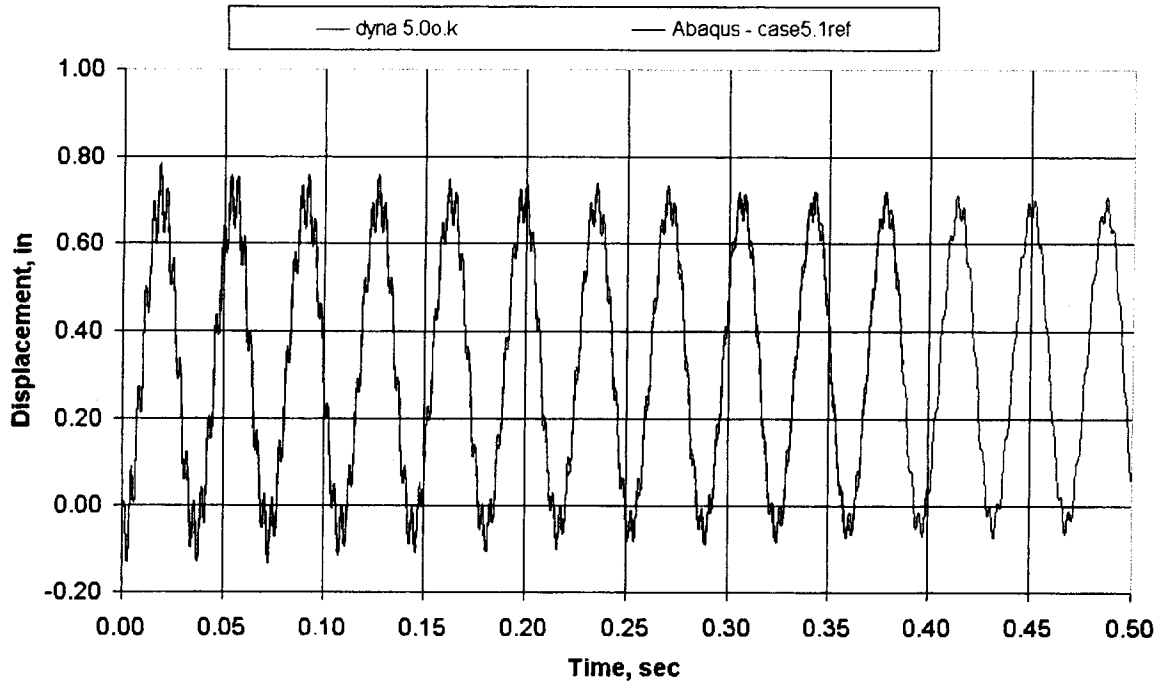
**Figure 6-2. X Displacement of the top center versus time for Case 5 without damping.**

There is excellent agreement between the ABAQUS and LS-DYNA solutions for the undamped inverted pendulum. Based on the observed oscillations, the primary natural period of pendulum is shown to be approximately 0.04 seconds.

6.5.2 Mass Proportional Damping of Inverted Pendulum Results

This section focuses on the inverted pendulum response using mass proportional damping. Based on Equation 6-1 and the principal period identified in Section 6.5.1, the critical mass proportional damping factor is calculated to be 314.0 sec^{-1}. Using this as a basis, three analyses were performed in ABAQUS and LS-DYNA:

1. 283 sec^{-1} mass proportional damping (90% critically damped),

2. 314 sec^{-1} mass proportional damping (critically damped), and

3. 345 sec^{-1} mass proportional damping (110% critically damped).

The resulting lateral deflection at the top center of the pendulum versus time for the three damping cases considered are presented in Figure 6-3.
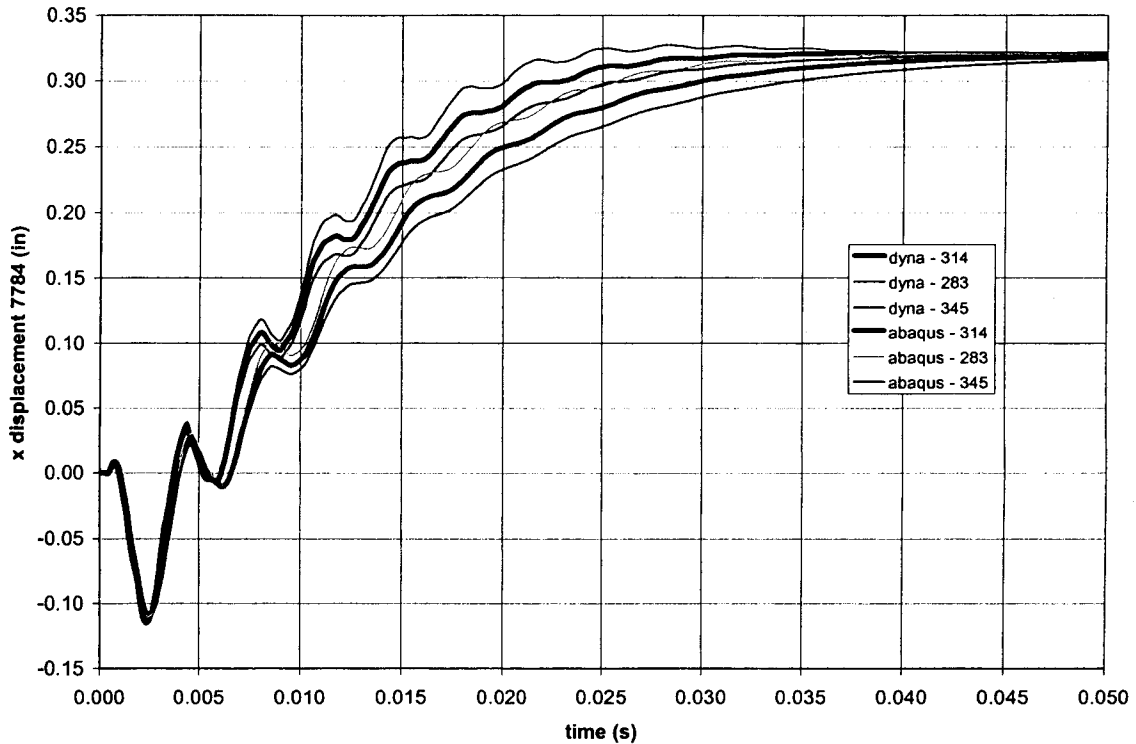
Figure 6-3. Lateral deflection of the top center of the inverted pendulum versus time for Case 5 using different mass proportional damping coefficients.

Initially, there is only a minimal variation between the two analysis codes, irrespective of the mass proportional damping used. However, as the time increases from 0.005 to 0.04 seconds, the variations between codes and damping coefficients becomes more significant. In general, over this time period, the 90% critically damped ABAQUS solution most closely resembles that of the 110% damping solution in LS-DYNA. Variations in time steps did not significantly alter the displacement time history so it is not believed that this variation can be attributed to any time scale factor.

Based on the deflection history, it is possible to assess the applied damping factor relative to the critical damping behavior. The peak deflection for the three analyses are presented in Table 6-2.

Table 6-2 Case 5 with Mass Proportional Damping Peak Lateral Deflection

Damping Values (1/sec)	Maximum deflection (top center node, x dir, inch)	
	ABAQUS	LS-DYNA
283	0.32082	0.32773.
314	0.32000	0.32126
345	0.31998	0.31976

56

As expected, there are variations in the peak deflection trends. The 314 sec^{-1} damping coefficient produces a peak lateral deflection identical to the applied 0.320 inch deflection in ABAQUS. The same damping coefficient in LS-DYNA results in a slightly under-damped condition as indicated by the peak deflection of 0.32126 inches. Also, the range on peak deflections encountered by varying the damping from 90-110% is significantly less in ABAQUS than in LS-DYNA. Despite these variations, it appears that the two codes are in good agreement to how they implement mass proportional damping.

6.6   Inverted Pendulum (Case 5) Conclusions

Case 5 considered an inverted pendulum modeled using three-dimensional, solid elements. Both undamped and mass proportionally damped structures were considered. Using the results from the undamped condition, an estimate of the critical mass damping was calculated. Comparisons between the ABAQUS and LS-DYNA solutions were made using this critical damping value and ±10% damping values. Good agreement was obtained in the structural deflection and the estimation of a critically damped condition.

7 Additional Material Models

Two material models addressing strain-rate plasticity and strain-failure damage modeling were examined in addition to the work associated with the Cases 1 to 5. It was deemed that the use of two unit problems would be sufficient to present the comparison of the ABAQUS and LS-DYNA solutions. This section documents the solutions related to these cases and the conclusions that can be drawn from them.

7.1 Strain-Rate Material Unit Problem (Case 9)

Case 9 applied an axial loading of varying rates to a single shell element utilizing a strain-rate dependent material model.

7.1.1 Strain-Rate Material Unit Problem Geometry

A single shell element 1.0-inches square and 0.1-inch thick was used in this model. ABAQUS utilized the S4R model described in Section 2.3.1.2. LS-DYNA used a type 16 element with 9 integration points as described in Case 1.

7.1.2 Strain-Rate Material Unit Problem Material Definition

It is possible to present material yield stress as a functional relationship involving the plastic strain, plastic strain rate, applied temperature, and additional fields such as environmental degradation. Case 9 only expresses the material yield surface as a function of the plastic strain and plastic strain rate.

An elastic, isotropic hardening material was created in both ABAQUS and LS-DYNA using tabular data defining different effective stress-logarithmic plastic strain curves for various strain rates. A summary of these values is provided in Table 7-1.

Table 7-1. Case 9 Strain-Rate Dependent Material Definition

Strain Rate (in/in/sec)	Stress-Strain Pairs					
	Pair 1		Pair 2		Pair 3	
	$\bar{\sigma}$ (psi)	$\bar{\varepsilon}^{pl}$ (in/in)	$\bar{\sigma}$ (psi)	$\bar{\varepsilon}^{pl}$ (in/in)	$\bar{\sigma}$ (psi)	$\bar{\varepsilon}^{pl}$ (in/in)
0.0	45,000	0.0	52,500	0.0470	66,000	0.1801
1.0	45,450	0.0	53,025	0.0470	66,660	0.1801
10.0	45,900	0.0	53,550	0.0470	67,320	0.1801
40.0	47,250	0.0	55,125	0.0470	69,300	0.1801
60.0	48,150	0.0	56,175	0.0470	70,620	0.1801
100.0	49,500	0.0	57,750	0.0470	72,600	0.1801

The material input in Table 7-1 shows that the material becomes stronger as the strain rate increases, which is typical of many metals.

7.1.3 Loading Conditions

In order to investigate the strain-rate effects on the material presented in Section 7.1.2, different axial loading conditions were applied to the model described in Section 7.1.1. The nominal strain rates used in each analysis are presented in Table 7-2.

Table 7-2 Nominal Applied Strain for Case 9

| Case	Nominal Strain Rate (in/in/sec)	Analysis Duration (sec)
9.1	1.0	1.00
9.2	10.0	0.10
9.3	100.0	0.01
9.4	50.0	0.02

The loading was intended to apply a complete loading cycle with the axial displacement progressing from 0.0 inches to +0.25 inches to -0.25 inches to 0.0 inches. The duration of the loading was determined by relating the applied displacement to the desired strain rate. It should be noted that the load application is done using a nominal strain rate, not the logarithmic plastic strain rate used to define the material model.

7.1.4 Strain-Rate Material Unit Problem Results

The strain-rate material unit problem results will be presented in the form of stress and strain quantities from each code.

ABAQUS results for the true axial stress versus true axial strain for the four strain rates identified in Table 7-2 are presented in Figure 7-1.
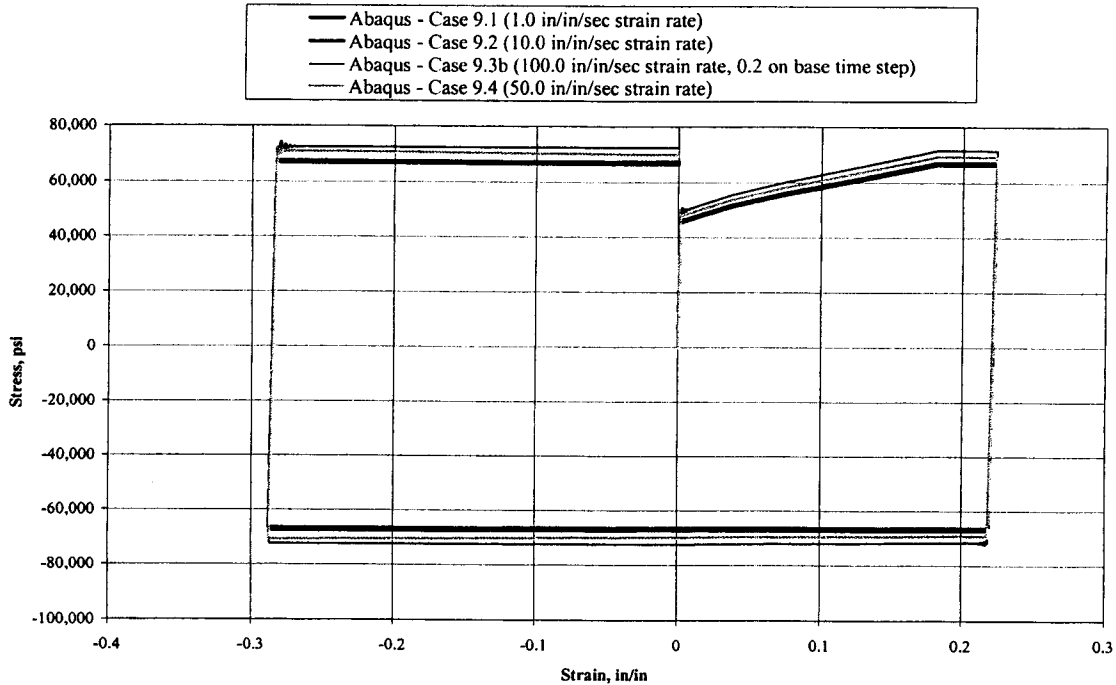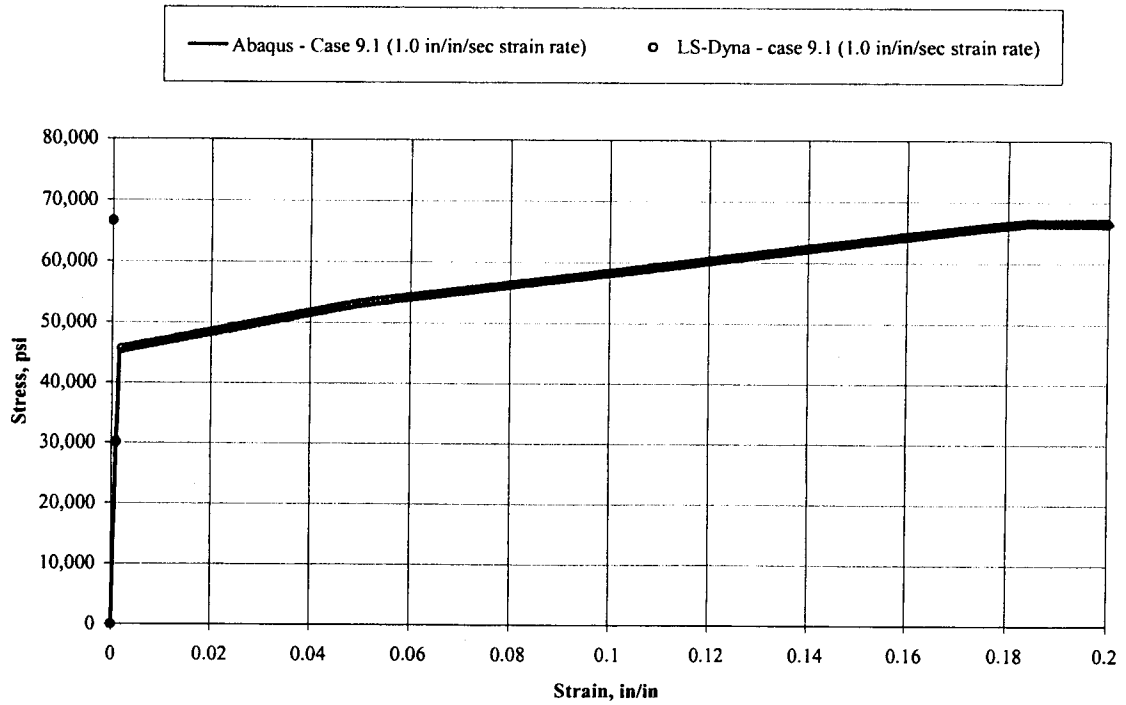

Figure 7-1. Axial stress versus axial strain for Case 9 models using ABAQUS.

This figure shows several important feature of this material model:

- Stiffer material behavior as the strain rate increases from 1.0 to 100.0 in/in/sec,

- Perfectly plastic material after exceeding last input yield stress for the first time, and

- Oscillations in solution during final loading from -0.25 inch deflection back to original length.

The fact that the model goes perfectly plastic after reaching the last yield stress point and during the full unloading cycle is a result of using the isotropic hardening option. The oscillations in the solution are similar to those observed in Section 2.3.1.5.2 and are a result of utilizing a time step that is slightly larger than ideal for a problem that is transitioning to a perfectly plastic solution. As was the case in Section 2.3.1.5.2, the impact of this can be minimized by reducing the fixed time incrementation in ABAQUS.

The overall trends of the LS-DYNA results are very similar to those in ABAQUS. For instance, Figure 7-2 shows the axial stress versus axial strain developed for a nominal strain rate of 1.0 in/in/sec.

60

Figure 7-2. Comparison of axial stress versus axial strain for Case 9 models at 1.0 in/in/sec strain rate.

At this level of magnification, there is no difference between the two codes. Each appears to indicate that there are four slopes for the initial loading condition as anticipated (initial elastic, two plastic, and a the final perfectly plastic slope). However upon zooming in on the region between 49,000 and 57,000 psi axial stress, as shown in Figure 7-3, differences between the two solutions become evident.
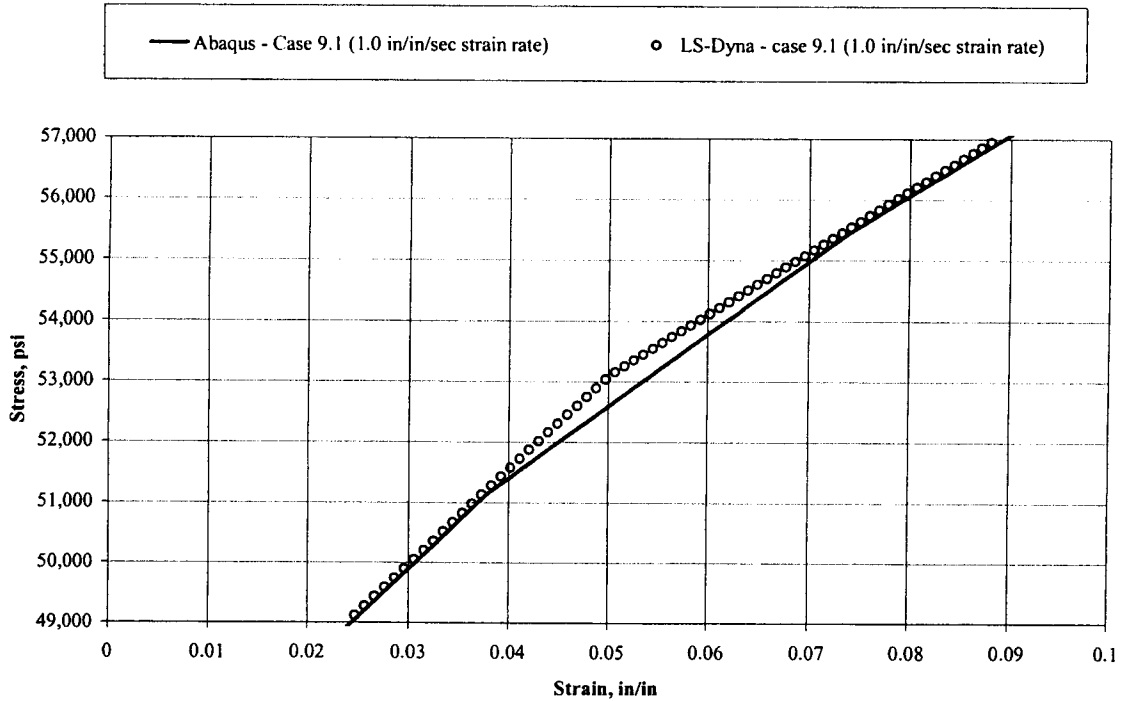
Figure 7-3. Close up of stress-strain curve for Case 9.1 showing additional slope in ABAQUS solution for a 1.0 in/in/sec nominal strain rate.

The codes exhibit excellent agreement at stress levels less than 51,000 psi and greater than 55,000 psi. However, there are variations for stress values between the two bounds. In this area, the LS-DYNA solution reflects the anticipated two slopes with the change in stiffness occurring at approximately 53,200 psi. The ABAQUS solution, on the other hand, includes an additional slope.

## 7.1.5 Investigation of Alternate Strain-Rate Dependent Material (Case 9.5)

A second material model was examined to investigate the additional slope anomaly. This material model was slightly different than the base model presented in Section 7.1.2. The primary difference is that the material model used in Case 9.5 used only two strain rates with the true stress-logarithmic plastic strain pairs presented in Table 7-3.

Table 7-3. Case 9.5 Strain-Rate Dependent Material Definition

Strain Rate (in/in/sec)	Stress-Strain Pairs					
	Pair 1		Pair 2		Pair 3	
	$\bar{\sigma}$ (psi)	$\bar{\varepsilon}^{pl}$ (in/in)	$\bar{\sigma}$ (psi)	$\bar{\varepsilon}^{pl}$ (in/in)	$\bar{\sigma}$ (psi)	$\bar{\varepsilon}^{pl}$ (in/in)
0.0	45,000	0.0	52,500	0.0470	66,000	0.1801
1.0	45,450	0.0	53,025	0.0470	66,660	0.1801

The model was then loaded by an axial extension of 0.25-inches over 0.25 seconds (corresponds to a nominal strain rate of 1.0 in/in/sec).

The results for this comparison were very similar to those for Case 9.1 provided in Section 7.1.4. In this case, the close-up of the axial stress versus axial strain provided in Figure 7-4 indicates that an additional slope is observed, similar to that appearing in Case 9.1.
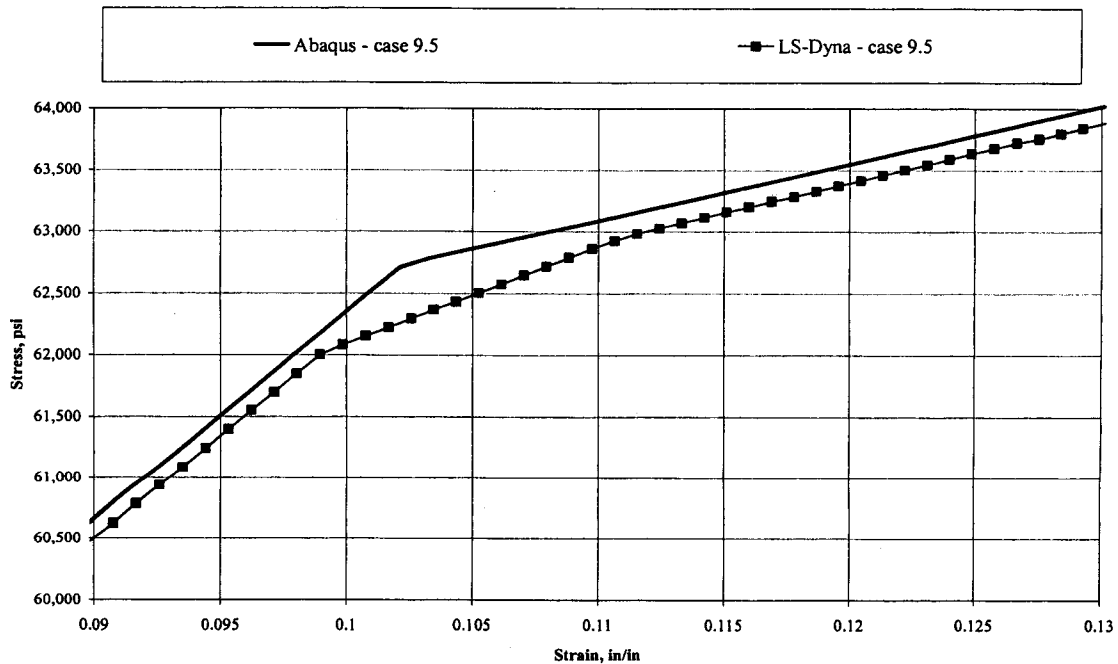
Figure 7-4. Close up of stress-strain curve for Case 9.5 showing additional slope in LS-DYNA solution for a 1.0 in/in/sec nominal strain rate.

There is one significant difference between Case 9.1 and 9.5 however. In this case, the additional stress-strain slope in Case 9.5 is observed in the LS-DYNA solution not the ABAQUS solution as in Case 9.1

7.1.6 Strain-Rate Material Model Conclusions

The investigation into the modeling of strain-rate material behavior of ABAQUS and LS-DYNA was successful at a global level. However, differences were observed between the codes in some cases when transitions were made between the various plastic moduli. The differences did not appear to be consistent and were not confined to a single code. Provided that the analysis is not highly sensitive to these transition regions, the two models can provide similar results. Care must be taken though as variations do exist in the solutions.

7.2 Strain Failure Material Modeling Problem (Case 10)

Another material model aspect investigated was the application of a strain failure criterion. This modeling allows the finite element analysis to remove the stiffness contribution of elements if a strain threshold is exceeded. This section documents the formulation of strain-failure materials in ABAQUS and LS-DYNA and their application in a plate bending problem.

7.2.1 Geometry

The strain-failure material model problem geometry consisted of a 0.10-inch thick, 10-inch square plate that is subjected to a lateral pressure. The plate is fixed from displacement and rotations along all edges and a uniform lateral pressure is applied over the entire plate.

7.2.2 Strain-Failure Material Model

The implementation of strain-failure material models in the two codes will be addressed in this section. The inelastic mechanical properties will be presented first followed by a brief discussion of how ABAQUS and LS-DYNA handle strain-failure.

The base material definition was an piecewise linear, isotropic hardening material:

- 30×10^6 psi Elastic modulus
- 0.3333 Poisson's ratio
- 7.40×10^{-4} lb sec^2 in^{-4} density
- 45,000 psi yield stress

The piecewise linear hardening definition used the true stress and logarithmic plastic strain pairs presented in Table 7-4.

Table 7-4. Piecewise Linear, Isotropic Hardening Material Model for Case 10

True Stress (psi)	Logarithmic Plastic Strain (in/in)
45,000	0.0000
52,500	0.0470
66,000	0.1801

Perfect plasticity is encountered once the material reaches the final true stress level in Table 7-4 of 66,000 psi.

Case 10 included a strain-failure parameter to the base material model that is assessed in each analysis code by comparing the current strain at all the integration points in each element with the specified maximum allowable plastic strain. When the current plastic strain exceeds the specified failure strain, the integration point's contribution to the global stiffness matrix is reduced to zero. This results in either an immediate or gradual reduction in element stiffness. For instance, if first-order, reduced-integration solid elements are used there will be an immediate elimination of the element's stiffness once the failure strain is exceeded whereas failure can progress through a shell element's thickness until the failure strain is obtained at all section points.

In this case, a maximum allowable plastic strain of 0.20 in/in was defined for each analysis code. It was assumed that the equivalent plastic strain at failure was independent of plastic strain rate, pressure-deviatoric stress ratio, temperature, and any predefined fields.

7.2.3   Element Selection

The geometry selected for the strain failure material model unit problem permits the use of shell elements. As such, the analyses performed utilized the ABAQUS S4R and LS-DYNA type 16 shell elements described in Section 1.

7.2.4   Loading Conditions

No rotation or displacements were permitted along the plate perimeter. The lateral pressure applied was linearly ramped from 0 psi at 0.000 seconds to 750 psi at 0.005 seconds.
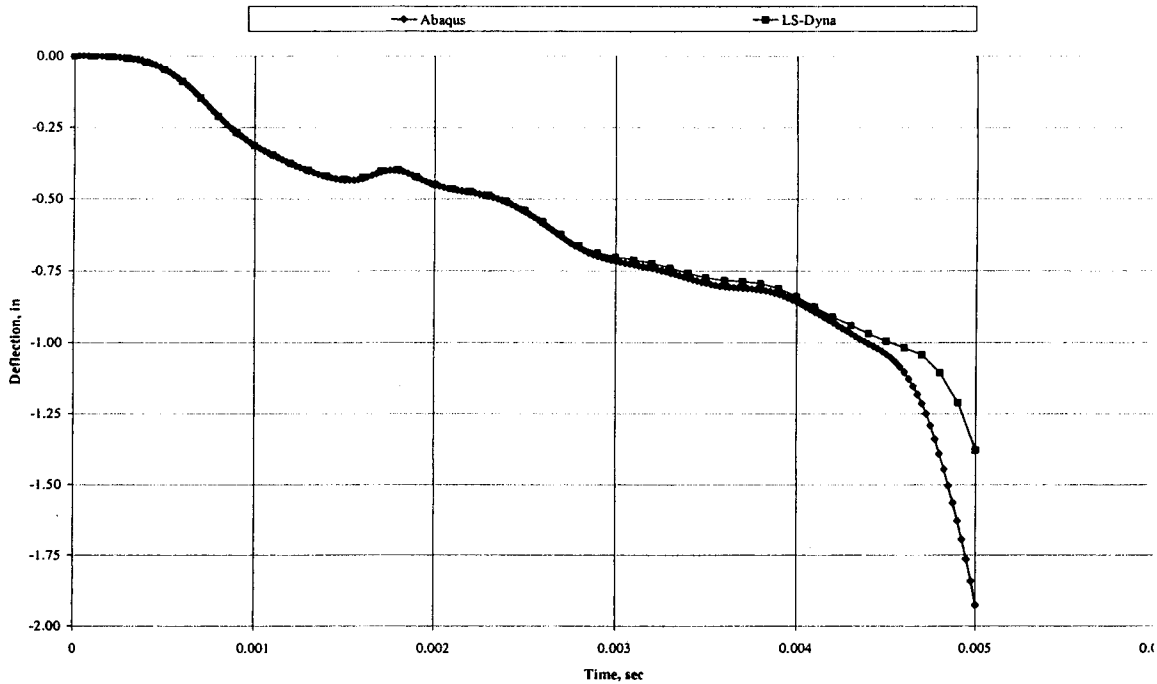
7.2.5   Strain Failure Material Model Unit Problem Results

The results obtained for the strain failure material model unit problem, Case 10, using both ABAQUS and LS-DYNA were compared considering:

- Lateral deflection at the center of the plate and
- Equivalent plastic strain along one of the plate edges

These results will provide an indication of agreement between the Case 10 solutions.

The lateral deflection of the plate versus time is presented in Figure 7-5.

Figure 7-5. Lateral deflection at the center of the plate versus time for strain failure material model unit problem (Case 10).

The lateral deflection time history indicates excellent agreement between the two analysis methods through approximately 0.004 seconds. After this point, the two codes begin to experience significant variations between the solutions. The explanation for this deviation lies in failure of elements along the boundaries.

Two different locations were selected along the plate perimeter to examine the equivalent plastic strain and, hence, strain failure behavior as a function of time. Two points were selected along an edge: one at the center of the edge 5.0 inches from a corner and the second 2.5 inches from the same corner. These locations provide an indication of not only the strain failure of the individual elements but also the propagation of the failure along the edge. Note that due to symmetry of the problem, it is not necessary to specify which edge is being considered as each edge will have the same response.

Figure 7-6 shows the plastic strain developed at the center of the edge at the element's upper, middle, and lower surfaces with time.
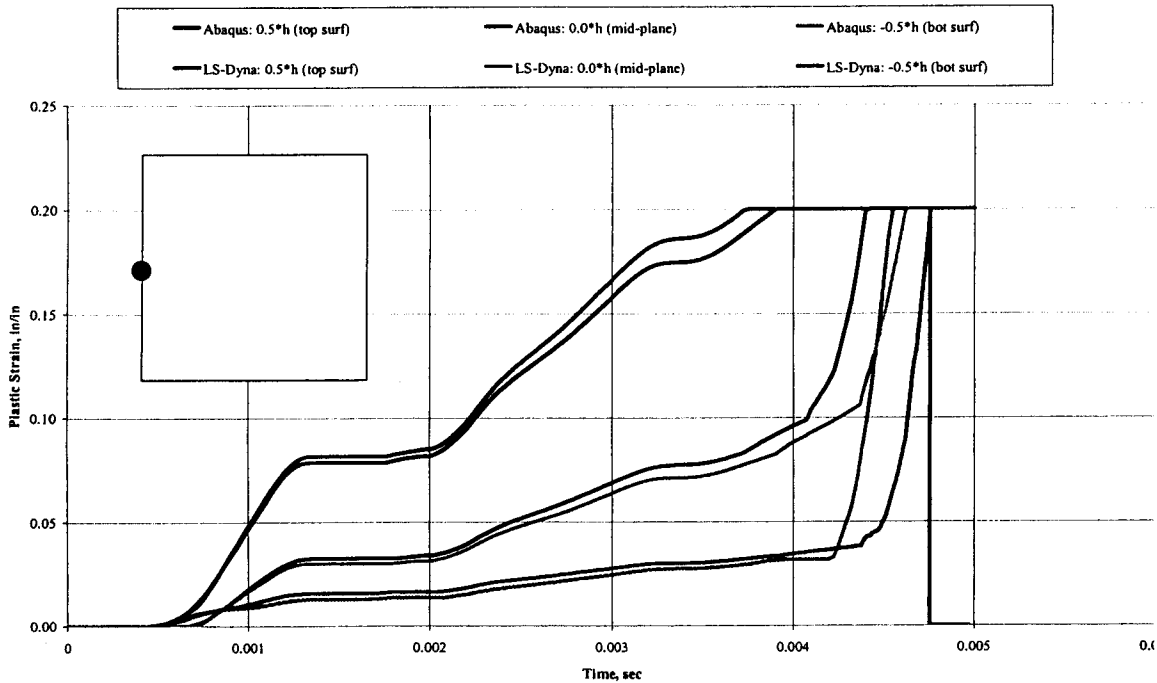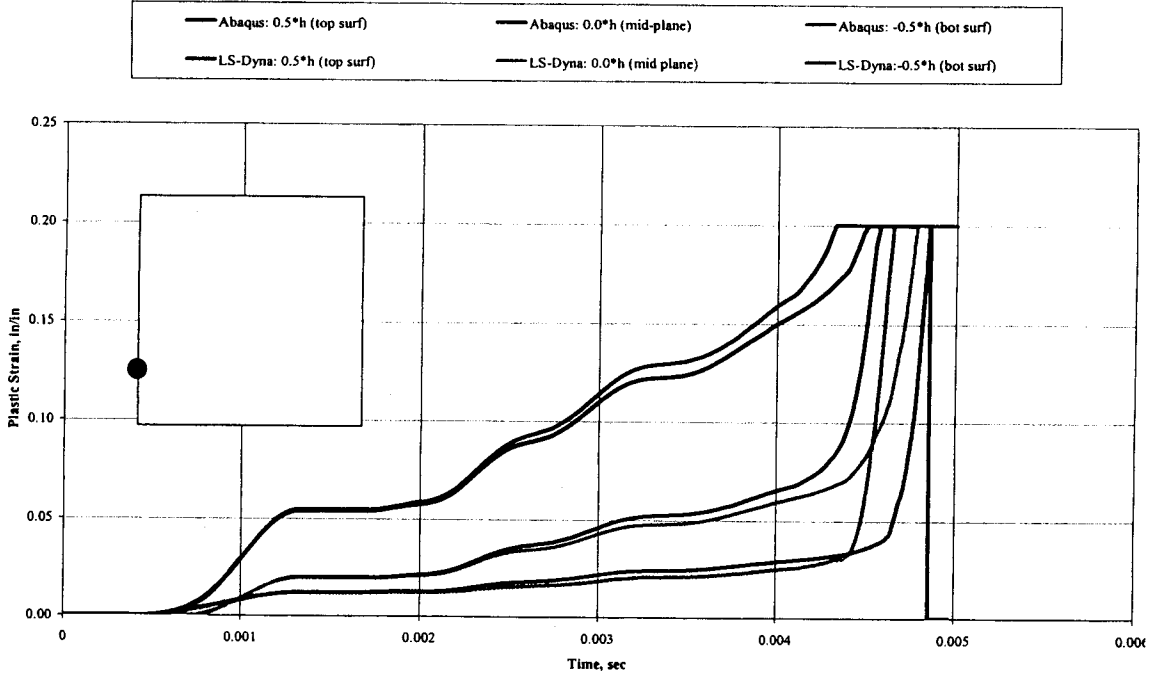
Figure 7-6. Equivalent plastic strain versus time at element 5.0 inches from plate corner for strain failure material model unit problem (Case 10).

For each point through the thickness, the equivalent plastic strain in the ABAQUS solution is slightly higher than that present in the LS-DYNA solution. The variation between the strain values through 0.0014 seconds is negligible. At this point, the LS-DYNA solution deviates slightly from that in ABAQUS. For the top surface of the element at the center of the edge, the ABAQUS equivalent plastic strain of 0.0815 in/in is approximately 3.7 percent higher than that in LS-DYNA. The magnitude of the variation remains fairly constant until approximately 0.003 seconds at which time the LS-DYNA strain solution increases at a slower rate than the ABAQUS solution. This results in the top surface of the element reaching the maximum allowable plastic strain of 0.20 in/in in ABAQUS prior to LS-DYNA. Once this happens, the variation in strain solutions become greater as the effective element cross section is no longer constant between the two analyses. As the load increases, the failed section points progress from the upper surface to the lower surface in both the ABAQUS and LS-DYNA solutions. The end result is that the center element along the edge is removed from the analysis (no stiffness contribution) earlier in ABAQUS than LS-DYNA, 0.00455 seconds compared to 0.00476 seconds, respectively. This variation in the element failure corresponds to a failure pressure of 682.5 psi in ABAQUS compared to 714.0 psi in LS-DYNA, or 4.4 percent lower load.

Figure 7-7 presents the time history plot of the equivalent plastic strain at the upper, middle, and lower surfaces for the element at 2.5 inches from the plate corner.

Figure 7-7. Equivalent plastic strain versus plate versus time at element 2.5 inches from plate corner for strain failure material model unit problem (Case 10).

As was the case at the center of the edge, the two solutions track each other well until the upper surface in the ABAQUS solution reaches a strain of approximately 0.09 in/in. As the applied load magnitude increases, the variation between the two codes also increases until the maximum allowable strain levels are reached in each code.

The resulting time to complete element strain failure for the two edge locations are presented in Table 7-5.

Table 7-5. Case 10 Element Failure Time

Analysis Code	Element Location	Complete Element Failure Time
ABAQUS	5.0 in from corner (Center of edge)	0.00455
	2.5 in from corner	0.00465
LS-DYNA	5.0 in from corner (Center of edge)	0.00476
	2.5 in from corner	0.00486

As expected, the failure time for both codes are shortest at the center of the edge. As the distance to the corner is reduced, the failure time increases.

68

7.2.6 Conclusion

A strain-failure material model was utilized in the ABAQUS and LS-DYNA analyses for a clamped plate subjected to a uniform lateral pressure. A combination of plate displacement and equivalent plastic strain results indicate that the LS-DYNA model tended to experience lower strains that those in ABAQUS. These initially small differences increased with increasingly lateral loading and resulted in the LS-DYNA solution indicating element failures after ABAQUS. Despite these variations, the two solutions were similar to one another with the variations being less than 5% throughout the majority of the analysis. Overall, the two codes appear to implement a strain-failure mechanism that is similar to each other when applied to a model similar to that presented.

8 Deformable to Rigid Validation with Bouncing Ball

This case was run to show that using the *DEFORMABLE_TO_RIGID command to change a deformable material to rigid material will yield very similar results compared to the unchanged condition if used under the correct situation. It is desired to change parts of the model to rigid (producing rigid body motion) after they have undergone most of their deformation to gain bulk body motion while reducing cpu times.

This case utilizes a deformable ball impacting a rigid plate. The ball undergoes deformation as it impacts and rebounds from the plate. In the unchanged run the ball is left as deformable for the whole run. In the "deformable to rigid" run the ball is switched to a rigid material at a given time after impact. These calculations were performed only with LS-DYNA because ABAQUS does not have a deformable-to-rigid option. As such, this model will use LS-DYNA features previously validated against ABAQUS including:

- Solid elements,
- Rigid surface, and
- Elastic, perfectly plastic material model.

8.1 Geometry

Figure 8-1. Initial geometry for Deformable to Rigid.

The center of a 0.5 inch diameter sphere is located 3 inches from a rigid plate (Figure 8-1). Initial velocity of the ball is 1,200 in/s in the –x direction (toward the rigid wave). There are 350 elements in the sphere utilizing a butterfly type mesh.

8.2 Material Definition

8.2.1 Ball

An elastic, perfectly plastic material was used:

- Elastic modulus of 30×10^6 psi,
- 0.333 Poisson's ratio,
- Density of 7.40×10^{-4} lb sec^2 in^{-4}, and
- Yield stress of 25,000 psi.

8.2.2 Wall

The wall is defined utilizing the *Rigidwall_planar command to define an infinite plane.

8.3 Element Formulation

8.3.1 LS-DYNA

Solid element type 2 – Fully Integrated S/R Solid.

8.4 Loading Conditions

The ball was given an initial velocity of 1,200 in/s in a direction normal to the rigid plane.

8.5 Results

The ball undergoes substantial deformation after impact with the rigid surface as is shown in Figure 8-2. A maximum effective plastic strain of 0.2276 in/in is seen in the elements.

DEFORM4.K
Time - 0.005005
Contours of Effective Plastic Strain
max ipt. value
min=0, at elem# 51
max=0.227568, at elem# 28

Fringe Levels

2.276e-01
2.048e-01
1.821e-01
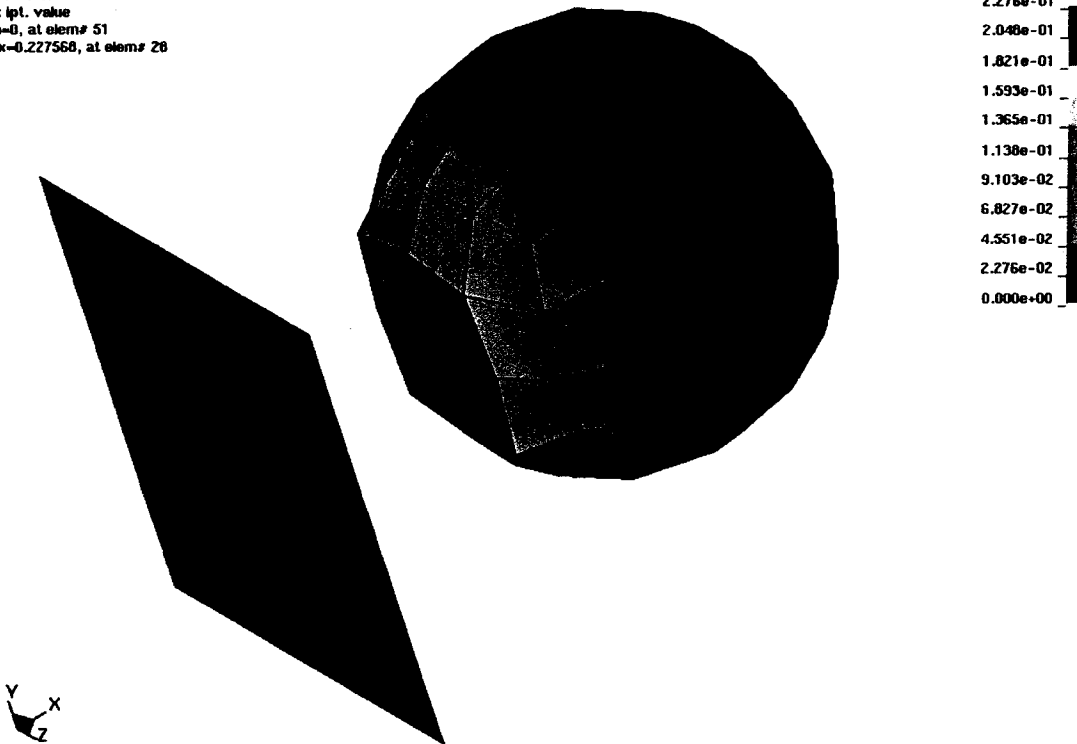1.593e-01
1.365e-01
1.138e-01
9.103e-02
6.827e-02
4.551e-02
2.276e-02
0.000e+00

**Figure 8-2. Ball deformation after impact with rigid plate.**

From Figures Figure 8-3, Figure 8-4, and Figure 8-5, the x displacement, velocity and acceleration for node 1 on the ball is shown. The ball is originally given a velocity in the negative x direction. It is seen that there is no noticeable difference in the displacement of the ball in the "unchanged" and "deformable to rigid" run. However, the velocity and acceleration plots show the "deformable to rigid" run do not produce the same reverberations after changing to rigid that the "deformable" run does. This is to be expected due to the solid becoming rigid.
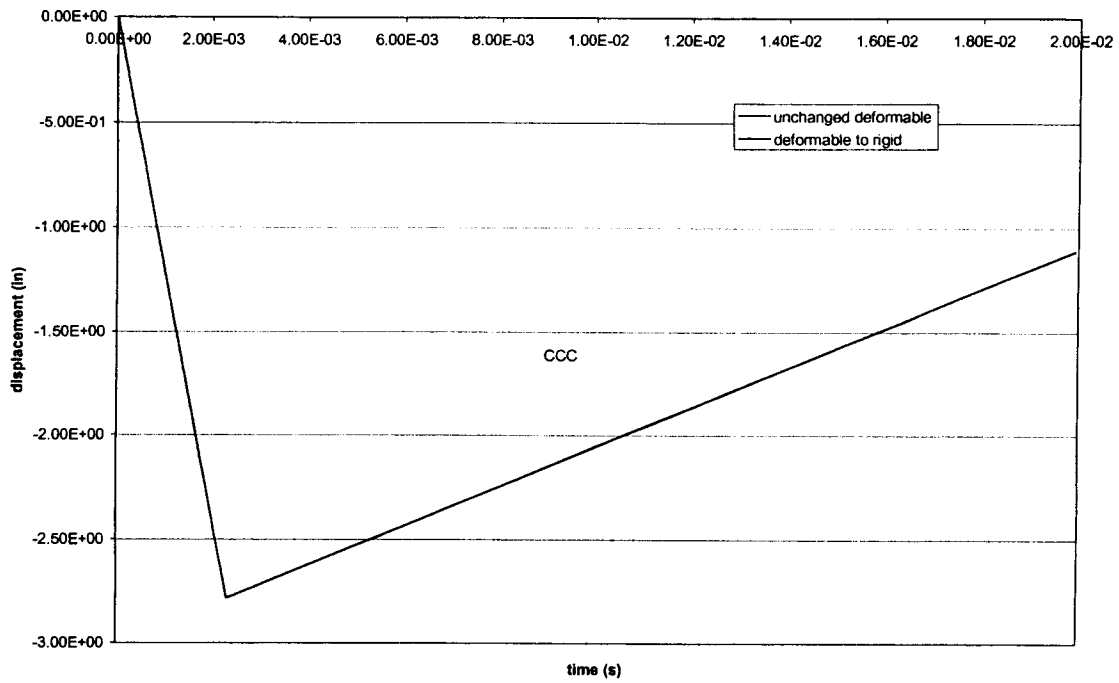
Figure 8-3. X Displacement for Node 1 on Ball.
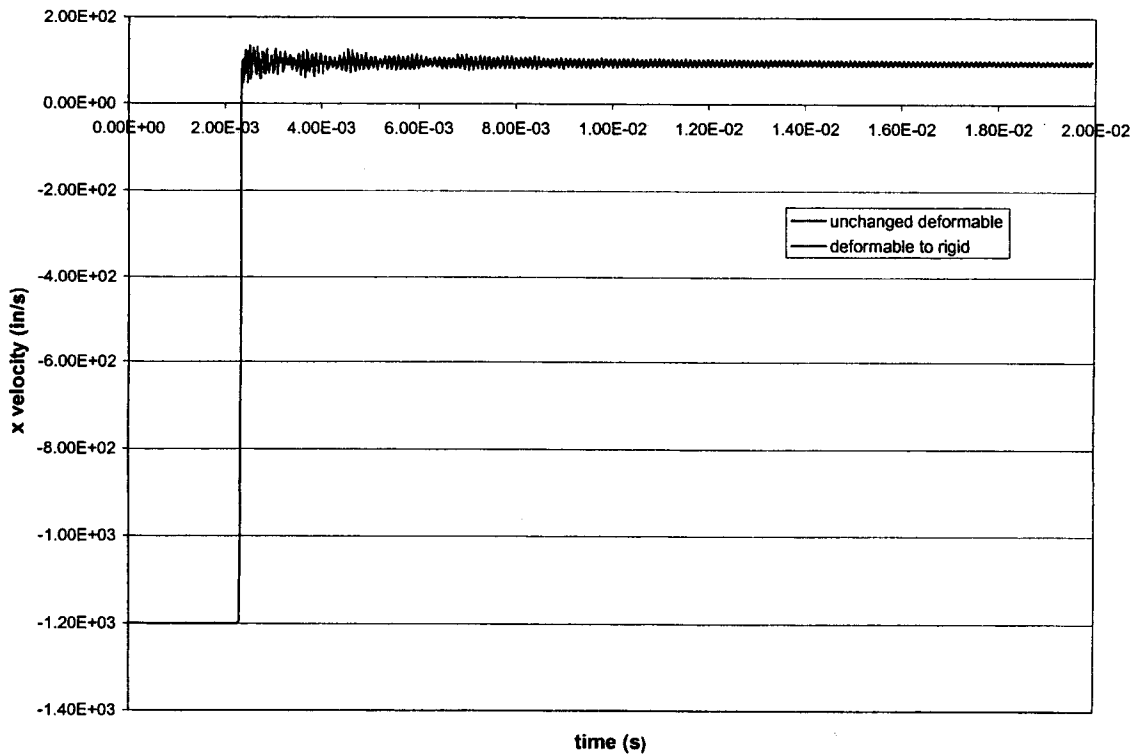
Figure 8-4. X Velocity for Node 1 on Ball.
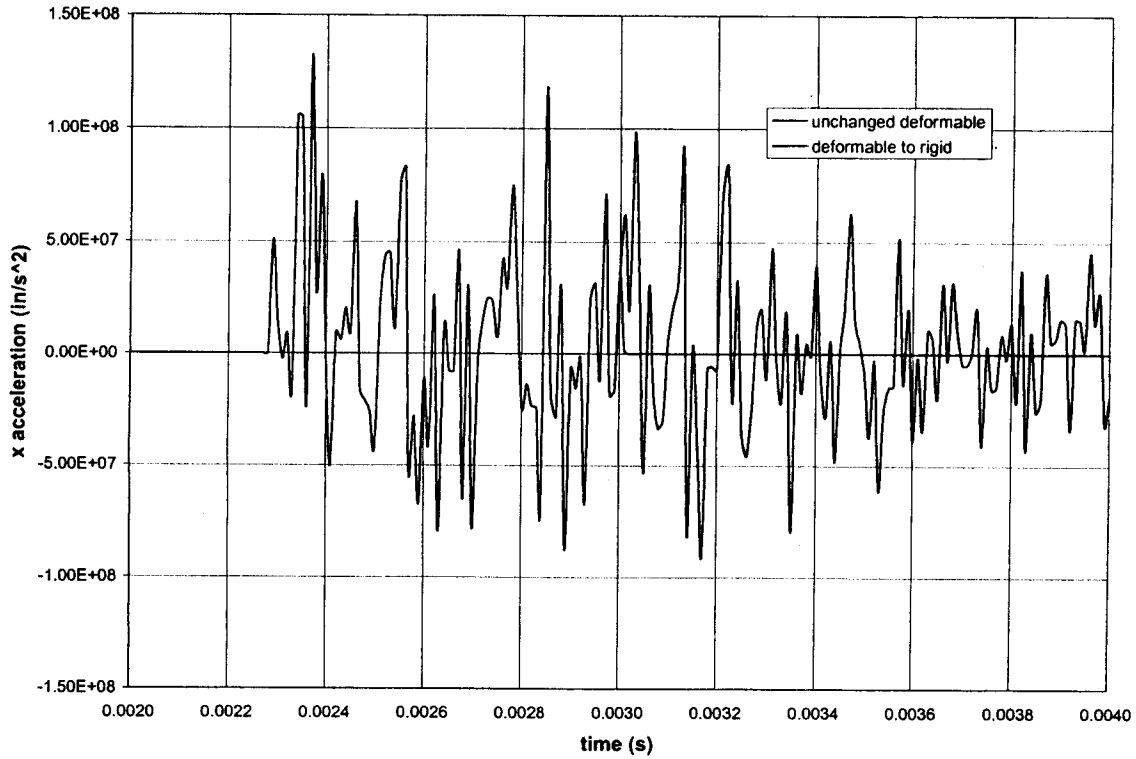
Figure 8-5 X Acceleration for Node 1 on Ball.

8.6 Conclusion

The purpose of this analysis was to determine the validity of using the *Deformable_to_Rigid command in LS-DYNA. Converting a deformable body to a rigid one is usually performed to gain bulk body motion of a part after a relatively short dynamic event has occurred. By changing deformable parts to rigid, a substantial computational cost savings is realized. The test case considered examined a ball impacting a rigid wall. The results from this case indicate that the assumed rigid body behavior is consistent with that observed for the deformable body, even though some of the computational detail in the part is lost.

9 Conclusions

The goal of this program was to validate features of LS-DYNA utilized in previous analyses performed for the CNWRA against ABAQUS. To achieve this, a series of cases were examined that addressed a combination of different features including:

- Element formulation
  - Three-dimensional solid element
  - Three-dimensional shell element
  - Three-dimensional beam element
  - Rigid elements
- Material modeling
  - Elastic material
  - Elastic, perfectly plastic material
  - Multi-linear, isotropic hardening material
  - Strain-rate dependent material
  - Strain failure criterion
  - Mass damping
- Boundary conditions
  - Boundary node constraints
  - Load curves
- Load application
  - Pressure loads
  - Gravity
  - Load curves
- Contact interaction
  - Surface to surface contact
  - Surface to node contact
  - Spot welds

In addition to these features, rigid body motion and the deformable-to-rigid conversion methods were examined in LS-DYNA by comparing against previously validated features in LS-Dyna, since ABAQUS lacks the ability to perform deformable to rigid conversions.

From these studies, some cautions were noted. LS-Dyna results are typically more flexible under large deflections. It was also noted that after initial spotweld failure subsequent failures may vary substantially due to the resulting oscillatory nature of the forces present in the remaining spotwelds. Caution should be taken to understand the contact algorithms used and to

make sure it is working satisfactorily. Slight differences between the codes were seen in the plastic moduli transition areas when using strain rate dependant material models.

Overall, good agreement between the code solutions was obtained, provided the codes featured comparable physical models. Variations between the codes for displacement, stress, strain, and observed failures was consistent with the formulation of each code and was typically less than 10 percent.

Input decks for the analyses described in this document are included on the enclosed compact discs.